Investigations Regarding the Design and Management of Aquifer Storage and Recovery Operations in Victoria County

Prepared for:

Victoria County Groundwater Conservation District

Prepared by:

INTERA
GEOSCIENCE & ENGINEERING SOLUTIONS

INTERA Incorporated
9600 Great Hills Trail
Suite 300W
Austin, TX 78759
512.425.2000

May 2019

This page intentionally left blank.

Investigations Regarding the Design and Management of Aquifer Storage and Recovery Operations in Victoria County

Prepared By

Steve C. Young, Ph.D., P.G., P.E.

Ross Kushnereit

INTERA
GEOSCIENCE & ENGINEERING SOLUTIONS

This page intentionally left blank.

TABLE OF CONTENTS

LIST OF FIGURES

LIST OF TABLES

Acronyms and Abbreviations

%	percent
ft	feet
ft^3/day	cubic feet per day
ac-ft	acre-feet
ASR	aquifer storage and recovery
CFR	code of federal regulation
EPA	Environmental Protection Agency
GCD	groundwater conservation district
gpm	gallons per minute
SDWA	Safe Drinking Water Act
TAC	Texas Administrative Code
TCEQ	Texas Commission on Environmental Quality
TWDB	Texas Water Development Board
UIC	underground injection control
USDW	united states drinking water standard
USGS	United States Geological Survey
UT	University of Texas at Austin
VCGCD	Victoria County Groundwater Conservation District
VCGFM	Victoria County Groundwater Flow Model

This page intentionally left blank.

1.0 INTRODUCTION

The Texas Water Development Board ([TWDB], 2018) defines aquifer storage and recovery (ASR) as "the storage of water in a suitable aquifer through a well during times when water is available, and the recovery of water from the same aquifer during times when it is needed." During the last decade, ASR facilities have been increasingly recognized as a viable option for helping industries and communities in Texas to address water supply problems. When comparing ASR systems to surface water reservoirs, there are two main benefits. One benefit is that no water loss occurs as a result of evaporation, and the other benefit is that there is no loss of storage capacity due to sedimentation.

This report provides an initial assessment of approaches for evaluating and modeling ASR operations conducted for the Victoria County Groundwater Conservation District (VCGCD). According to the Texas Commission on Environmental Quality (TCEQ), an ASR project should be designed and operated to isolate the recharge water (i.e., water added to the aquifer) from the native groundwater such that the same water that is stored can be subsequently recovered. The ability of an ASR project to recover the stored water is called recoverability. A 70 percent (%) ASR recoverability indicates that 70% of the water withdrawn from an ASR consists of stored water (i.e., water injected into the aquifer by an ASR well) and 30% native groundwater.

This report discusses the concepts of ASR recoverability and provides a framework for simulating ASR operations using a numerical groundwater model developed for the County of Victoria. After this introduction, the report contains three main sections, which are described below:

- Section 2 – This section describes the general design and operation of ASR systems and their potential benefits for managing water supplies. This section also overviews ASR systems in Texas and discusses the impact that House Bill 655 has on how the TCEQ regulates ASR wells.
- Section 3 - This section explains the terms and concepts that are important to defining recoverability with respect to water injected by an ASR well. This section explains why the calculation of recoverability is required as part of the application process for operating an ASR project in Texas. This section also describes and demonstrates groundwater modeling approaches for estimating ASR recoverability.
- Section 4 - This section uses a groundwater flow model to demonstrate an approach for estimating ASR recovery. Simulations are performed for six candidate locations for ASR wells in Victoria County. The simulations are based on simple assumptions regarding regional pumping and the operation schedule for the ASR.

This page intentionally left blank.

2.0 INTRODUCTION TO AQUIFER STORAGE AND RECOVERY

This section describes the general design and operation of ASR systems and their potential benefits for managing water supplies. This section also overviews ASR systems in Texas and discusses the impact that House Bill 655 has on how the TCEQ regulates ASR wells.

2.1 General Description

The TWDB (2018) defines ASR as “the storage of water in a suitable aquifer through a well during times when water is available, and the recovery of water from the same aquifer during times when it is needed.” The fundamental objective of an ASR system is to recover a high percentage of injected water (i.e., to maximize the recovery efficiency) at a quality that is (nearly) ready to be put to beneficial use.

More than 200 sites in 27 different states in the United States have either implemented or investigated ASR (American Water Works Association, 2015). Most existing systems involve storage of potable water, but a number of wells use untreated raw surface water or groundwater in an ASR system for later withdrawal and treatment. ASR systems are designed to inject water into an aquifer during relatively wet periods when water availability exceeds demand and recover the injected water during periods of high demand. Water from various sources can be used for injection, including storm water, river water, reclaimed water, desalinated seawater, rainwater, or even groundwater from other aquifers.

ASR systems typically include the following seven major components: (1) capture of available water; (2) pretreatment of the water prior to injection, (3) injection of the pretreated water into the aquifer; (4) storage of the water in the aquifer; (5) recovery of the water from the aquifer; (6) post treatment of the water; and (7) distribution of the water for its end use. In the United States, surface water is usually the capture water, and the pretreatment achieves drinking water standards. The most common mechanisms for recharging water into an aquifer are injection wells, spreading basins, and infiltration galleries. Recovery is usually performed by pumping wells and is preceded by minimal water treatment that includes disinfection.

In the United States, ASR wells are regulated under U.S. Environmental Protection Agency (EPA)’s Underground Injection Control (UIC) program that was promulgated under the Safe Drinking Water Act (SDWA). The EPA’s authority to govern UIC programs is codified at 40 Code of Federal Regulation (CFR) 144 through 148. The UIC program requirements were developed to ensure that emplacement of fluids via injection wells do not endanger current and future underground sources of drinking water (USDW). Several states have primacy over ASR operations, but state-specific ASR regulations do not supersede federal regulations that protect potable water supplies. Federal UIC regulations state:

> “No owner or operator shall construct, operate, maintain, convert, plug, abandon, or conduct any other injection activity in a manner that allows the movement of fluid containing any contaminant into underground sources of drinking water, if the presence of that contaminant may cause a violation of any primary drinking water regulation under 40 Code of Federal Regulations (CFR) part 142 or may otherwise adversely affect the health of persons.” (40 CFR 144.12L)

ASR operations can be differentiated based on whether they inject into a confined or unconfined aquifer. These two types of ASR operations are described below and illustrated in **Figure 2-1**.

- *Injection into a confined aquifer*. In this case, water from secondary sources, such as treated wastewater or collected rainwater, is pre-treated and injected into a confined geologic unit. The water can then be recovered from the same well, or designated recovery well(s), and treated for a specific end use. The hydraulic head changes in accordance with pressure changes induced during injection and withdrawal. Components of this ASR type are shown in **Figure 2-2a**.
- *Injection into an unconfined aquifer*. For many applications, water is injected into an unconfined aquifer. Injection through a spreading basin, infiltration basin (or gallery), or well can result in mounding of the groundwater table under these conditions. These practices are sometimes referred to as artificial recharge (AR) rather than ASR if there is no recovery component. Components of this ASR type are shown in **Figure 2-2b**.

During ASR operations, the injected water forms a “bubble” by displacing the native water closest to the point of introduction and mixing with native water for some distance away from the injection point. The point at which only native groundwater is present in pore space defines the edge of the injection bubble. In Figure 2-2, the injection bubble is represented as stored water. Between the zone of stored injected water and the native groundwater is a region called the buffer zone, which consists of a mixture of native groundwater and injected water. The native groundwater zone consists of native groundwater unaffected by the buffer zone. The permeability, porosity, and spatial boundaries of the aquifer will determine injection/extraction rates and the injection bubble geometry for storage.

ASR offers several benefits to managing water supplies. In regions where significant fluctuations in raw water supplies and/or demands occur throughout the year, ASR may allow the water utility to size its treatment plants for average conditions rather than seasonal high demands; thereby saving capital infrastructure costs. ASR can also defer the need for additional capital investment by increasing the use of existing treatment facilities but allowing the facilities to be used during non-peak hours to pretreat ASR source water for storage. When comparing ASR systems to surface water reservoirs, there are two main benefits. One benefit is that no water loss occurs as a result of evaporation, and the other benefit is that there is no loss of storage capacity due to sedimentation.

A concern with operating ASR wells is the chemical compatibility of the injected water with the native groundwater and the aquifer mineralogy. One type of problem that can be related to water quality is clogging. Geochemical reactions that can contribute to clogging include biological fouling and incrustations that precipitate across the well screen and in the gravel pack. In their review of 204 ASR sites in the United States, Bloetscher and others (2014) report that clogging was a problem at 18 active sites and 29 inactive sites. Another type of water quality problem is the release of potential contaminants from the aquifer matrix in the ASR bubble. Of particular concern is the injection of oxygen-rich surface waters into an aquifer, which can cause the release of trace metals into the stored water (Jones, 2015). Out of the inactive ASR wells surveyed by Bloetscher and others (2014), 10 wells were affected by water quality issues. Five of those were related to arsenic in Florida (Arthur and others, 2001; Reese, 2002) and four were associated with arsenic, manganese, iron, or a combination of metals (Austin, 2013).

2.2 ASR Operations and Studies in Texas

In Texas, activities on ASR date back to the 1940s and 1950s, with studies in El Paso and Amarillo (Sundstrom and Hood, 1952; Moulder and Frazer, 1957). In the 1960s, operational systems were in place in Texas (TWDB, 1997; Malcolm Pirnie, 2011). In 1995, the passage of House Bill 1989 by the 74th Texas Legislature established the statutory framework for ASR and called for further studies of potential ASR applications in Texas.

The Texas Administrative Code (TAC), Title 30, Rule 331.2(8) defines ASR as: “The injection of water into a geologic formation, group of formations, or part of a formation that is capable of underground storage of water for later retrieval and beneficial use.” [30 TAC § 331.2(8)]. Implicit in this TAC definition is that ASR facilities inject water into the aquifer using injection wells. Currently, there are two ASR facilities (the City of Kerrville facility and the Twin Oaks Aquifer Storage and Recovery facility in San Antonio) and one hybrid ASR facility (El Paso Water Utilities) in Texas. The ASR facility at the City of Kerrville began operating in 1998, and the San Antonio Water System’s Twin Oaks facility began operating in 2004. Both systems continue to perform successfully and are viewed by their operators as a beneficial component of their water management plans. The El Paso Water Utilities hybrid ASR facility was established in 1985. With this system, water is added to the aquifer using wells and spreading basins, and stored water is recovered from wells that are not the same as the ones used for injection.

In the 2017 State Water Plan, seven regional water planning groups (Regions E, F, G, J, K, L, and O) included ASR as a recommended water management strategy. Collectively, there are 49 recommended water management strategies in the plan that meet the water needs of water user groups. If these strategies are implemented, ASR would yield an estimated 152,000 acre-feet (ac-ft) of new water supply per year by decade 2070, constituting about 1.8% of all recommended water management strategies. **Figure 2-3** is a map showing decommission and currently operating ASR facilities, ongoing ASR studies, and 2017 recommended water ASR projects in Texas compiled by the TWDB (2018).

2.3 House Bill 655

In 2015, the Texas 84th Legislature enacted House Bill 655, which repealed some of the existing requirements for ASR projects. House Bill 655 established the same regulatory framework for all ASR projects, regardless of the source of the stored water, by giving TCEQ exclusive jurisdiction over both the injection and recovery of stored water under its existing ASR UIC program. The new law specifies how ASR facilities must account for the water they inject and recover. It requires ASR project developers to meter all wells and report total injected and recovered amounts monthly to the TCEQ and to any applicable groundwater district, as well as results of annual water quality testing of injected and recovered water.

For ASR projects within the jurisdiction of a groundwater conservation district (GCD), the amount of water that a project may recover is limited to the lesser of the total amount injected or the amount the TCEQ determines can be recovered. If the project withdraws more water than the amount authorized by the TCEQ, the ASR operator must report the excess volume to the GCD. A GCD’s spacing, production, and permitting rules and fees apply only to the excess volume (Parker, 2016). The requirements in House Bill 655 do not apply to the regulation of an ASR project in the Edwards Aquifer Authority, the Harris-Galveston Subsidence District, the Fort Bend Subsidence District, the Barton Springs Edwards Aquifer Conservation District, or the Corpus Christi Aquifer Storage and Recovery Conservation District.

House Bill 655 requires the TCEQ to assess the impacts of an ASR project on the water in the receiving aquifer. In adopting rules or issuing permits, the commission must consider (Parker, 2016):

- Whether the injection of water will comply with the federal SDWA;
- The extent to which the water injected for storage can be successfully recovered for beneficial use;
- The project's effect on existing water wells; and
- Whether the injected water could degrade the quality of the native groundwater so that it might be harmful or require an unreasonably higher level of treatment to be suitable for beneficial use.

House Bill 655 prohibits the TCEQ from adopting or enforcing groundwater quality protection standards for injected water that are more stringent than applicable federal standards. During rulemaking, the TCEQ amended ASR rules to be consistent with current EPA requirements. Under the new TCEQ rules, which became effective May 19, 2016, water no longer must meet drinking water standards before it is injected. Instead, the operator must assure that injected water will not endanger any drinking water sources.

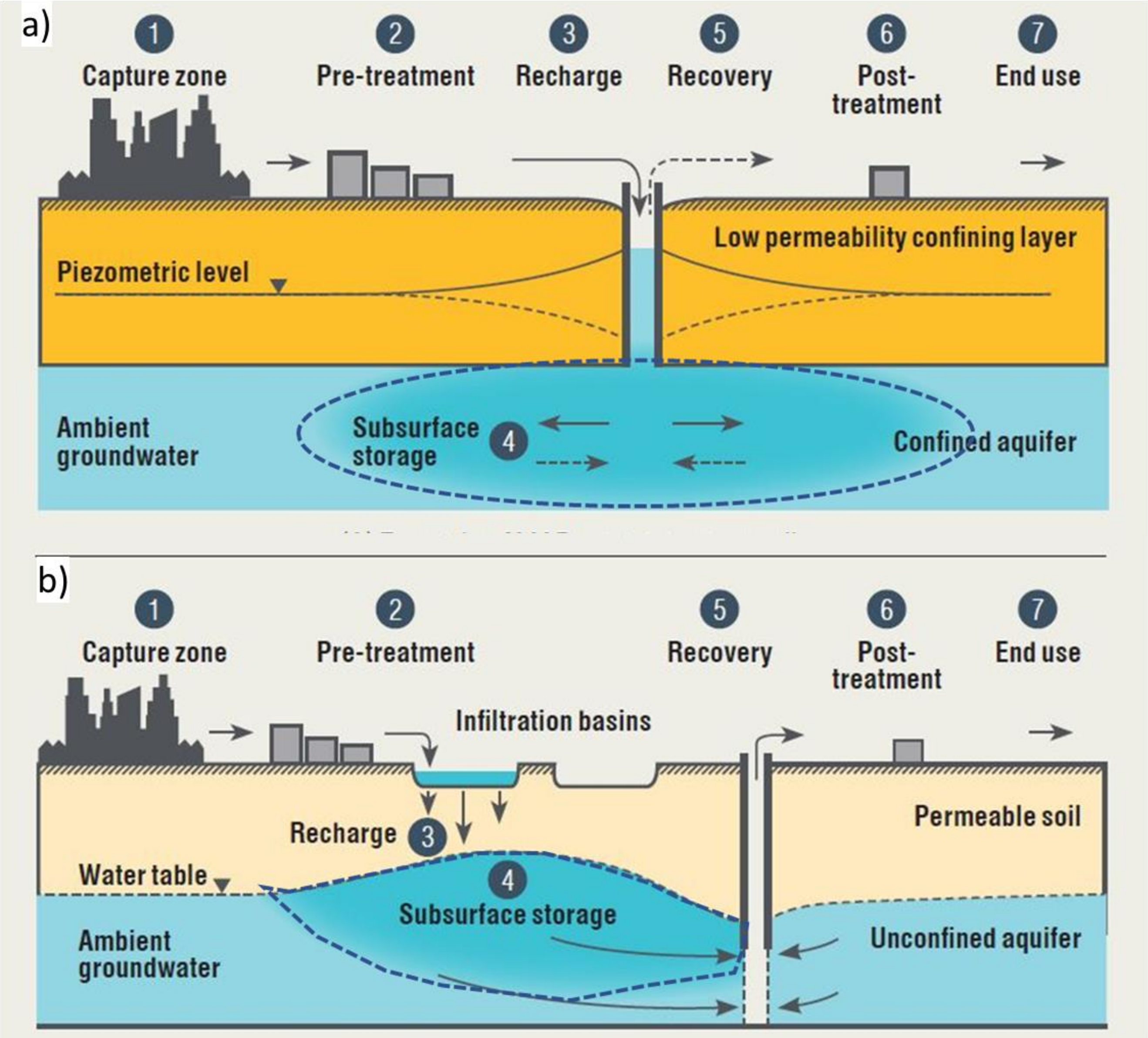

Figure 2-1 Two major types of ASR operations for water storage and recovery: (a)injection into a confined aquifer and (b) injection into an unconfined aquifer. The dotted blue lines represent the outer edge of the injected water (modified from Ward and Dillion, 2009).

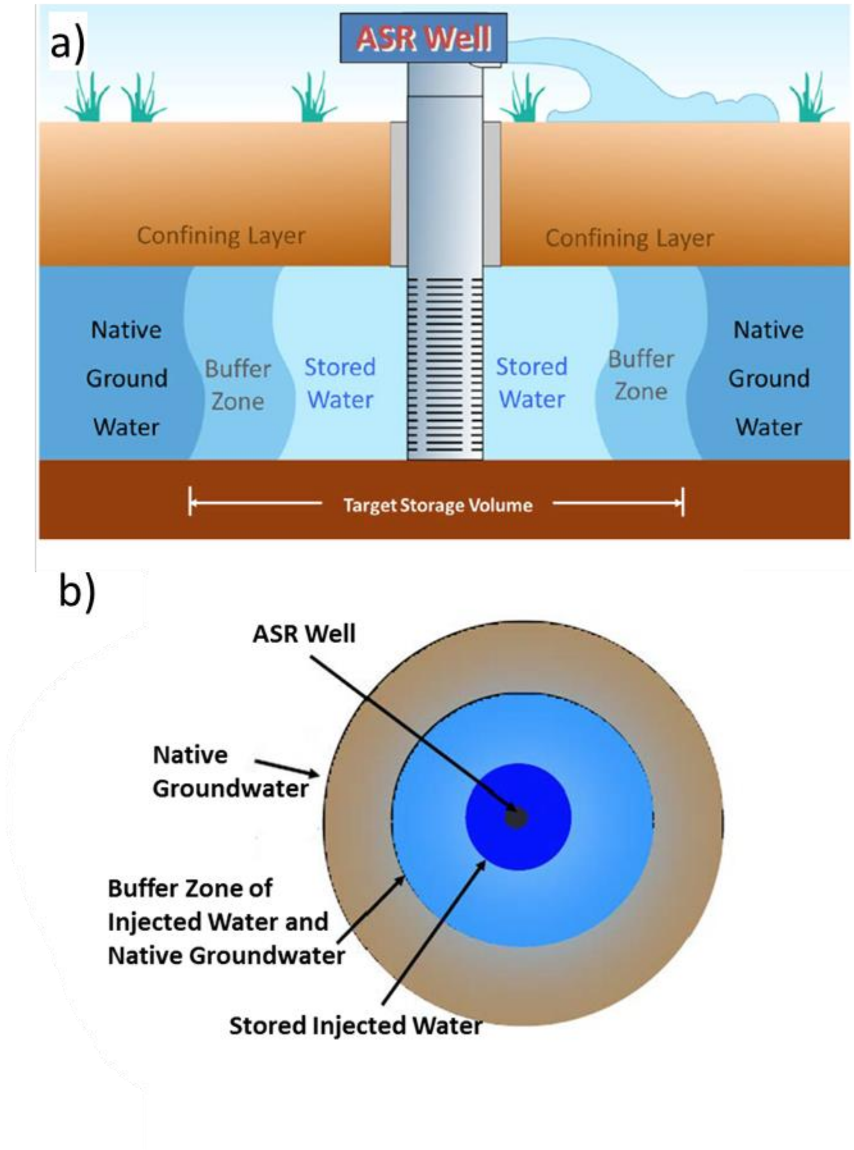

Figure 2-2 Schematic illustrating the concept of an ASR bubble created by injecting water into a confined aquifer. The bubble includes the region where the stored injected water has displaced the native groundwater and the buffer zone where the injected water has mixed with the native groundwater water. (a) Side view of the ASR bubble showing the confining layers above and below the ASR bubble and (b) top view of the ASR bubble showing the radial extent of water with different mixtures of injected water and native groundwater.

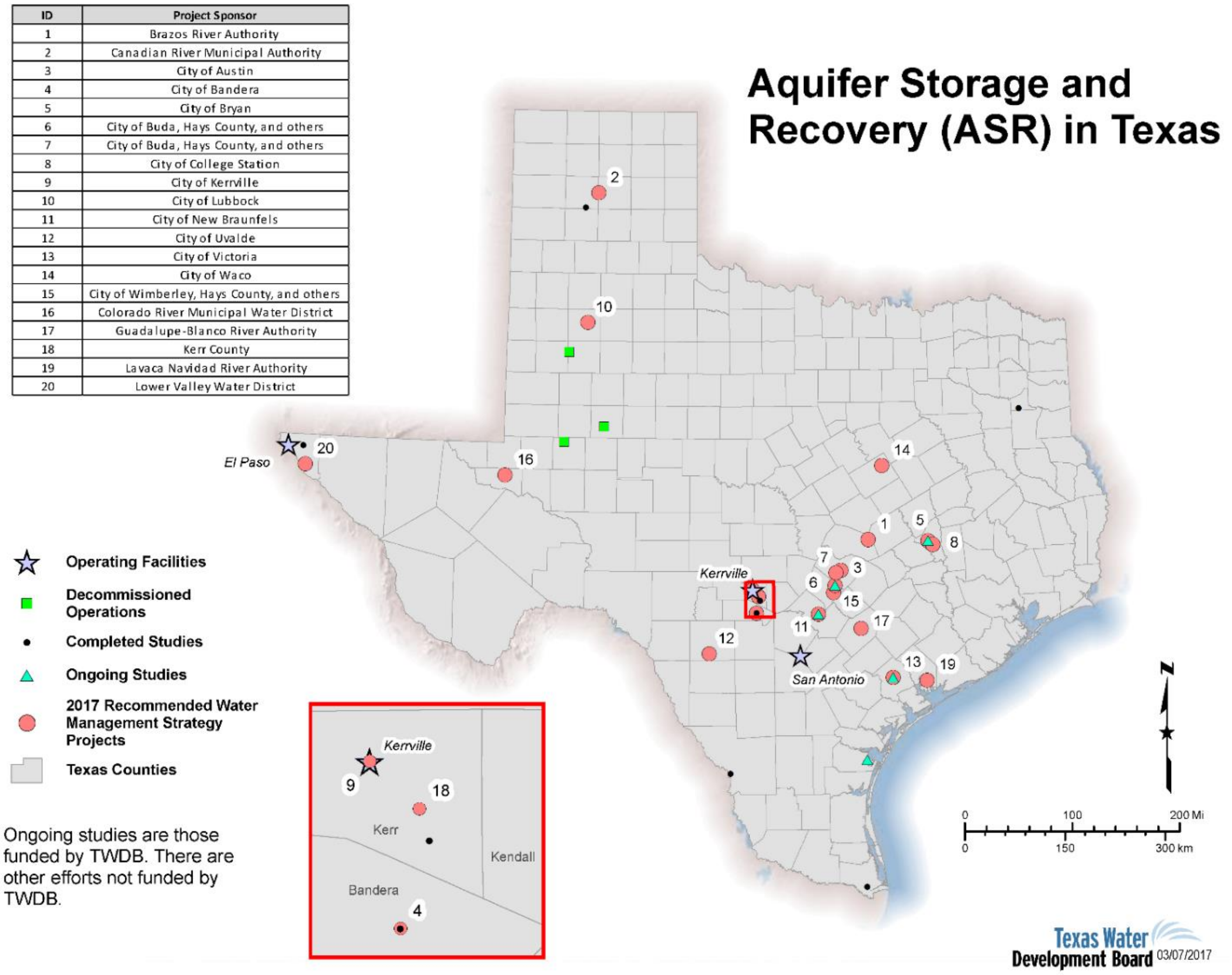

ID	Project Sponsor
1	Brazos River Authority
2	Canadian River Municipal Authority
3	City of Austin
4	City of Bandera
5	City of Bryan
6	City of Buda, Hays County, and others
7	City of Buda, Hays County, and others
8	City of College Station
9	City of Kerrville
10	City of Lubbock
11	City of New Braunfels
12	City of Uvalde
13	City of Victoria
14	City of Waco
15	City of Wimberley, Hays County, and others
16	Colorado River Municipal Water District
17	Guadalupe-Blanco River Authority
18	Kerr County
19	Lavaca Navidad River Authority
20	Lower Valley Water District

Figure 2-3 Map of ASR showing decommissioned and currently operating facilities, ongoing studies, and 2017 recommended water projects in Texas complied by the TWDB (2018).

This page intentionally left blank.

3.0 ASR SYSTEM PERFORMANCE AND RECOVERABILITY

This section explains the terms and concepts that are important to defining recoverability with respect to water injected by an ASR well. This section explains why the calculation of recoverability is required as part of the application process for operating an ASR project in Texas. This section also describes and demonstrates groundwater modeling approaches for estimating ASR recoverability.

3.1 The Concept of Recovery Efficiency and Recoverability

One measure of the performance of an ASR system is recovery efficiency. For this study, recovery efficiency is defined as a percentage of the recovered water that is the injected water. The TCEQ refers to recovery efficiency as recoverability, which is defined per **Equation 3-1**. Typically, recovery efficiency is measured on an individual operation cycle basis.

$$R = V_R/V_I * 100\% \qquad \text{Equation 3-1}$$

Where:

R = Recoverability
V_i = Volume of injected water
V_r = Volume of the injected water that is recovered

Figure 3-1 explains the meaning of recovery efficiency using images that represent water injected with an ASR well and water recovered by the same ASR well. The flow patterns shown in Figure 3-1 are for idealized aquifer conditions where the regional groundwater flow direction is uniform and constant over time. Figure 3-1a shows a series of concentric ovals that represent the migration over time of 120 ac-ft of water injected with the ASR well. Figure 3-1b shows a series of concentric ovals that represent 100 ac-ft of water captured by pumping the ASR well after injection of water had stopped. Figure 3-1c superimposes the footprints for the injected water and the recovered water. The footprints are divided into three areas: (1) the area once occupied by native groundwater that was recovered; (2) the area occupied by injected water that was not recovered; and (3) the area occupied by injected water that was recovered. The recovery of 30 ac-ft of the 120 ac-ft of injected water results in a recoverability of 25%.

The shapes that define the zone of injected water and the zone of captured water in Figures 3-1a and 3-1b are affected by the relative difference between the flow to and from the ASR well compared to the regional groundwater flow. In the absence of a regional groundwater flow, both the zone of injected water and the zone of captured water would be circular and centered on the ASR well. The greater the regional groundwater flow compared to the injected flow rate at the ASR well, the more elongated the zone of injected water will be. In the absence of a regional groundwater flow and where the injection and withdrawal rates are the same, recoverability of the injected water will be 100% because the zone of captured water will overlap 100% with the zone of injected water. As a general rule, an increase in the ambient regional groundwater flow will lead to a decrease in the recoverability of the injected water.

An aquifer characteristic that will affect recoverability rates is spatial variability in the aquifer hydraulic properties. One of the reasons that spatial variability exists in hydraulic properties is the vertical layering of deposits in an aquifer that have different permeabilities. In general, low permeable clayey deposits confine groundwater flows, whereas high permeable sandy deposits facilitate groundwater flow. **Figure 3-2** is a schematic showing injected water preferentially entering the higher transmissivity zones. The non-uniformity in groundwater flow is the result of the permeable deposits serving as high transmissivity zones and the low permeability deposits serving as confining strata. In situations where there are large contrasts in the permeability of the deposits intersected by an ASR well screen, a three-dimensional groundwater model may be warranted to simulate recoverability for different pumping scenarios.

3.2 TCEQ Application for Class V Underground Injection Control Wells for an ASR Project

The TCEQ application for a Class V UIC Well for an ASR project states that:

> "An ASR project should be designed and operated to isolate the injected water from native groundwater. By providing such isolation, the injected water can be stored underground for later retrieval and beneficial use without its quality being affected by the native groundwater, and without the quality of the injected water being affected by the native water. Vertical containment of the injected water is achieved by confining layers above and below the stored water, and horizontal containment is achieved by maintaining a buffer zone. The 'target storage volume' is that volume of water contained in the stored water zone and the buffer zone." (TCEQ, 2018)

With regard to the recovery of water from an ASR well, TCEQ (2018) makes several statements that indicate that recoverability calculated using Equation 3-1 needs to be based on the retrieval of the same water that was injected and not of a like volume of water. The TCEQ application for a Class V UIC Well for an ASR project states (TCEQ, 2018):

> "The purpose of ASR is the underground storage of water and the subsequent retrieval of that *same* water. ASR is not injection of a volume of water and the subsequent retrieval of a like volume of water with no regard as to the source of the recovered water."

Table 3-1 lists the eight sections that comprise the TCEQ application for Class V UIC Wells for an ASR Project. The application requires comprehensive documentation of the site hydrogeology and geochemistry in order to support the design of the ASR well field and operations. One of the key objectives of the hydrogeologic characterization is to support and guide the estimate of recoverability of injected water. Section VIII requires a detailed discussion of the methods and modeling used to estimate recoverability. The instructions for Section VIII is the following paragraph:

> "In order for the commission to make a determination as to whether injection of water into a geologic formation will result in a loss of injected water or native groundwater, as required under TWC, §27.154(b), please provide an analysis of the volume of injected water that will be recovered. This analysis should consider the geologic, hydrogeologic, and hydrochemistry of the injection zone, the quality of the injected water, and the operational conditions proposed for the project. The commission anticipates that this analysis will require groundwater modeling. Please provide a detailed discussion of how the applicant estimated the percentage of injected water that will be recovered. If this

estimated percentage of the injected water volume that is estimated is based on groundwater modeling, please describe the modeling performed, with justification for all assumptions and input parameter values." (TCEQ, 2018)

Table 3-1 The eight sections that comprise the TCEQ (2018) application for an ASR project

Application Section	
Number	**Description**
1	General Information
2	Information Required to Provide Notice
3	ASR Project Area
4	Area of Review
5	Well Construction and Closure Standards
6	Injection Well Operation
7	Project Geology, Hydrogeology, and Geochemistry
8	Demonstration of Recoverability

3.3 Modeling Approaches for Determining Recoverability

This subsection discusses modeling approaches for simulating groundwater flow associated with ASR operations to determine recoverability. The modeling approaches are divided into the general categories of analytical models and numerical models. Example applications of each model type are provided.

3.3.1 Introduction to Groundwater Modeling

Models are approximations that describe physical systems. Groundwater models describe the groundwater flow and transport processes using mathematical equations based on simplifying assumptions. The assumptions typically involve the direction of flow, geometry of the aquifer, the heterogeneity or anisotropy of sediments or bedrock within the aquifer, the contaminant transport mechanisms and chemical reactions. Because of the simplifying assumptions embedded in the mathematical equations and the many uncertainties in data required by a groundwater model, a groundwater model represents an approximation of the real physical aquifer system. Different sets of simplifying assumptions will result in different models, each approximating the groundwater system in a different way.

Although groundwater flow and transport in a porous medium occurs in three-dimensions, there are situations where a two-dimensional model can provide useful simulations for estimating recoverability. The flow conditions that justify using a two-dimension model include where groundwater flow is primarily horizontal and where the vertical variations in aquifer hydraulic properties are small. Formally, a two-dimensional horizontal flow model is obtained by averaging each of the three-dimensional variables over the aquifer's thickness such that the aquifer properties are assumed to be a function of only the horizontal coordinates.

To estimate the recoverability for an ASR project, both a conceptual model and a mathematical model for the groundwater flow system is needed. The conceptual model is the hydrologist's written description of a groundwater system's geohydrology including estimates of aquifer properties. The mathematical model is comprised of the equations and parameters used to represent the processes expressed in the conceptual model. Once the mathematical model is created, the resulting equations can be solved either analytically, if the model is simple, or numerically.

3.3.1.1 Analytical Models

Analytical models are based on exact mathematical solutions to simplified groundwater flow equations. The types of simplifications that are made include uniform aquifer thickness, infinite aquifer extent, uniform aquifer hydraulic properties, constant pumping, and uniform hydraulic gradients. Analytical solutions are relatively easy to apply and produce continuous and accurate results for simple problems. Application of analytical solutions is relatively quick, and the opportunity for their misuse is low. Unlike numerical solutions, analytical solutions give a continuous output at any point in the problem domain. Analytical solutions are most useful where approximate answers are sought or where there are insufficient site characterization data to justify using more sophisticated models. Because analytical solutions are based on simplifying assumptions, analytical solutions may not provide a sufficiently accurate representation of the real physical groundwater system where the aquifer is spatially heterogeneous and where there are significant temporal variability in the groundwater flow field. For complex groundwater flow systems that involve heterogeneous conditions or changes in regional flow directions, numerical models may be more appropriate than analytical models for predictive evaluation and decision assessment of ASR projects. Nonetheless, for complex groundwater flow systems, analytical models should be used to provide benchmark simulations to check the accuracy of the numerical groundwater flow model for calculating recoverability.

3.3.1.2 Numerical Models

Numerical methods were developed to handle the complexity of groundwater systems such as spatial variability in aquifer hydraulic properties or changes in the hydraulic gradient over time. Numerical models (e.g., finite difference, finite volume, or finite element) solve the partial differential groundwater flow or solute transport equations through numerical approximations using matrix algebra and discretization of the modeled domain. The model domain is represented by a network of grid cells or elements and the time of the simulation is presented by time steps. In some numerical models, the vertical discretization is determined by the number of model layers. Numerical models allow different properties and boundary conditions to be assigned to grid cells in order to reflect the spatial variability in the real physical system.

The most widely used numerical groundwater flow model is MODFLOW, which is a three-dimensional model, originally developed by the United States Geological Survey (USGS) (McDonald and Harbaugh, 1988). Since its initial development, the USGS MODFLOW model has developed into a series of codes that represent a continuum of enhanced capabilities. Throughout their development, the family of MODFLOW-based groundwater codes have maintained a modular structure wherein the MODFLOW code consists of a Main Program and a series of highly-independent subroutines called modules. The modules are grouped in packages. Each package deals with a specific feature of the hydrologic system that is to be simulated, such as flow from rivers or flow into drains, or with a specific mathematical technique for solving groundwater equations.

3.3.2 An Analytical Modeling Approach for Simulating ASR Recoverability

The analytical modeling approach to assess ASR recoverability presented here is based on work performed by The University of Texas at Austin (UT). UT has a contract with the TCEQ to provide information for a guidance document to help complete TCEQ's application for an ASR project. Among UT tasks are to (1) identify important data needs for an ASR project, (2) identify calculation and modeling approaches using these data to assess the feasibility of water injection, storage and recovery, and (3) identify tracer study approaches to confirm injected water recovery in pilot studies (Dr. Charles Werth, personal communication). As part of their TCEQ contract, UT has surveyed analytical solutions for evaluating ASR recoverability and has selected a solution by Bear and Jacobs (1965). The paper by Bear and Jacobs (1965) is published in the Journal of Hydrology and is titled "On the Movement of Water Bodies Injected into Aquifers."

Using the mathematical equations provided by Bear and Jacob (1965), UT developed an analytical model and used that model to help INTERA performed several simulations for this study. The analytical model is capable of determining the recoverability for a single ASR well into a confined aquifer where uniform regional groundwater flow occurs. The solutions assumes the following conditions:

- Two-dimensional flow
- Homogeneous aquifer hydraulic properties
- Uniform Aquifer thickness
- Infinite aquifer extent
- Uniform regional groundwater flow
- Constant injection rate and pumping rate for ASR well
- Groundwater moves through porous media as plug flow. No mixing occurs between flow lines.
- No density differences between the injected water and native groundwater

Bear and Jacobs (1965) developed their solution by solving a dimensionless form of the groundwater flow equation using superimposing of complex potentials. **Figure 3-3** shows a graphic representation of the output from the ASR analytical model. The figures shows the superimposing of the zone of injected water and the zone of capture. As in Figure 3-1, the overlap area of the two zones represents the amount of the injected water that is recovered.

UT developed the analytical model in Python, which is a object-oriented programming language. 2). The accuracy of the completed model was tested using the example problems provided by Bear and Jacobs (1965). The required inputs to the model are:

- Q_i= injection rates
- Q_p= pumping rates
- t_i= injection time
- t_p= pumping time
- t_d= delay time
- B= thickness of aquifer
- n= porosity of aquifer
- K= hydraulic conductivity of aquifer
- dh/dx = regional hydraulic gradient in aquifer
- q_o= (K * dh/dx) specific discharge (i.e., groundwater flow per unit thickness and unit width)

3.3.3 A Numerical Modeling Approach for Simulating ASR Recoverability

The numerical modeling approach for assessing ASR recoverability involves coupling a MODFLOW-based flow code with a particle-tracking code. Particle tracking is a well-established and accepted technique for simulating the advective transport of groundwater through porous media (Pollock, 1989, 1994, 2012; Zheng, 1990, 1992; Konikow and others, 1996). Particle tracking of groundwater flow assumes that no mixing occurs between flow paths and that groundwater moves as plug flow through the porous media. The assumption of plug flow, which was also assumed in developing the ASR analytical solution discussed in Section 3.3.2, was used to conceptualize formation of the ASR bubble discussed in Section 2.1. In reality, the spatial variation in the aquifer hydraulic properties will prevent plug flow from occurring so results from particle tracking will over estimate recoverability compared to a similar modeling approach that allows mixing to occur between flow paths.

Several particle tracking codes have been developed for use with MODFLOW-based models (Pollock, 1989, 1994, 2012; Zheng, 1990, 1992). Many of these particle tracking codes represent an enhanced version of the original particle tracking code developed by the USGS called MODPATH (Pollock, 1989) The code mod-PATH3DU (Muffles and others, 2018) was used to track advective groundwater flow for this study. Among the reasons for selecting mod-PATH3DU are the following:

- Compatible with all grid cell geometries that can be constructed using structured and unstructured grids supported by the MODFLOW-based family of groundwater codes including nested, quadpath, quadtree, Voronoi, and triangular grids
- Compatible with all MODFLOW-based groundwater codes including MODFLOW 96 (Harbaugh and McDonald, 1996); MODFLOW 2000 (Harbaugh and others, 2000), MODFLOW 2005 (Harbaugh, 2005), MODFLOW-NWT (Niswonger and others, 2011) and MODFLOW-USG (Panday and others, 2013) and MODFLOW-6 (Langevin and others, 2017; Hughes and others, 2017)
- Uses the state-of-the-art method (Ramadham, 2015) for interpolating intra-cell velocities to represent flow to a well using an exact solution to simulate capture by a pumping well
- Uses an adaptive time-stepping scheme that can account for curvature in the flow field in order to improve the tracking of particles through grid cells near sources and sinks

Based on INTERA’s experience with modeling groundwater flow, the two most useful MODFLOW codes for modeling ASR projects are MODFLOW-NWT (Niswonger and others, 2011) and MODFLOW-USG (Panday and others, 2013). The primary difference between these two codes is that MODFLOW-USG offers the advantage of supporting local grid refinement around an ASR well. However, MODFLOW-USG is considerably more complicated to set up and run than MODFLOW-NWT (Niswonger and others, 2011).

The coupling between a MODFLOW model and mod-PATH3DU occurs through the groundwater flow vectors simulated for each grid cell. The groundwater flow vectors are generated as output from the MODFLOW model based on the flow mass balance it generates for each grid cell. Mod-PATH3DU reads the flow vectors as input and uses them to track particles through the model domain one grid cell at a time. **Figure 3-4** illustrates the groundwater flow vectors that MODFLOW-NWT generates for each of the six sides of a grid cell. PATH3DU inputs the geometries and the flow vectors for each grid cell and calculates groundwater velocity vectors by dividing the groundwater flow vectors by the cross-sectional area of the grid face through which groundwater is flowing. Mod-PATH3DU tracks the particle migration though the grid in three-dimensions using a procedure that has been simplified to two dimensions in

Figure 3-5. To track a particle through an intra-cell velocity field, mod-PATH3DU uses an algorithm to determine an adequate number of time steps to properly account for the groundwater velocity changes in three-dimensions within the volume of the grid cell.

The numerical modeling approach can be divided into the components of simulating hydraulic heads, calculating groundwater velocities, and tracking particles using the groundwater velocities. **Figures 3-6**, **3-7**, and **3-8** have been generated to visualize these three components in two dimensions.

Figure 3-6 shows contours of hydraulic heads. Figure 3-6a shows hydraulic head contours associated with uniform regional groundwater flow prior to operating the ASR well. Figure 3-6b shows hydraulic head contours associated with outward flow from the ASR well during injection where the highest hydraulic head exists in the ASR well. Figure 3-6c shows hydraulic head contours associated with inward radial flow to the ASR well during pumping, where the lowest hydraulic head exists in the ASR well.

Figure 3-7 shows groundwater flow velocity vectors. Figure 3-7a shows velocity vectors associated with uniform regional groundwater flow prior to operating the ASR well. Figure 3-7b shows velocity vectors associated with outward radial flow from the ASR well during injection where the highest hydraulic head exists in the ASR well. Figure 3-7c shows velocity vectors associated with inward radial flow to the ASR well during pumping where the lowest hydraulic head exists in the ASR well.

Figure 3-8 shows groundwater flow velocity vectors and the tracking of particles over time. Figure 3-8a shows velocity vectors and particle migration associated with uniform regional groundwater flow prior to operating the ASR well. Figure 3-8b shows velocity vectors and particle migration associated with outward radial flow from the ASR well during injection where the highest hydraulic head exists in the ASR well. Figure 3-8c shows velocity vectors and particle migration associated with inward radial flow to the ASR well during pumping where the lowest hydraulic head exists in the ASR well.

3.4 Simulation of ASR Recoverability

Numerous factors should be considered in development of a modeling approach for estimating ASR recoverability. Among these factors are the availability of field data, pre-existing groundwater models, the complexity of the site hydrogeology, the proximity of nearby wells, and the proposed ASR operations schedule. In this section, hypothetical ASR scenarios are simulated using analytical and numerical models in order to demonstrate the potential benefits and limitations of each type of modeling approach.

3.4.1 Recoverability Simulated Using Numerical and Analytical Models

Of paramount importance to any approach for simulating recoverability is that the groundwater modeling be reproducible and accurate. This concern is particularly relevant to the application of numerical models because their accuracy is affected by the size of the grid cells and time steps used to represent the physical aquifer system. Where numerical models are used to simulate ASR recoverability, the modeling approach should include validating the numerical model using an analytical model. For this study, we used the Bear and Jacob analytical model developed by UT to validate our numerical modeling approach using MODFLOW and Mod-PATH3DU to simulate flow of injected water.

Our verification of the numerical modeling approach involves checking the simulated recoverabilities for a base case ASR scenario against those produced by the Bear-Jacob analytical model. The base case ASR scenario created for the purpose of model validation is described by the parameters in **Table 3-2**. The parameters in Table 3-2 are organized based on the inputs required to use the Bear and Jacob analytical model. The aquifer has uniform properties that include a thickness of 100 feet (ft), a hydraulic conductivity of 20 ft/day, a porosity of 30%, and a regional hydraulic gradient of 0.001 ft/ft. The ASR operation involves injecting at a constant rate of 20,000 cubic feet per day (ft^3/day) (104 gallons per minute [gpm]) for 330 days and then pumping the aquifer at a constant rate of 220,000 ft^3/day (1,142 gpm) for 30 days. During its 360 days of operation, the ASR well injects a total of 6,600,000 ft^3 (152 ac-ft) of water and then withdrawals a total of 6,600,000 ft^3 (152 ac-ft) of water.

Table 3-2 Parameters that describe an ASR scenario used for benchmarking and validating the recoverability simulated by the analytical and numerical approaches

Parameter		Value	Units
Q_i	Injection rate	20,000	ft^3/day
Q_p	Pumping rate	220,000	ft^3/day
t_i	Injection time	330	days
t_d	Delay time	0	days
t_p	Pumping time	30	days
n	Porosity in aquifer	0.3	-
K	Hydraulic conductivity	20	ft/day
dh/dx	Regional hydraulic gradient	0.001	ft/ft
B	Thickness of aquifer	100	ft
V_i	Injection Volume	6.60E+06	ft^3
Vp	Pumping Volume	6.60E+06	ft^3

For the ASR scenario described in Table 3-2, the analytical and numerical models generated ASR recoverabilities of 96.2 and 96.0%, respectively. The similar recoverabilities produced by the two models serve to help validate the accuracy of both models.

Figures 3-9, **3-10**, and **3-11** were created to help explain several aspects associated with the numerical modeling approach used to predict a recoverability of 96.0%.

Figure 3-9 provides information on the hydraulic boundary conditions for the numerical model. Figure 3-9 consists of three parts, which are described below:

- Figure 3-9a shows the domain for the numerical model. The domain is a square with sides that are 29.5 miles long. Uniform regional groundwater flow in the longitudinal direction is established by assigning no-flow boundaries on the eastern and western side boundaries and constant head boundaries on the north and south side boundaries. At the location of the ASR well in the middle of the grid (grayed area), the grid cells are 20 by 20 ft squares. Outside of the grayed area, the grid cell sizes gradually increase in size until they extend to a maximum side length of 1,440 ft (0.25 mile). The small grid cell sizes near the middle of the model provide the capability to accurately represent large changes in hydraulic heads near the well. The large distances between the well and the model boundaries allows the model to accurately represent flow in an infinitely-wide aquifer, which is an assumption in the Bear and Jacob (1965) analytical solution.

- Figure 3-9b shows that the base case scenario has a regional hydraulic gradient of 0.001, which indicates that the hydraulic head changes 1 foot for every 1,000 ft of distance (or about 5.28 ft for every mile). Figure 3-9b also shows the hydraulic head contours generated by the numerical model for a regional hydraulic gradient of 0.001. In the model, regional groundwater flow only occurs in the longitudinal direction, that is, no flow occurs in the lateral direction (Figure 3.9b).
- Figure 3-9c shows the injection and pumping schedule and the water balance as a function of time for the ASR system described in Table 3-2. During injection, the amount of water that is added into the aquifer increases linearly from 0 at time 0 to 6.0E+06 ft^3 (about 152 ac-ft) at day 330. After the 30-day extraction period, the total volume of water removed equals the total volume of water injected into the aquifer.
-

Figure 3-10 shows hydraulic heads generated by the numerical model that show changes in the hydraulic head contours caused by the ASR well operation. Figure 3-10 consists of four parts, which are described below:

- Figure 3-10a shows contours of hydraulic head after injecting water for 330 days at a constant rate of 20,000 ft^3/day (104 gpm). The arrows show that the direction of groundwater flow is radially outward from the ASR well. The spacing of the contours indicates groundwater velocities decrease away from the well. Near the well, the greatest groundwater velocities are due south.
- Figure 3-10b shows contours of hydraulic head change between the start and end of the 330-day injection period. The maximum change is an increase of 15 ft, which occurs at the grid cell containing the ASR well. At a radial distance of about 450 ft, the increase in the hydraulic head is about 7 ft.
- Figure 3-10c shows contours of hydraulic head after extracting water for 30 days at a constant rate of 220,000 ft^3/day (1,142 gpm). The arrows show that the direction of groundwater flow is radially inward toward the ASR well. The spacing of the contours indicates groundwater velocities are significantly higher near the well.
- Figure 3-10d shows contours of hydraulic head change between pre-ASR conditions and at the end of the 30-day extraction period. The maximum change is a decrease of 152 ft, which occurs at the grid cell containing the ASR well. At a radial distance of about 450 ft, the decrease in the hydraulic head is about 52 ft.

Figure 3-11 provides results from the particle tracking generated by the numerical model. During the ASR injection period, 16 particles were released into the aquifer once every day to represent the injected water. The 16 particles were equally spaced along a circle that is centered at the ASR well location. The locations of the particles were updated daily unless they were captured and removed by the ASR well when it was pumping. Figure 3-11 consists of two parts, which are described below:

- Figure 3-11a shows the location of the injected particles after the ASR well has been injecting water for 330 days. Each of the 5,280 particle locations are color coded based on their elapsed time of travel. The figure is annotated to show the maximum distances that the injected water migrated away from the ASR well in the down dip direction, up dip direction, and lateral direction, which are 282, 252, and 264 ft, respectively.
- Figure 3-11b shows the location of the injected particles after the ASR well has completed 30 days of extraction. The figure shows that 211 of the 5,280 injected particles remain at the end of extraction. Each particle is color coded to represent the elapsed time of travel. Each particle represents approximately 1,250 ft^3 of water. So the remaining 211 particles represent approximately 6 ac-ft of water, which is approximately 4% of the injected water.

3.4.2 Sensitivity of Simulated Recoverability to Aquifer Properties and ASR Operation Parameters

An important aspect of any groundwater modeling is identifying sources of uncertainty in the field data, the site conceptual model, or the numerical model. Among the important questions to ask regarding these sources of uncertainty is their potential impact on the simulated recoverability. A common approach used to quantity the impact of uncertainty in the model parameters is to perform a sensitivity analysis.

A sensitivity analysis provides a means to quantify the impact of varying specific model inputs on model predictions. A sensitivity analysis was performed on the base case ASR scenario described in Table 3-2. The input variables that were modified include aquifer properties and ASR operation parameters. Changes were recorded in predictions of ASR recoverability, hydraulic head, and the size of the plume created by the injected water. The sensitivity analysis consisted of changing the value for one input parameter at a time from its “base case” value. This type of sensitivity analysis is called an “one-off” sensitivity analysis.

Tables 3-3 presents the sensitivity of predicted ASR recoverability to four aquifer parameters (hydraulic gradient, thickness, hydraulic conductivity, and porosity) and two ASR operation parameters (injected volume and storage period). For each of the six parameters, two “one-off” sensitivity runs were conducted to evaluate the impact of changes in these parameters on the predicted recoverability. A total of twelve sensitivity runs were conducted. The predicted recoveries varied between 63 and 99%. Very similar ASR recoverabilities were predicted by the numerical and the analytical models. Over 90% of the simulations have less than a 1% difference in the recovery predicted by the two types of models.

Table 3-4 presents the sensitivity of simulated hydraulic head and the size of the plume of injected water to changes in the aquifer and ASR operation parameters. The metric used to quantify the sensitivity of hydraulic head was the maximum change in hydraulic head at the ASR well location at the end of the injection period and at the end of the extraction period. For both time periods, the change in hydraulic head was measured relative to the water level at the ASR well location for non-pumping conditions. The maximum change in the hydraulic head at the end of the injection period ranged between 4 and 46 ft. The maximum change in the hydraulic head at the end of the extraction period ranged between -37 and -469 ft. The metric used to quantify the sensitivity of the injected water migration distance was the maximum distance of the particles from the location of the ASR well in the up dip, down dip, and lateral directions. The maximum distances ranged from 133 to 445 ft in the up dip direction, 163 to 505 ft in the down dip direction, and 144 to 458 ft in the lateral direction.

Table 3-5 summarizes key results from the sensitivity analysis embedded in Tables 3-3 and 3-4. These results show that sensitivity analysis can be a useful tool for helping to understand and quantify the impact of uncertainty in model input parameters on predicted outputs. The results show that all six of the model parameters have the potential to affect recoverability, the migration extent of the injected water, and the change in groundwater head. As a result, all six model parameters should be included in sensitivity analyses for evaluating ASR recoverability.

One of the more important aquifer parameters that affect the performance of ASR operations is the regional hydraulic gradient. In general, an increase in the regional hydraulic gradient will decrease the simulated recoverability for an ASR well. This relationship is shown by the modeling results in **Figure 3-12** for the modeling scenarios based on regional hydraulic gradients of 0.01, 0.001, and 0.0001. For the case of a low regional hydraulic gradient of 0.0001, over 99% of the injected water is withdrawn during 30 days of pumping. The high recovery rate occurs because the regional groundwater flow is very small compared to the radial flow caused by operating the ASR well. The strong radial flow component near the well is evident in Figure 3-12a, where the injected particles are aligned on 16 straight lines extending outward from the ASR well. Figure 3-12c shows that a hydraulic gradient of 0.01 has a notable impact on the migration of particles outward from the ASR well. Figure 3-12c shows a large amount of deviation from radial flow lines because of a strong southward longitudinal flow component contributed by the regional groundwater flow. For the case of a much higher regional hydraulic gradient of 0.01, only about 64% of the injected water is withdrawn during 30 days of pumping.

Table 3-3 The sensitivity of simulated recoverability to changes in aquifer and ASR operations parameters

Value for Sensitivity Parameter	Recoverability	
	Numerical Model	Analytical Model
Hydraulic Gradient		
0.01	63.6%	63.6%
0.001	**96.0%**	**96.2%**
0.0001	99.5%	99.6%
Thickness		
50 feet	97.0%	97.3%
100 feet	**96.0%**	**96.2%**
200 feet	94.3%	94.6%
Hydraulic Conductivity		
6.8 ft/day	98.5%	98.8
20 ft/day	**96.0%**	**96.2%**
60 ft/day	82.4%	82.9%
Porosity		
30%	**96.0%**	**96.2%**
20%	95.1%	95.3%
15%	93.0%	93.3%

Injected Volume		
2.2E+06 ft³	92.8%	93.0%
6.6E+06 ft³	**96.0%**	**96.2%**
1.2E+07 ft³	97.5%	97.8%
Storage Period		
No Delay	**96.0%**	**96.2%**
100 days	94.4%	94.6%
200 days	92.7%	92.9%

Bold text indicates base case simulation

Table 3-4 The sensitivity of simulated hydraulic head change and injected water migration distance to changes in aquifer and ASR operations parameters

Value for Sensitivity Parameter	Hydraulic Head Change (ft)		Maximum Distance (ft) Injected Water Migrated		
	At End of Injection Period	At End of Extraction Period	Up Dip (north)	Down Dip (south)	Lateral (east or west)
Hydraulic Gradient					
0.01	15	-152	143	432	241
0.001	**15**	**-152**	**252**	**282**	**265**
0.0001	15	-152	265	268	267
Thickness					
50 ft	29	-305	361	391	375
100 ft	**15**	**-152**	**252**	**282**	**265**
200 ft	7	-76	175	204	187
Hydraulic Conductivity					
6.8 ft/day	46	-469	262	271	266
20 ft/day	**15**	**-152**	**252**	**282**	**265**
60 ft/day	3.5	-37	204	337	259
Porosity					
30%	15	-152	252	282	265
20%	**15**	**-152**	**304**	**348**	**323**
15%	15	-152	416	505	453
Injected Volume					
2.2E+06 ft³	3.5	-37	133	163	144
6.6E+06 ft³	**15**	**-152**	**252**	**282**	**265**
1.2E+07 ft³	44	-457	445	475	458
Storage Interval					
No Delay	**15**	**-152**	**252**	**282**	**265**
100 days	15	-153	252	288	265

200 days	15	-154	252	295	265

Bold text indicates base case simulation

Table 3-5 Key observations based on the results of the sensitivity analysis

Hydraulic Gradient (Base case is 0.001. Sensitivity runs range from 0.01 to 0.0001)	
1	Recoverability decreases with increases in hydraulic gradient
2	Changes in hydraulic gradient do not notable affect the maximum change in hydraulic head
3	Decrease from 0.001 to 0.0001 causes minimal changes in recoverability and the maximum distance of injected water migration
4	Increase from 0.001 to 0.01 causes significant changes in recoverability and the maximum distance of injected water migration
Aquifer Thickness (Base case is 100 ft. Sensitivity runs range from 50 to 200 feet)	
1	Recoverability decreases with increases in aquifer thickness
2	The magnitude of change in the maximum hydraulic head change is linearly correlated with the magnitude of change in the aquifer thickness
3	Doubling or halved the aquifer thickness changes the recoverability percentage by less than 2%
4	Decreasing the aquifer thickness increases the maximum distance of injected water migration and vice versa
Aquifer Hydraulic Conductivity (Base case is 20 ft. Sensitivity runs range from 6.8 to 60 ft)	
1	Recoverability decreases with increasing aquifer hydraulic conductivity
2	Changes in hydraulic conductivity caused a linear and proportional change in the maximum change in hydraulic head
3	Simulated recoverability changes in a non-linear fashion with changes in aquifer hydraulic conductivity and changes are negatively correlated meaning an increase in hydraulic conductivity decrease recoverability and a decrease in hydraulic conductivity increases recoverability
Aquifer Porosity (Base case is 30%. Sensitivity runs range from 15 to 20%.)	
1	Recoverability increases with an increase in porosity
2	The maximum change in hydraulic head is insensitive to porosity
3	Decreasing porosity increases the maximum distance of injected water migration
4	Doubling porosity from 15 to 30% changed recoverability by only 3%
Injected Volume (Base case is 6.6E+06 ft^3. Sensitivity runs range from 2.2E+6 to 1.2 E+07 ft^3)	
1	Recoverability increased with an increase in injected volume
2	Changes in injected volume cause a linear and proportional change in the maximum change in hydraulic head
3	A nine-fold increase in the injected volume increased the recoverability by approximately 5%.
4	Changes in the injected volume caused a linear and proportional change in the maximum distance of injected water migration
Storage Interval (Base case is no delay (0 days). Sensitivity runs range from 100 to 200 days.)	
1	Recoverability decreases with increases in the length of the storage interval
2	The maximum change in hydraulic head is insensitive to the storage interval
3	An increase in the storage interval from 0 to 200 days decreased the recoverability by 3%
4	Increases in the length of the storage interval increases the maximum distance that the injected water migrates

3.4.3 Sensitivity of Simulated Recoverability to Pumping from Nearby Wells

An important hydrological factor affecting ASR operations is the impact of pumping from nearby wells on the groundwater flow patterns that affect recoverability. To investigate the potential effects of pumping at nearby wells on ASR recoverability a sensitivity analysis was performed for two ASR operational scenarios that involve a single ASR well and a single well that is hydraulically downgradient of the ASR well. The two scenarios are:

ASR Scenario #1 – The ASR well injects water at 100 gpm for 11 months and then extracts groundwater at 1,100 gpm for 1 month. The recoverability is calculated after 24 months of operation.

ASR Scenario #2 – The ASR well injects water at 100 gpm for 9.5 years and then extracts groundwater at 1,900 gpm for 0.5 years. The recoverability is calculated after 10 years of operation.

The ASR scenarios are simulated for an aquifer that is 100 ft thick, has a uniform hydraulic conductivity of 20 ft/day, and has uniform porosity of 30%. These aquifer properties are the same as those in Table 3-2 for the aforementioned base case ASR scenario discussed in Section 3.4.2.

For both scenarios, the sensitivity analysis focused on changing the following three factors: (1) the pumping rate at the nearby well, (2) the distance between the ASR well and the nearby well, and (3) the regional hydraulic gradient. The sensitivity analysis included the cases where only the ASR well was operating and three cases where a pumping well was operating near the ASR well. For both ASR scenarios, ASR recoverability was determined for regional hydraulic gradients of 0.01, 0.001, and 0.0001.

Figure 3-13 shows the sensitivity analysis results for ASR Scenario #1. The three distances used for spacing the nearby well away from the ASR well were 1,100, 2,200, and 4,400 ft and the three pumping rates for the nearby well were 100, 550, and 1,100 gpm. Among the key observations are the following:

- Pumping from a nearby well that is spaced as far as 4,440 ft away from the ASR well can have a notable effect on reducing the simulated recoverability.
- Nearby wells pumping as little as 100 gpm should be considered when estimating aquifer recoverability.
- At a distance of 1,110 ft away from the ASR well, a nearby well pumping at a rate of 1,100 gpm reduces the ASR recoverability percentage by not less than 50% from the base line of no nearby pumping well.
- The commonly used well spacing criteria of 1 ft per 1 gpm pumped appears to be insufficient to prevent pumping at a nearby from adversely impacting the ability of an ASR well to recover its injected water.

Figure 3-14 shows the sensitivity analysis results for ASR Scenario #2. The three distances used for spacing the nearby well away from the ASR well are 1,900, 3,800, and 7,600 ft and the three pumping rates for the nearby well were 100, 1,000, and 1,900 gpm. Among the key observations are the following:

- Pumping from a nearby well that is spaced as far as 7,600 ft away from the ASR well can have a notable effect on reducing the simulated recoverability.
- At a distance of 1,900 ft away from the ASR well, a nearby well pumping at a rate of 1,000 gpm reduces the ASR recoverability percentage by not less than 55% from the base line of no nearby pumping well.

- The commonly used well spacing criteria of 1 ft per 1 gpm pumped appears to be insufficient to prevent pumping at a nearby well from adversely impacting the ability of an ASR well to recover its injected water.

3.4.4 Sensitivity of Simulated Recoverability to Numerical Model Grid Cell Size

An inherent concern with developing a numerical model is selecting how a model domain will be represented using grid cells. From a mathematical viewpoint, the greater the number of grid cells and the smaller the size the of grid cells, the more accurate the numerical solution will be. However, there is a point where further increases in the number of grid cells does not lead to a noticeable or needed improvement in the accuracy of the model prediction. To investigate the sensitivity of simulated recoverability, recoverability was simulated using numerical models with different size grid cells in the vicinity of the ASR wells. Table 3-6 shows a compares the simulated recoverability for the grid cells sizes of 20 ft, 100 ft, and 500 ft. The tabulated data shows that for each of the three regional hydraulic gradients, the recoverability for all three grid cell sizes were within 1%. These results indicate that grid cell sizes of 100 feet and greater can be used in some numerical simulations of ASR operations without an undesirable amounts of numerical error embedded in the simulated recoverability values.

Table 3-6 Results of sensitivity analysis between recoverability and model grid block size

Regional Hydraulic Gradient	Recoverability			
	Numerical Model			Analytical Model
	Grid Cell Size Near ASR Well			
	20 ft	100 ft	500ft	
0.01	63.6%	62.9%	64.0%	63.6%
0.001	**96.0%**	**96.3%**	**95.9%**	**96.2%**
0.0001	99.5%	99.5%	99.4%	99.6%

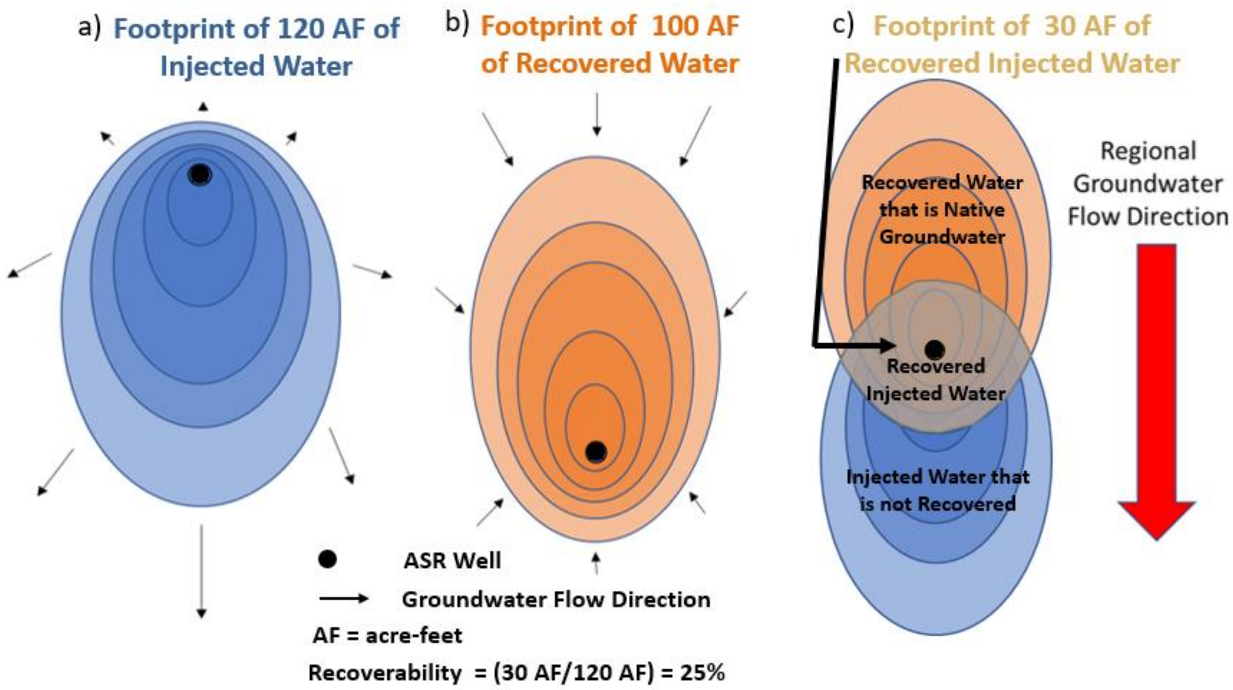

Figure 3-1 Schematic of recovered injected water by overlapping (a) a series of concentric ovals that represent the migration of 120 ac-ft of water injected with an ASR well over time, (b) a series of concentric ovals that represent 100 ac-ft of water captured by pumping the ASR well after the ASR stopped injecting water, and (c) superimposing the injected water (represented by the blue ovals) and the pumped water (represented by the orange ovals) to mark the 30 ac-ft of injected water recovered during pumping (represented by area where the blue and orange areas overlap).

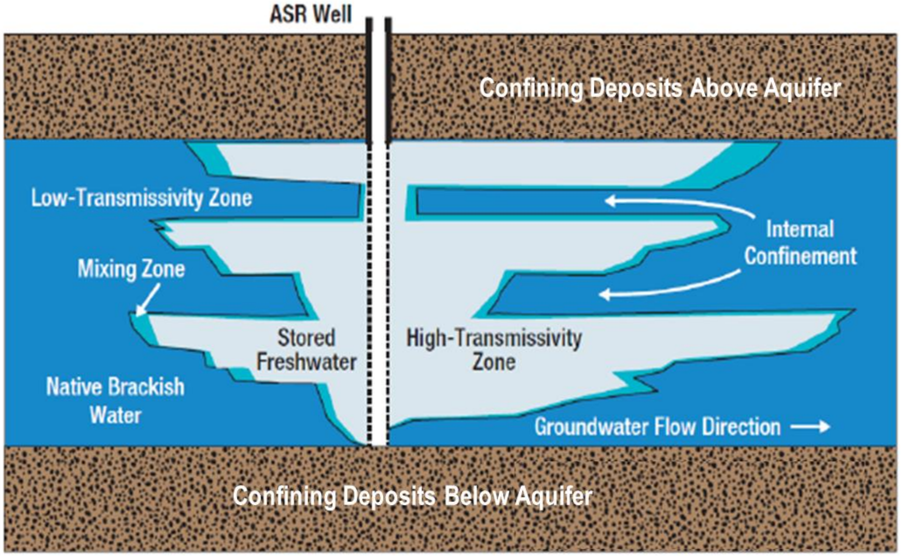

Figure 3-2 Schematic diagram of an ASR storage zone. Aquifer variability results in differential penetration of injected water to strata. High-transmissivity flow zones are confined by lower transmissivity strata within the storage zone (internal confinement). The aquifer heterogeneity promotes greater mixing and three-dimensional flow near the ASR well. (modified from Maliva and others, 2006).

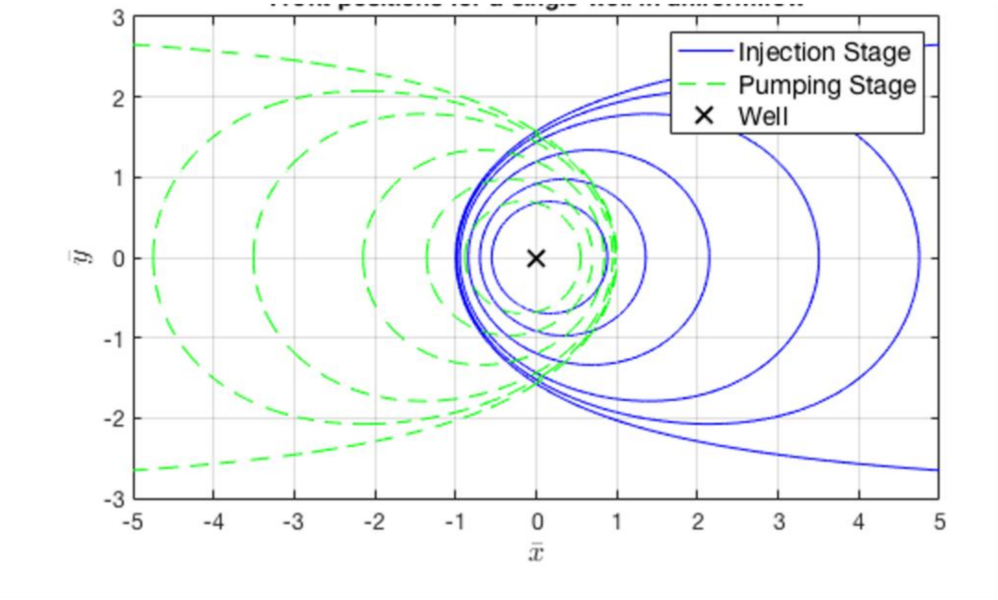

Figure 3-3 Schematic diagram showing the perimeter of the area covered by water injected and the perimeter of the source area of the groundwater pumped by the water extracted by an ASR well for different times.

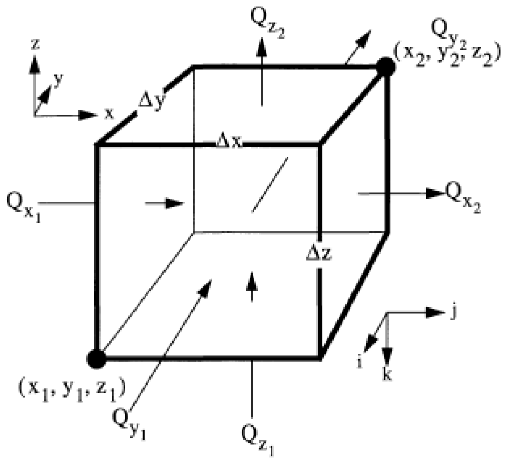

Figure 3-4 Schematic showing a grid cell from a three-dimensional, finite-difference numerical model based on coordinate axes x, y, and z. The schematic shows the flow vectors, labeled using the letter “Q”, associated with each of the six faces of the grid cell. The symbols “Δx”, “Δy”, and “Δz” represent the thickness of the grid cell in along the x, y, and z axis.(from Pollock, 1994)

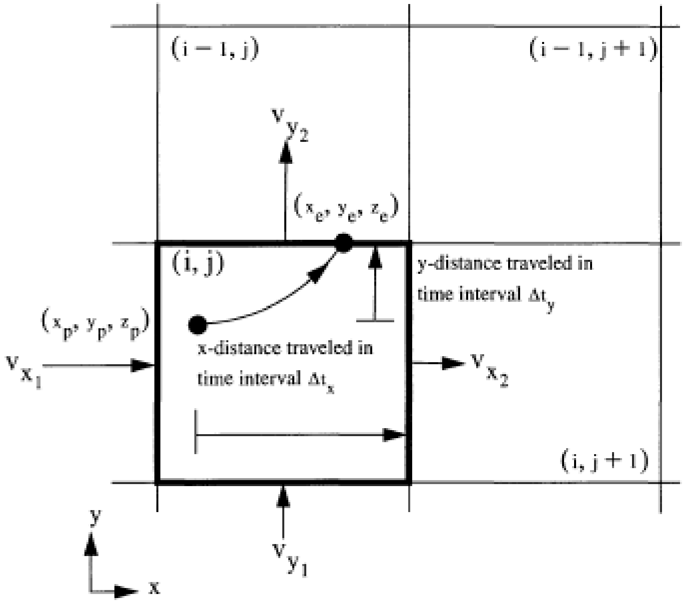

Figure 3-5 Schematic showing the computation of exit point and travel time for the case of two-dimensional flow in the x-y plane (from Pollock, 1994). For the grid block that is outlined in bold, the groundwater velocities in the x direction and y direction are represented by V_x and V_y, respectively. Movement of the particle along a streamline over time interval Δt_x is represented by the arrow that connects the starting location at point (x_p, y_p, z_p) to the ending location at point (x_e, y_e, z_e)

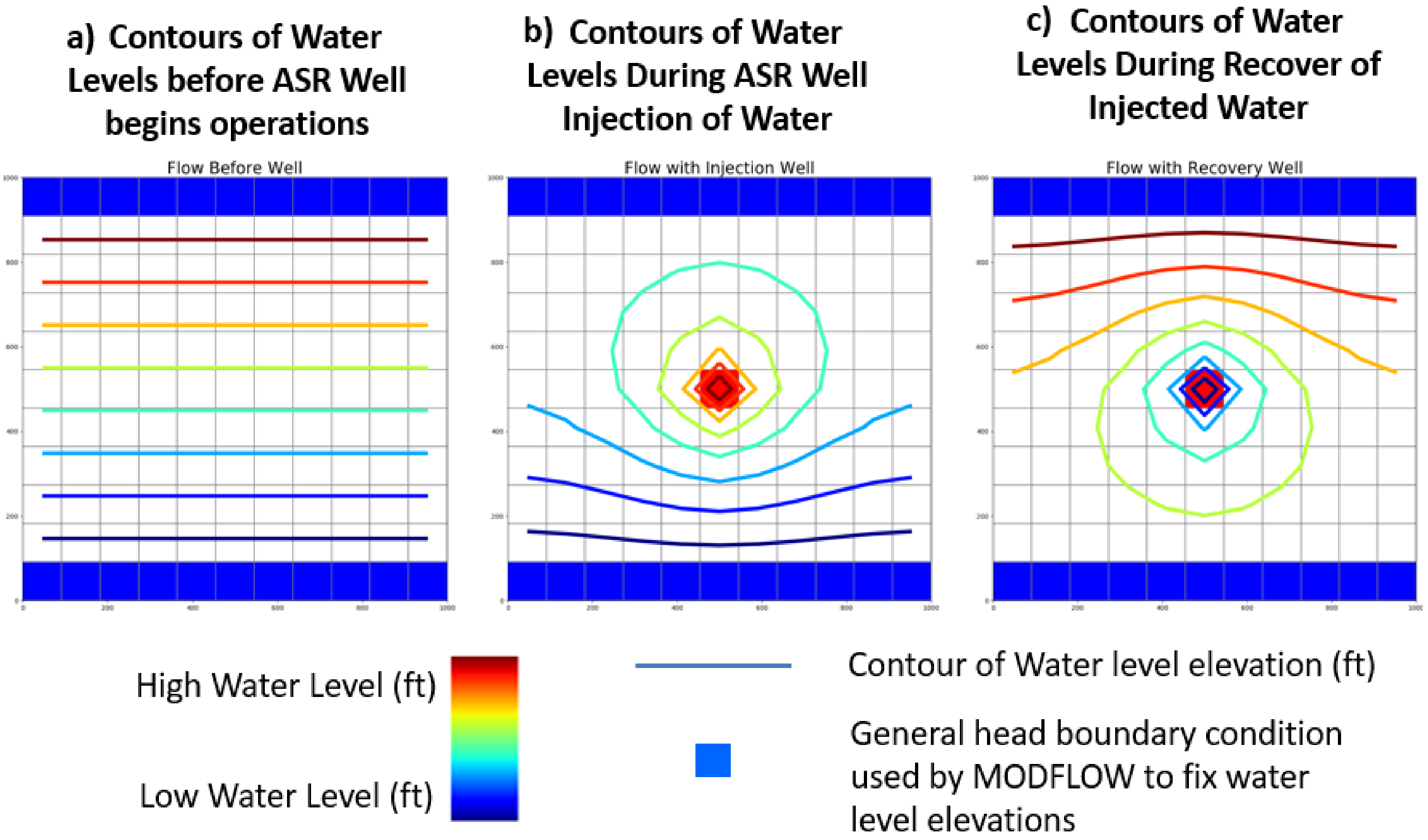

a) Contours of Water Levels before ASR Well begins operations

b) Contours of Water Levels During ASR Well Injection of Water

c) Contours of Water Levels During Recover of Injected Water

Figure 3-6 Schematic showing hydraulic head contours associated with (a) uniform regional groundwater flow prior to operating the ASR well, (b) outward radial flow from the ASR well during injection, and (c) inward radial flow to the ASR well during pumping.

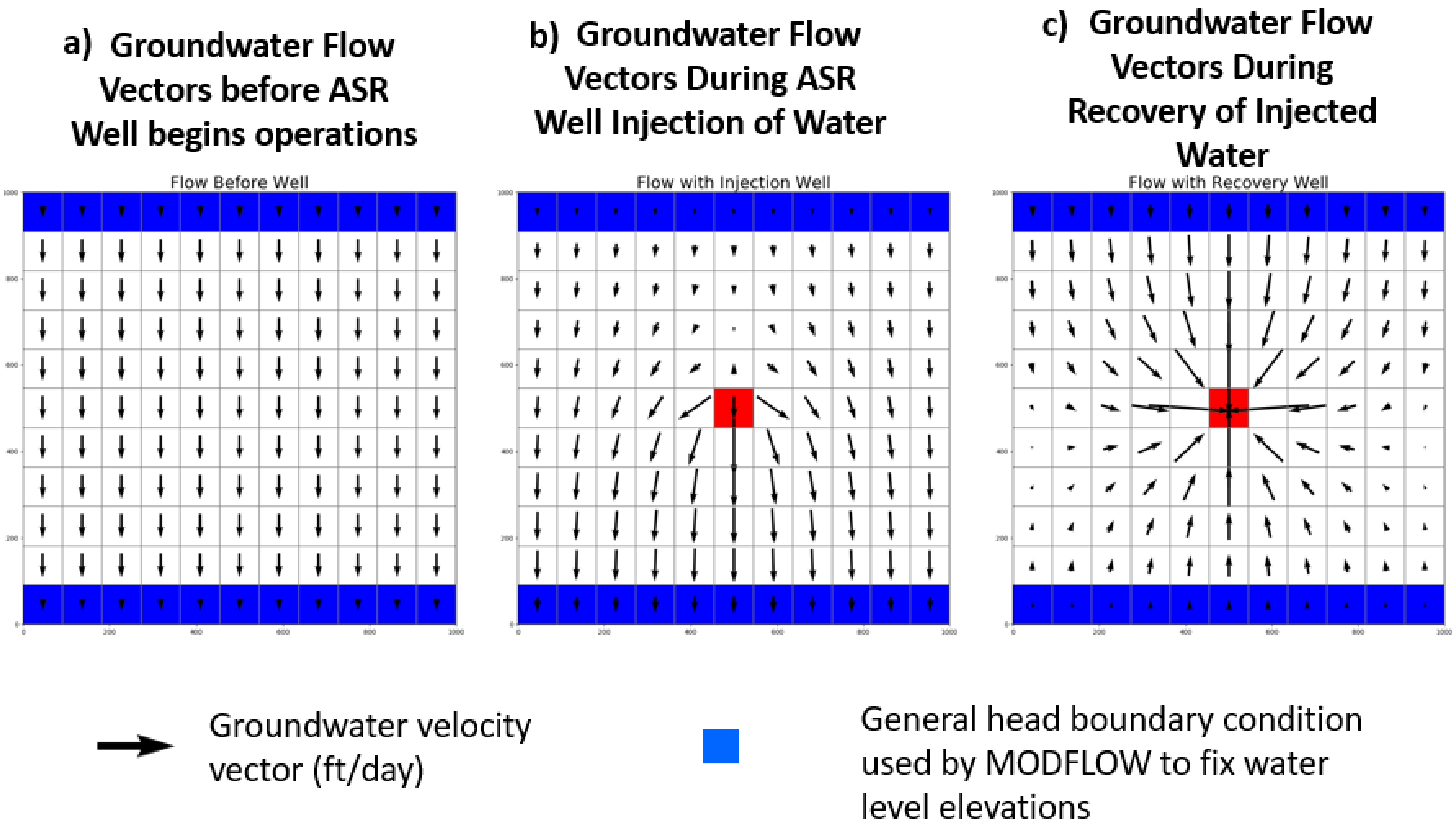

a) Groundwater Flow Vectors before ASR Well begins operations

b) Groundwater Flow Vectors During ASR Well Injection of Water

c) Groundwater Flow Vectors During Recovery of Injected Water

Figure 3-7 Schematic showing groundwater flow velocity vectors associated with (a) uniform regional groundwater flow prior to operating the ASR well, (b) outward radial flow from the ASR well during injection, and (c) inward radial flow to the ASR well during pumping.

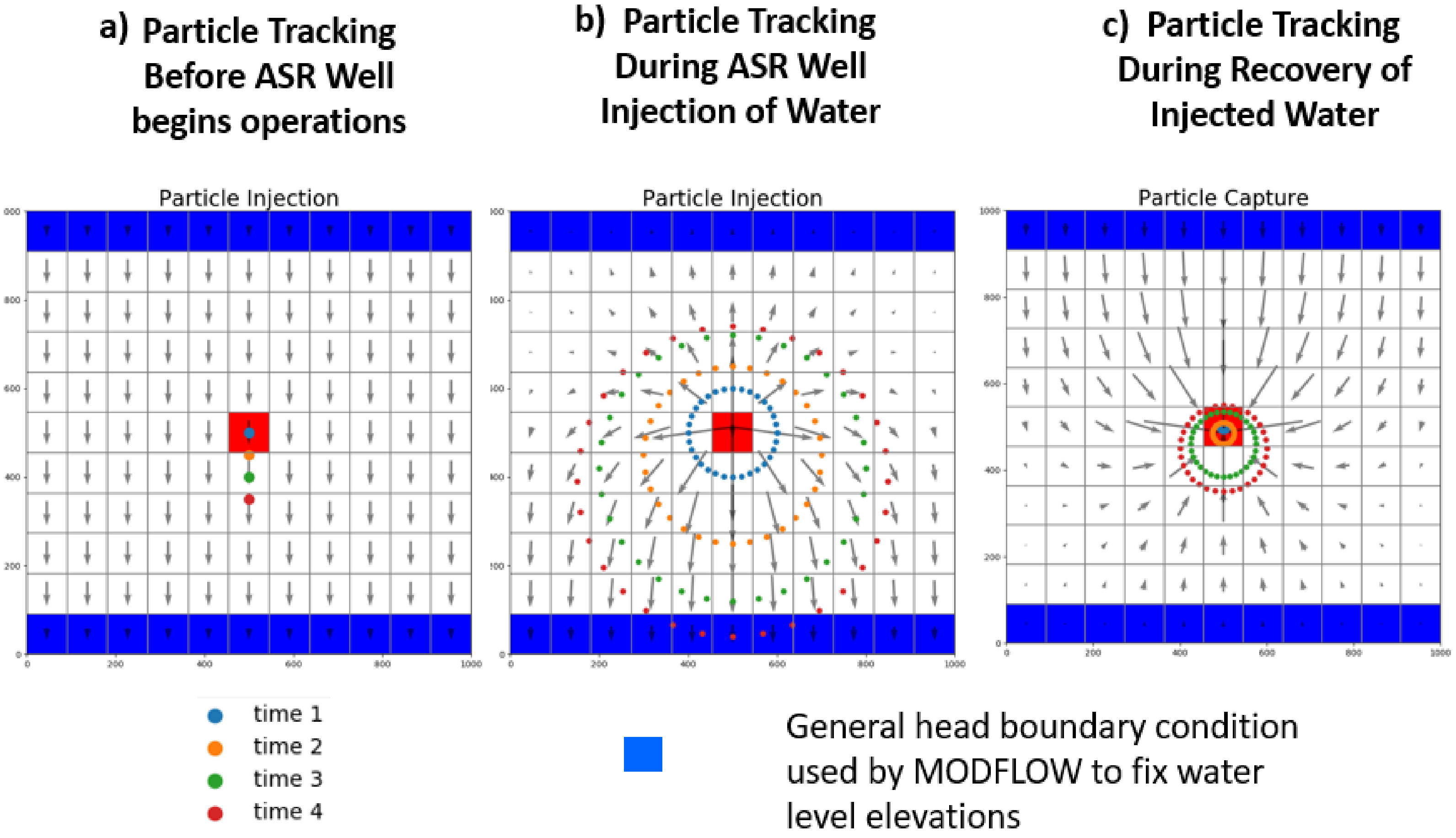

Figure 3-8 Schematic showing the groundwater flow velocity vectors and the tracking of particles over time for (a) uniform regional groundwater flow prior to operating the ASR wel, (b) outward radial flow from the ASR well during injection, and (c) inward radial flow to the ASR well during pumping.

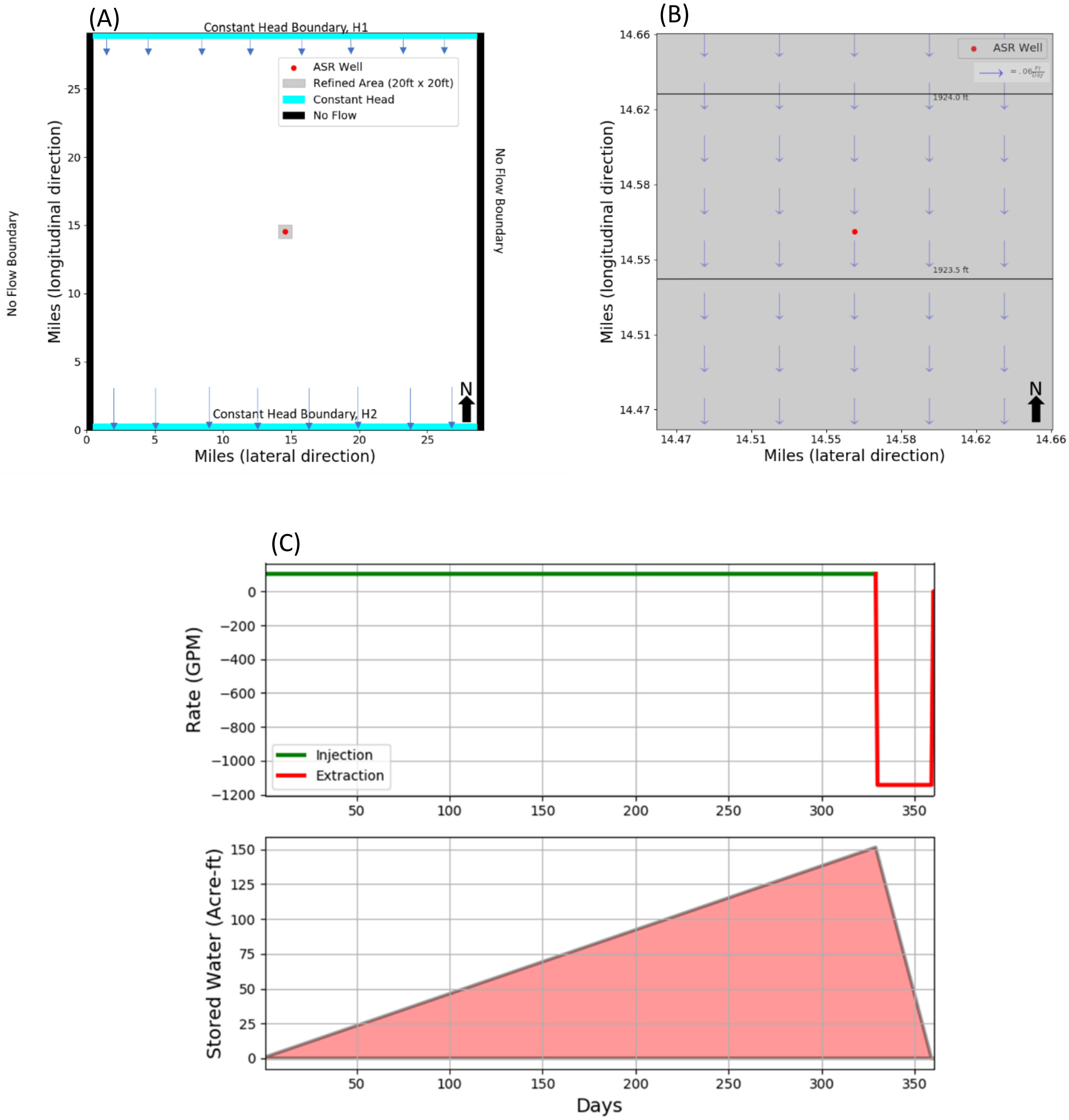

Figure 3-9 Schematic showing the hydraulic boundaries used in the numerical model to simulate the ASR base case scenario. (A) model domain with boundaries conditions used to simulate steady-state conditions for regional groundwater flow, (B) simulated regional groundwater hydraulic gradient of 0001, and (C) schedule for injecting and pumping the ASR well and stored water volume with time.

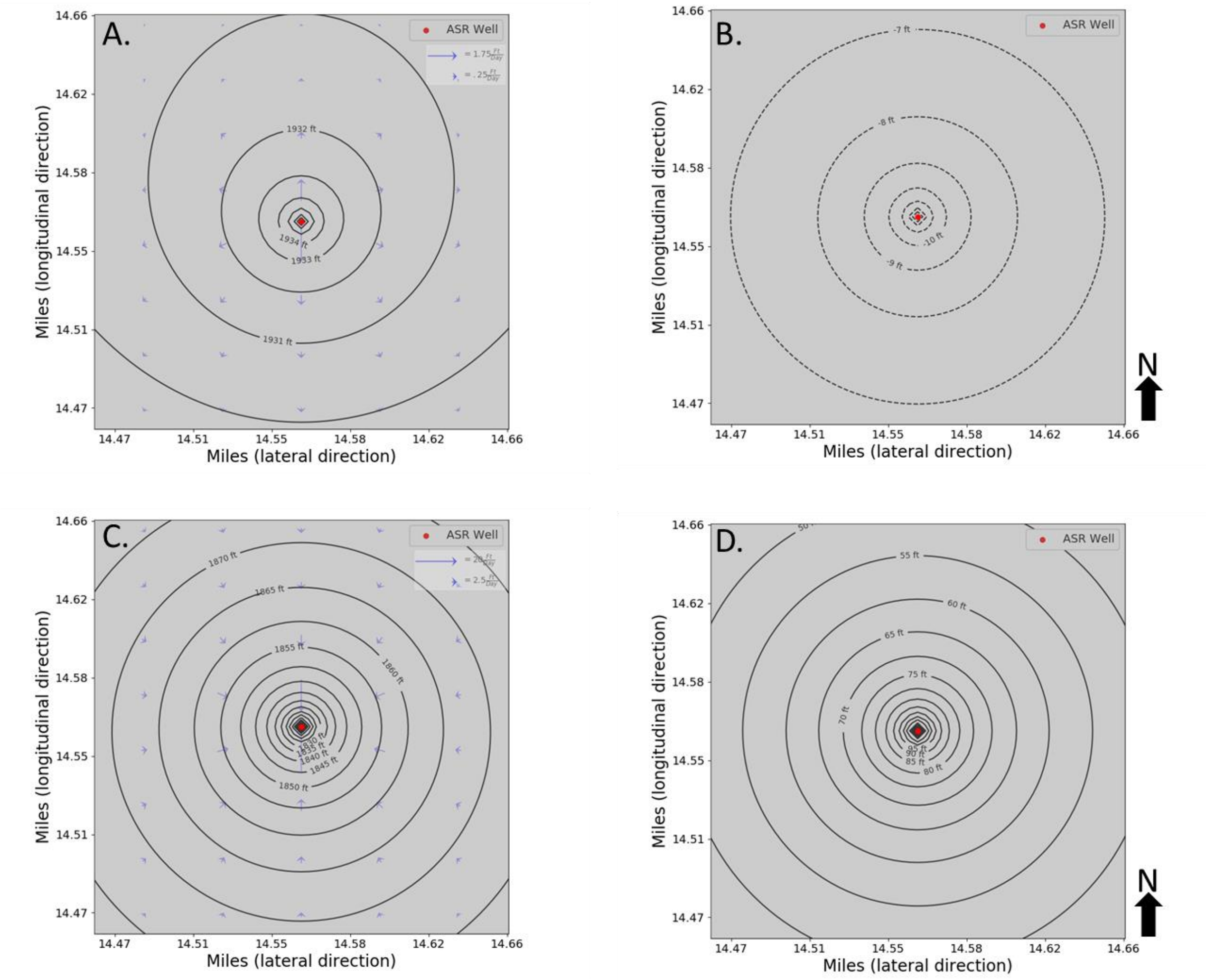

Figure 3-10 Groundwater conditions simulated by the numerical model for the ASR base case scenario. (A) contours of hydraulic heads after injecting water for 330 days; (B) contours of hydraulic head change between the start and the end of the 330-day injection period; (C) contours of hydraulic heads after pumping groundwater for 30 days; and (D) contours of hydraulic head change between pre-ASR conditions and at the end of the 30-day extraction period.

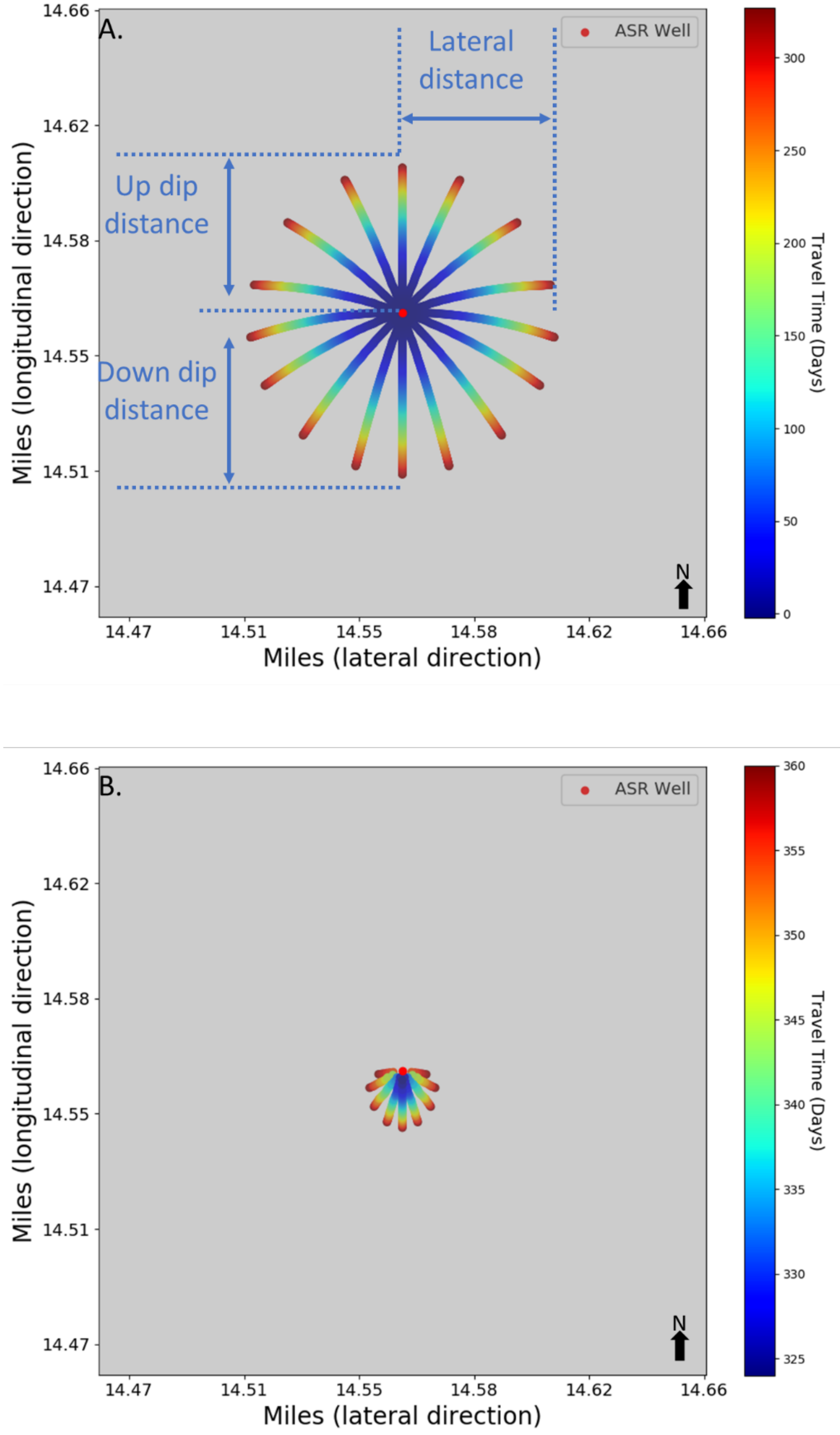

Figure 3-11 Particle tracking results showing the location and travel time of injected water for the base case ASR scenario (A) after 330 days of injection and (B) after 30 days of extraction

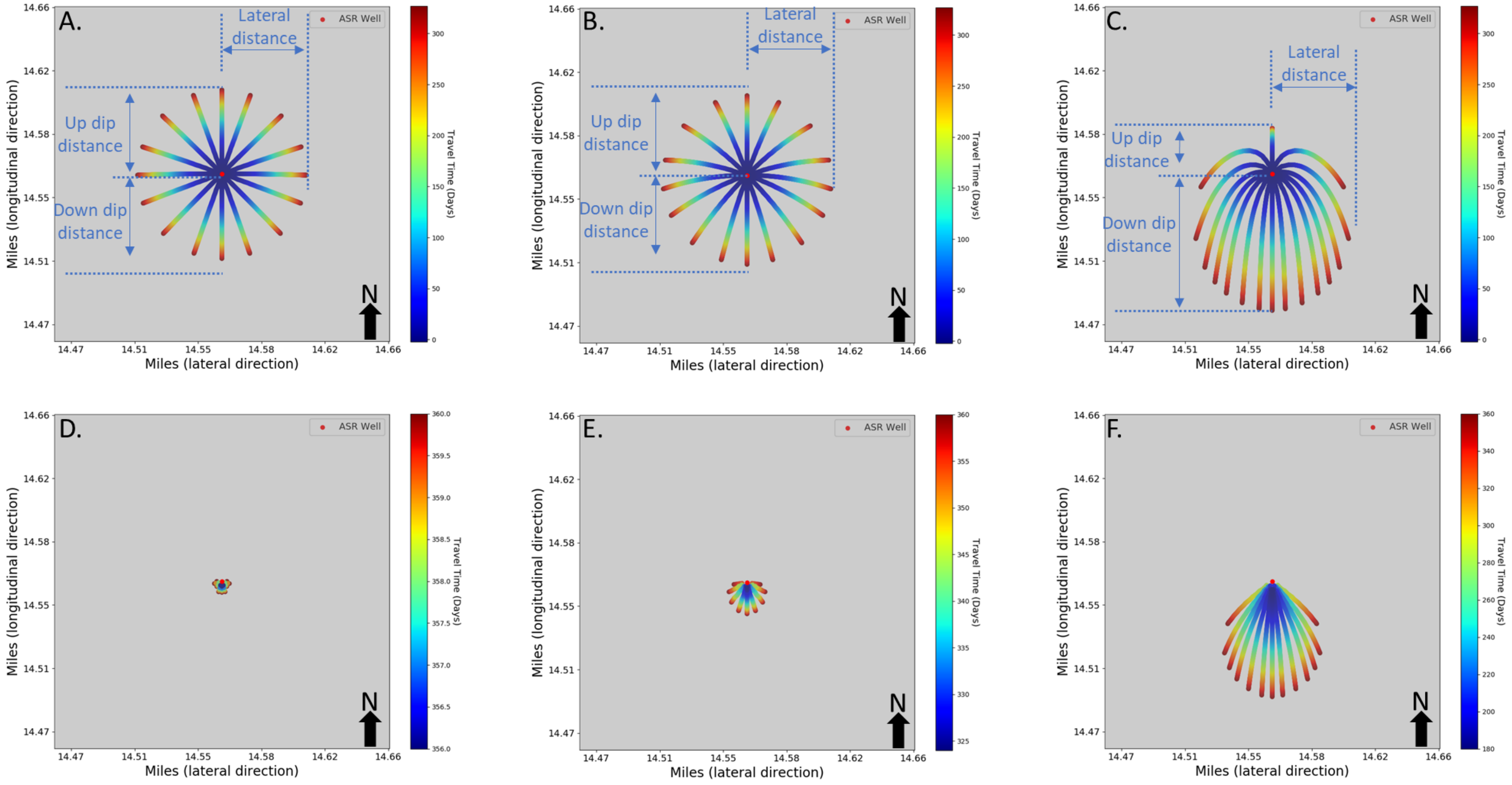

Figure 3-12 Particle tracking results showing the location and travel time of injected water after 330 days of injection with a regional hydraulic gradient of (A) 0.0001, (B) 0.001 and (C) 0.01 and after 30 days of extraction with a regional hydraulic gradient of (D) 0.0001, (E) 0.001, and (F) 0.01.

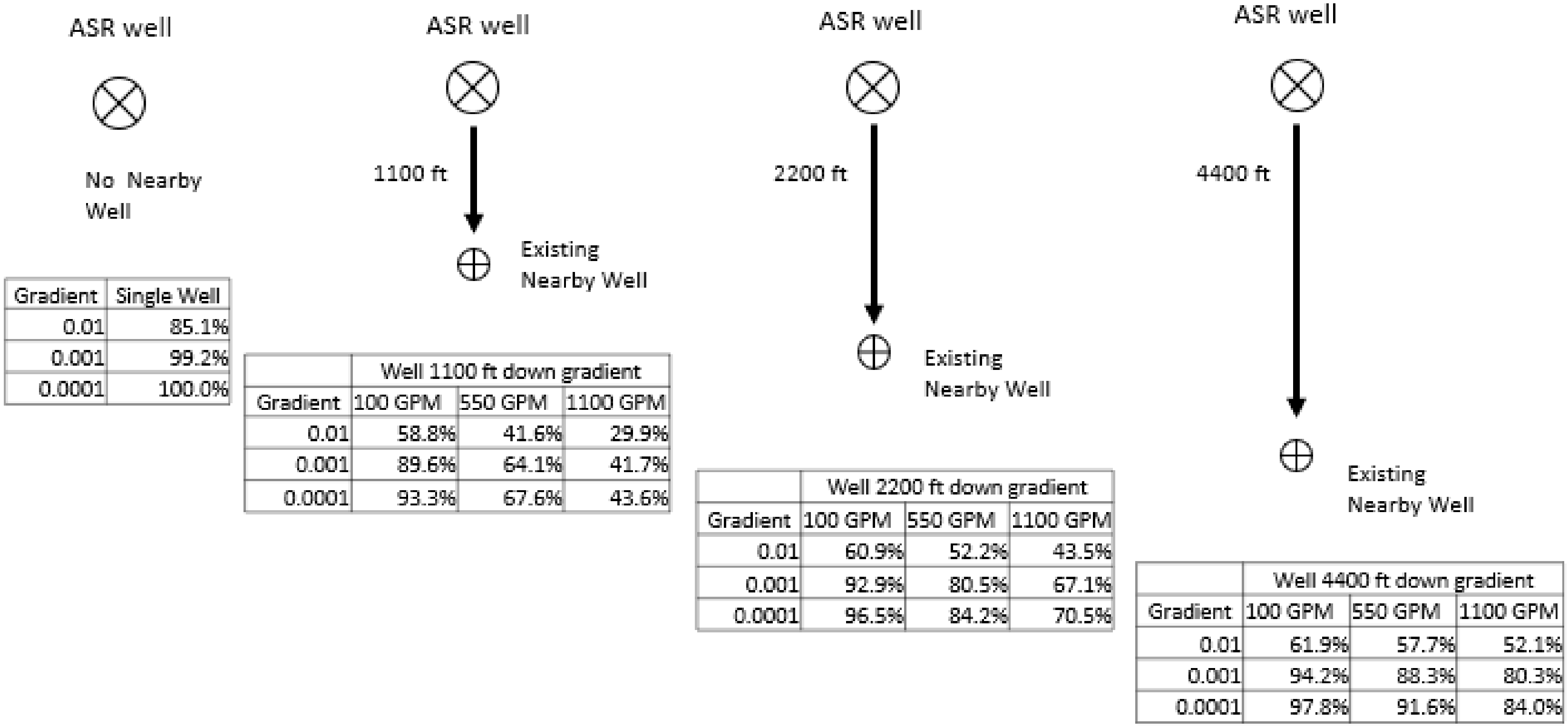

Gradient	Single Well
0.01	85.1%
0.001	99.2%
0.0001	100.0%

	Well 1100 ft down gradient		
Gradient	100 GPM	550 GPM	1100 GPM
0.01	58.8%	41.6%	29.9%
0.001	89.6%	64.1%	41.7%
0.0001	93.3%	67.6%	43.6%

	Well 2200 ft down gradient		
Gradient	100 GPM	550 GPM	1100 GPM
0.01	60.9%	52.2%	43.5%
0.001	92.9%	80.5%	67.1%
0.0001	96.5%	84.2%	70.5%

	Well 4400 ft down gradient		
Gradient	100 GPM	550 GPM	1100 GPM
0.01	61.9%	57.7%	52.1%
0.001	94.2%	88.3%	80.3%
0.0001	97.8%	91.6%	84.0%

Figure 3-13 The sensitivity of simulated ASR recoverabilities to pumping from a single well located down gradient from the ASR well with for regional hydraulic gradients of 0.01, 0.001, and 0.001 for ASR Scenario #1. The aquifer is 100 ft thick and has a hydraulic conductivity of 20 ft/day. The ASR well operation is to inject water at 100 gpm for 11 months and then extract at 1100 gpm for 1 month. The recoverabilities are calculated after 24 months of operation. The arrow indicates direction of regional groundwater flow. The tabulated flow rates are for the existing nearby well.

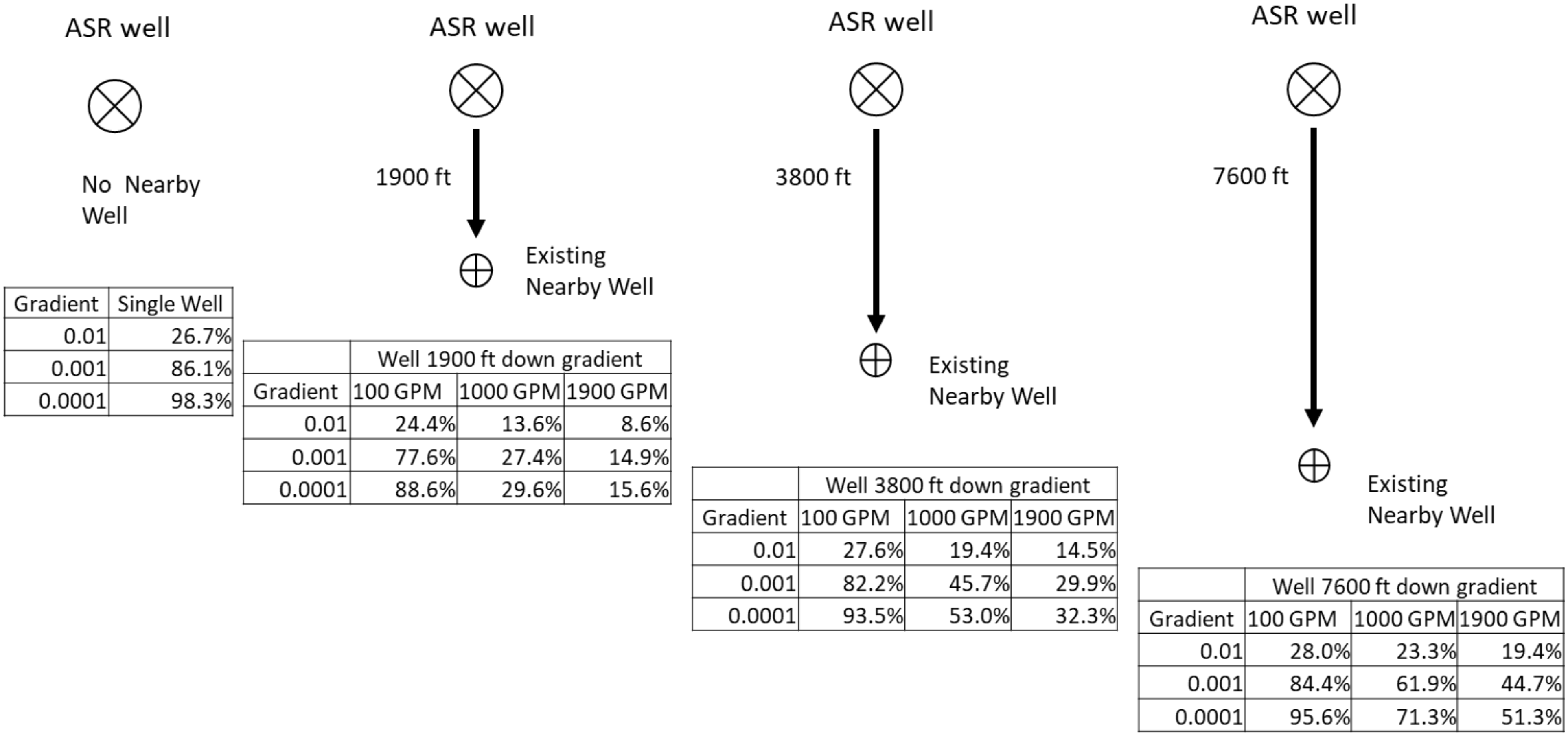

Gradient	Single Well
0.01	26.7%
0.001	86.1%
0.0001	98.3%

	Well 1900 ft down gradient		
Gradient	100 GPM	1000 GPM	1900 GPM
0.01	24.4%	13.6%	8.6%
0.001	77.6%	27.4%	14.9%
0.0001	88.6%	29.6%	15.6%

	Well 3800 ft down gradient		
Gradient	100 GPM	1000 GPM	1900 GPM
0.01	27.6%	19.4%	14.5%
0.001	82.2%	45.7%	29.9%
0.0001	93.5%	53.0%	32.3%

	Well 7600 ft down gradient		
Gradient	100 GPM	1000 GPM	1900 GPM
0.01	28.0%	23.3%	19.4%
0.001	84.4%	61.9%	44.7%
0.0001	95.6%	71.3%	51.3%

Figure 3-14 The sensitivity of simulated ASR recoverabilities to pumping from a single well located down gradient from the ASR well with for regional hydraulic gradients of 0.01, 0.001, and 0.001 for ASR Scenario #2. The aquifer is 100 ft thick and has a hydraulic conductivity of 20 ft/day. The ASR well operation is to inject water at 100 gpm for 9.5 years and then extract at 1900 gpm for 0.5 years. The recoverabilities are calculated after 10 years of operation. The arrow indicates direction of regional groundwater flow.

4.0 SIMULATION OF ASR RECOVERABILITY IN VICTORIA COUNTY

This section uses a groundwater flow model to demonstrate an approach for estimating ASR recovery for six candidate locations for ASR wells in Victoria County. The simulations were based on simple assumptions regarding regional pumping and the operation schedule for the ASR.

4.1 Development of a Groundwater Flow Model

The groundwater flow model was constructed by modifying the three-dimensional MODFLOW NWT groundwater model developed by Young and Kushnereit (2018) for use by the VCGCD to assess their brackish water supply. **Figure 4-1** shows the areal extend of the model. The model covers an area of 745 square miles and includes 14 counties. The model domain has been discretized using a numerical grid consisting of 250 rows, 310 columns, and 15 model layers (**Figure 4-2**). Across most of the model domain, grid cells are represented by 1-mile by 1-mile squares. Across most of Victoria County, the grid cells are represented by squares that measure 0.25-mile on a side. In the areas where hypothetical ASR wells were located, the grid cells have sides with lengths as short at 132 ft.

The vertical extend of the model extends to a depth of 5,425 ft and includes the nine formations listed in **Table 4-1** that comprise the Chicot Aquifer, Evangeline Aquifer, Burkeville Confining Unit, and Jasper Aquifer. The model uses 15 layers to represent these nine formations. For convenience, the groundwater flow model is named the Victoria County Groundwater Flow Model (VCGFM). The model layers were constructed using the formation surfaces provided by Young and others (2010). Six of the formations are each represented by a single model layer. These formations are the Beaumont, Lissie, Willis, Middle Lagarto, Lower Lagarto, and Oakville. The three formations that comprise the Evangeline Aquifer are represented by multiple model layers. The Upper Goliad, Lower Goliad, and Upper Lagarto formations are represented by four, three, and two model layers, respectively.

Table 4-1 Simplified stratigraphic and hydrogeologic chart of the Gulf Coast Aquifer System (Young and others, 2010)

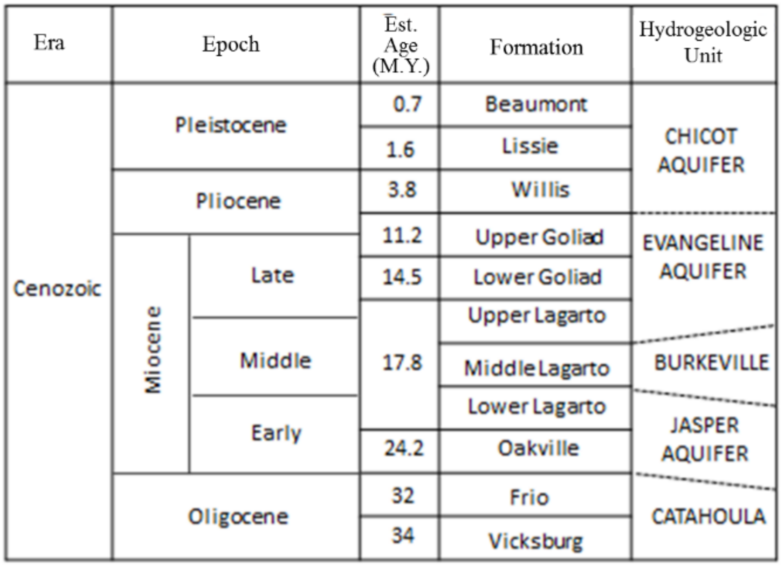

Era	Epoch		Est. Age (M.Y.)	Formation	Hydrogeologic Unit
Cenozoic	Pleistocene		0.7	Beaumont	CHICOT AQUIFER
			1.6	Lissie	
	Pliocene		3.8	Willis	
	Miocene	Late	11.2	Upper Goliad	EVANGELINE AQUIFER
			14.5	Lower Goliad	
		Middle	17.8	Upper Lagarto	
				Middle Lagarto	BURKEVILLE
		Early		Lower Lagarto	JASPER AQUIFER
			24.2	Oakville	
	Oligocene		32	Frio	CATAHOULA
			34	Vicksburg	

4.2 Candidate Locations for ASR Wells

VC GCD provided INTERA with six candidate locations for ASR wells. **Table 4-2** lists the six locations and **Figure 4-3** shows the six locations. All of the ASR wells were screened in the Evangeline Aquifer and across the Upper Goliad Formation. Table 4-2 lists the model layers in which the ASR well screens were placed.

Table 4-2 Six locations selected for candidate ASR wells screened in the Upper Goliad Formation

ASR Site		Latitude	Longitude	Model Layers	Depth to Top of Well Screen
1	ASR Demonstration Site	28.8107	-97.0197	5,6	511
2	Murphy Ranch Area	28.9334	-97.1387	6,7	240
3	Port of Victoria Area	28.6939	-96.9506	5,6	799
4	Growth Area	28.8750	-96.9918	5,6	509
5	Airline Rd Water Plants	28.8211	-96.9841	5,6	599
6	Victoria Water Treatment Plant Site	28.7810	-96.9935	5,6	659

4.3 Location of Pumping Near Candidate ASR Wells

In several of the groundwater model simulations, pumping is simulated in Victoria County. The pumping rates used in the modeling scenarios are based on pumping rates listed in well permits issued by VCGCD. Based on the well construction information associated with each permitted well, each well was assigned to one or more model layers. Appendix A lists the location and pumping rates assigned to each permitted well. **Figures 4-4** through **4-8** show the location and pumping rates by formation for the pumping wells that were used for the pumping scenarios.

4.4 Pre-Development and Post-Development Scenarios for Establishing Regional Flow Conditions

For the six ASR wells, ASR recoverabilities were estimated using the numerical groundwater flow model for two different steady-state flow conditions that existed prior to the ASR well operations. Steady-state occurs where hydraulic heads are not changing and the amount of flow entering the aquifer flow system equals the amount of flow leaving the aquifer flow system. The two steady-state situations are called Pre-development and Post-development. The Pre-development modeling scenarios assumes that no pumping is occurring at any well in Victoria County. **Figure 4-9** shows contours of hydraulic head in the Upper Goliad Formation for the Pre-development scenarios. In Figure 4-9, the hydraulic head contours indicate relatively uniform groundwater flow toward the Gulf Coast. The Post-development modeling scenarios assume that pumping is occurring at existing permitted wells. **Figure 4-10** shows contours of hydraulic head in the Upper Goliad formation for the Post-development scenarios. In Figure 4-10, the hydraulic head contours show several zones of depression caused by pumping in Victory County. The primary propose of the Pre-development and Post-development scenarios is to establish the regional conditions on top of which the ASR pumping is superimposed.

4.5 29-month and 64-month Scenarios for Describing Operation Conditions at the ASR wells

At all six ASR well locations, two schedules for injecting and extracting were simulated. The two schedules different in the length of time for injecting water. The injection length was 29 months for one scenario and 64 months for the other scenario. Both scenarios involved extracting for only 4 months. Because of different hydrological conditions among the six ASR locations, the pumping and extraction rates were not the same for all of the ASR locations. As shown in **Table 4-3**, the injection and pumping rates varied up to a factor of 3 between sites. For both scenarios for ASR operation, the total volume of injected water equals the total volume of extracted water.

Table 4-3 Injection and extraction rates used for the 3-year and 6-year modeling scenarios

ASR Well		Injection Rate (gpm) for the 29-month and 64-month Scenarios	Extraction Rate (gpm)	
ID	Name		29-month Scenario	64-month Scenario
1	ASR Demonstration Site	300	2,175	4,875
2	Murphy Ranch	100	725	1,625
3	Port of Victoria Area	300	2,175	4,875
4	Growth Area	200	1,450	3,250
5	Airline Rd Water Plants	300	2,175	4,875
6	Victoria Water Treatment Plant Site	300	2,175	4,875

4.6 Simulation of ASR Scenarios

At each ASR site, the 29- and 64-month ASR operational schedules were simulated for both the Pre- and Post-development scenarios. Thus, four scenarios were simulated for each ASR well.

Figures 4-11a through **4-22b** show the contours of hydraulic head associated with the 24 ASR scenarios that were modeled. Each figure consists of four plots. Three of these plots show contours of hydraulic head in the Upper Goliad Formation immediately prior to the start of ASR injection, at the end of the injection period, and at the end of the extraction period. The fourth plot shows the hydraulic head as a function of time for the grid cell containing the ASR well.

For each of the four modeling scenarios, the particle tracking approach used to calculate ASR recoverability is very similar to the approach described in Section 3.3.3. Recoverabilities were predicted for a porosity of 30% (**Table 4-4**) and 15% (**Table 4-5**). Two values for porosity are used because of the uncertainty with assigning an effective porosity value for the Upper Goliad Formation.

The results in Table 4-4 suggest that, except for Murphy Ranch, the ASR well sites have favorable conditions for achieving recoverability of above 70%. Three of the sites have estimated recoverabilities of 90% or better for both the 29- and 64-month ASR operating schedules. These results provide a good framework for more detailed modeling work to investigate more site-specific data to better represent the anticipated pumping schedules and ASR operation schedules.

Table 4-4 Simulated ASR recoverability based on a porosity of 30%

ASR Well		Pre-Development (%)		Post-Development (%)	
ID	Name	29-month	64-month	29-month	64-month
1	ASR Demonstration Site	98.7	97.7	87.3	83.9
2	Murphy Ranch	49.4	40.0	50.0	31.5
3	Port of Victoria Area	98.8	98.7	98.5	98.1
4	Growth Area	98.4	97.8	95.5	93.7
5	Airline Rd Water Plants	98.6	97.8	84.2	80.6
6	Victoria Water Treatment Plant Site	98.6	98.2	95.9	93.8

Table 4-5 Simulated ASR recoverability based on a porosity of 15%

Name	Pre-Development (%)		Post-Development (%)	
	29-month	64-month	29-month	64-month
ASR Demonstration Site	98.13	97.24	83.66	77.36
Murphy Ranch	49.07	40.06	50	32.48
Port of Victoria Area	98.53	98.22	98.06	97.31
Growth Area	97.99	96.79	93.68	90.79
Airline Rd Water Plants	98.1	97.79	80.17	72.48
Victoria Water Treatment Plant Site	98.1	97.18	93.64	90.93

For all six ASR well sites, the modeling scenario with the lowest recovery is based on Post-development conditions for regional groundwater flow and a 64-month injection/4-month extraction for the ASR well operation. The pathlines associated with the particle movement at the six ASR well locations for this modeling scenario are shown in **Figures 4-23** through **4-27**. Among the important issues that affect the performance of the ASR wells for this scenario is the proximity of nearby pumping. Any nearby pumping in the Upper Goliad Formation is shown in **Figures 4-23** through **4-27**. **Table 4-6** lists the closest wells to each ASR well location. The potential importance of pumping at nearby wells is evident in the tabulated and plotted results. In Tables 4-4 and 4-5, the three ASR well locations with the highest recoverabilities are same three ASR wells in Table 4-5 that have their closest pumping well more than a than a mile away. Moreover, an inspection of Figures 4-23 through 4-27 reveals that the more radial the particle pathways for an ASR well location, the greater the recoverability in Tables 4-4 and 4-5. Figures that show the movement of particles to nearby pumping wells, such as is the case for ASR well #2 (Figure 4-24) and ASR well #5 (Figure 4-26), have the lowest recoverabilities in Tables 4-4 and 4-5.

Table 4-6 Location of closest pumping well to ASR well in the Post-development scenarios

ASR Well Location		**Closest Existing Well**	
ID	**Name**	**Distance (ft)**	**Pumping Rate (gpm)**
1	ASR Demonstration Site	3200.0	395.9
2	Murphy Ranch	417.1	2.4
3	Port of Victoria Area	5800.0	41.7
4	Growth Area	15459.0	186.8
5	Airline Rd Water Plants	1145.0	716.0
6	Victoria Water Treatment Plant Site	11770.0	872.5

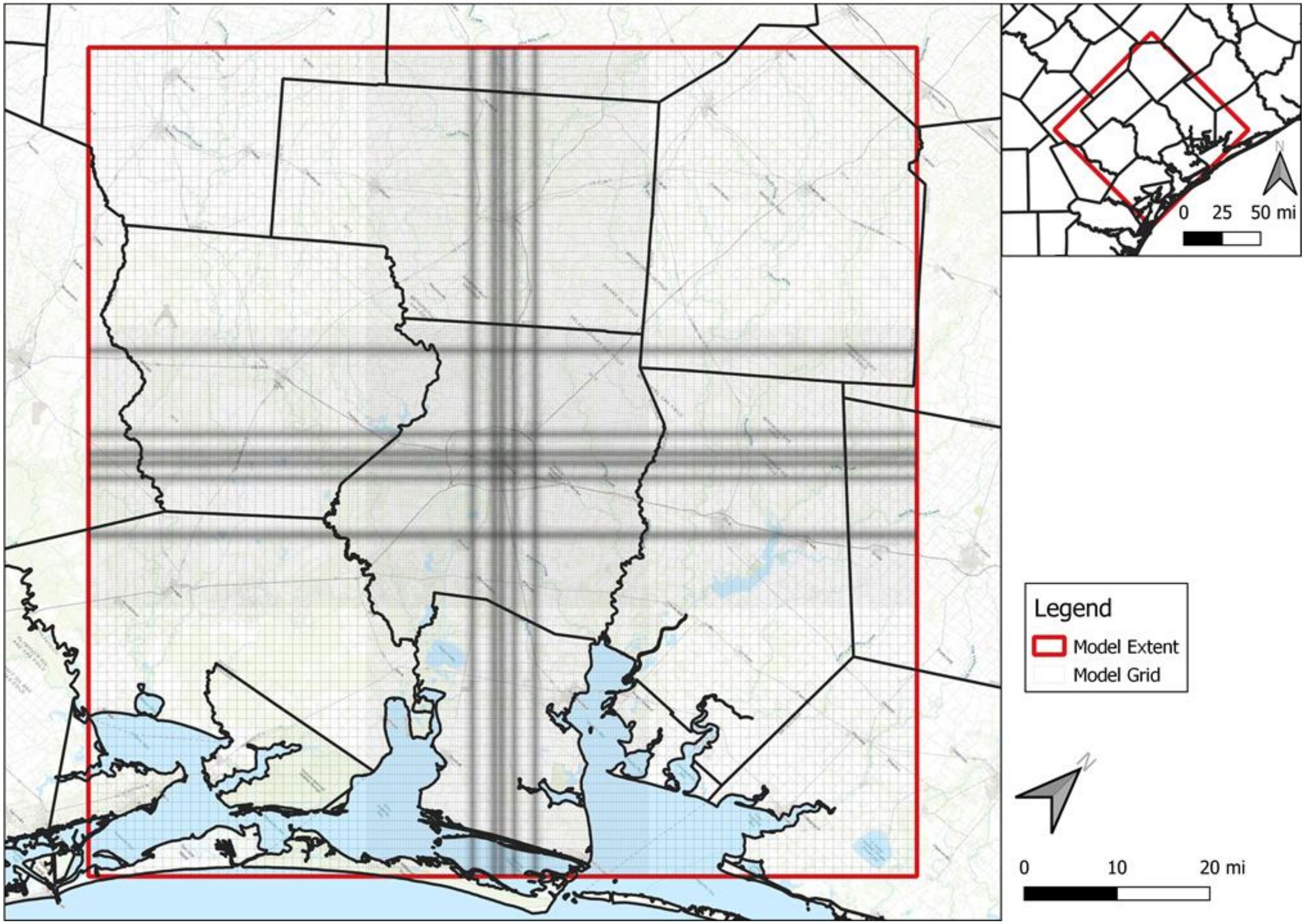

Figure 4-1 Model domain and numerical grid for the groundwater flow model used to simulate the impacts of injection and extraction from ASR wells on groundwater flow and ASR recovery in Victoria County.

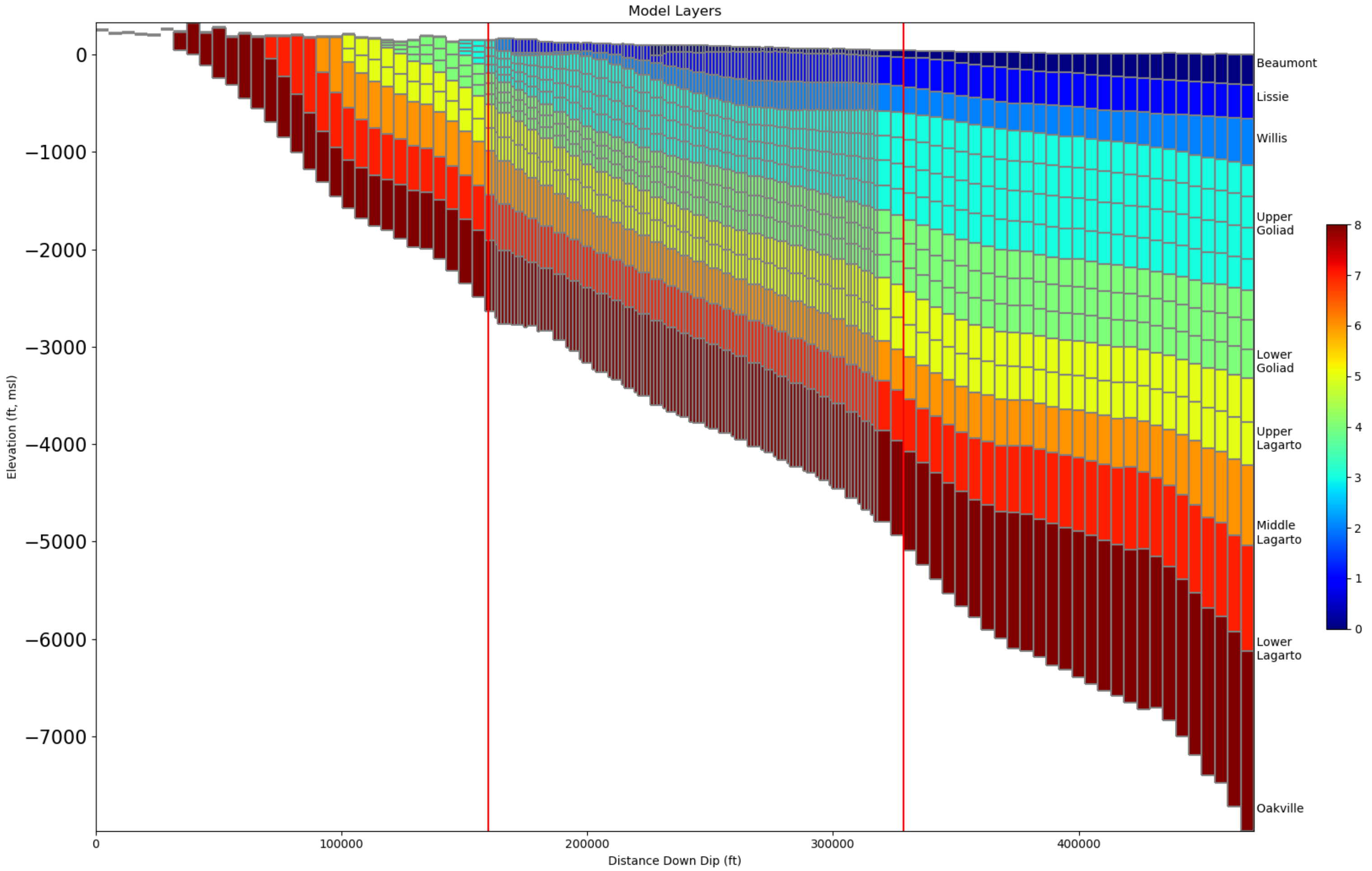

Figure 4-2 Northwest-southeast vertical cross-section showing the 15 model layers that comprise the numerical grid of the groundwater flow model along an axis that extends from up dip to down dip and crosses through the middle of Victoria County The red lines mark the boundaries for Victoria County.

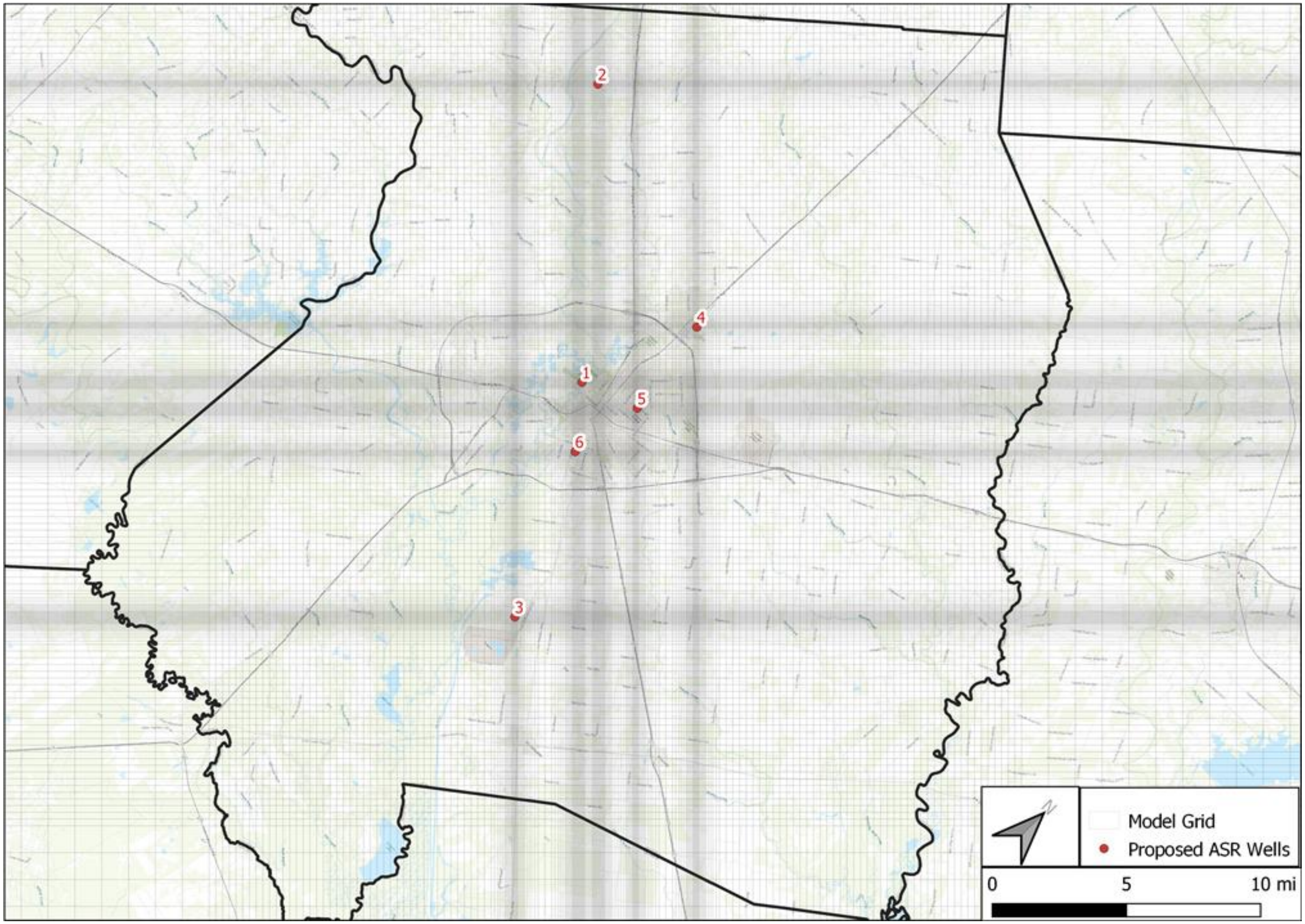

Figure 4-3 Locations of six candidate ASR wells and the numerical grid used by the groundwater flow model.

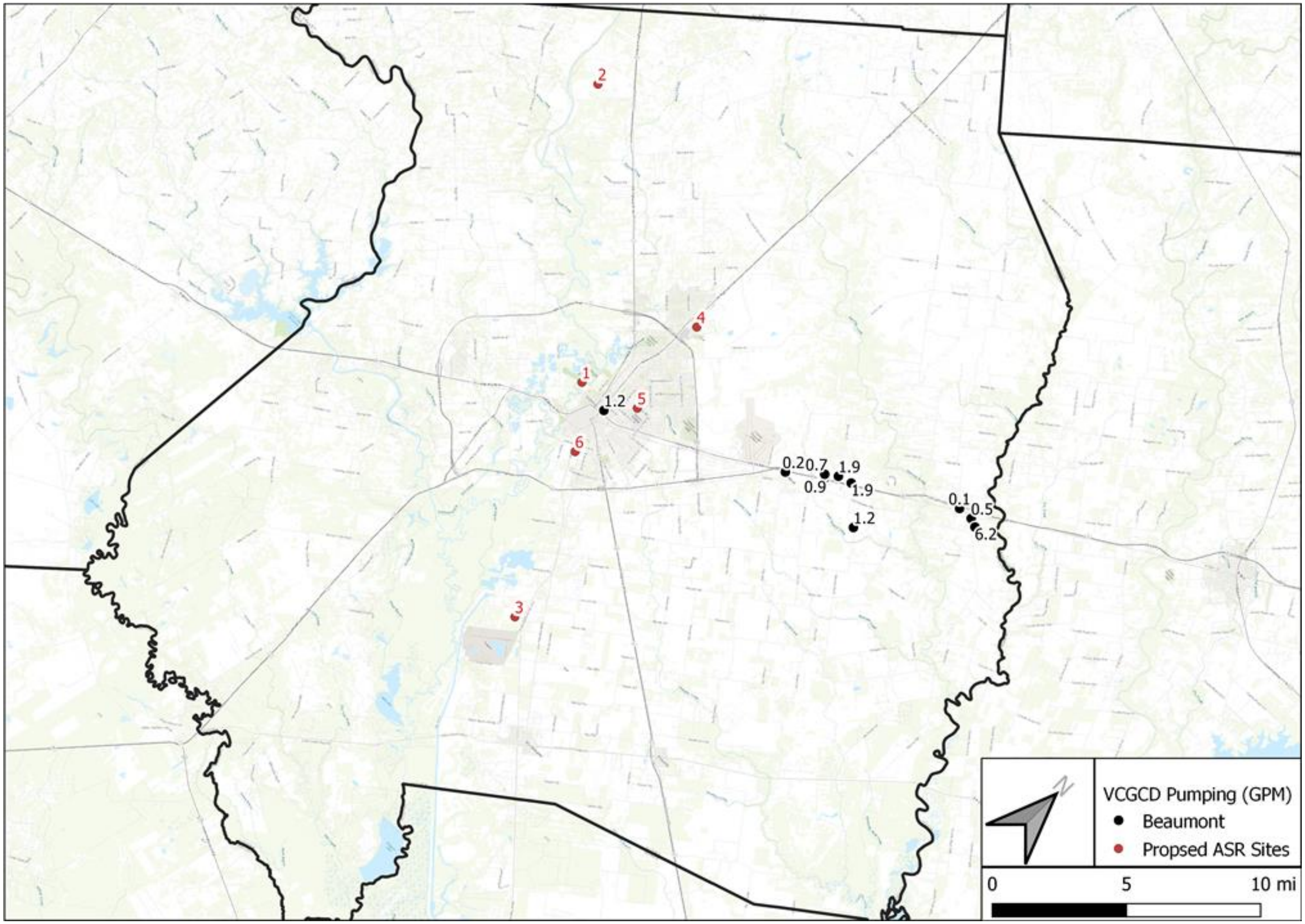

Figure 4-4 Location of permitted wells in the Beaumont Formation that were assigned pumping rates for the ASR Post-development modeling scenarios and the locations of the six candidate ASR wells.

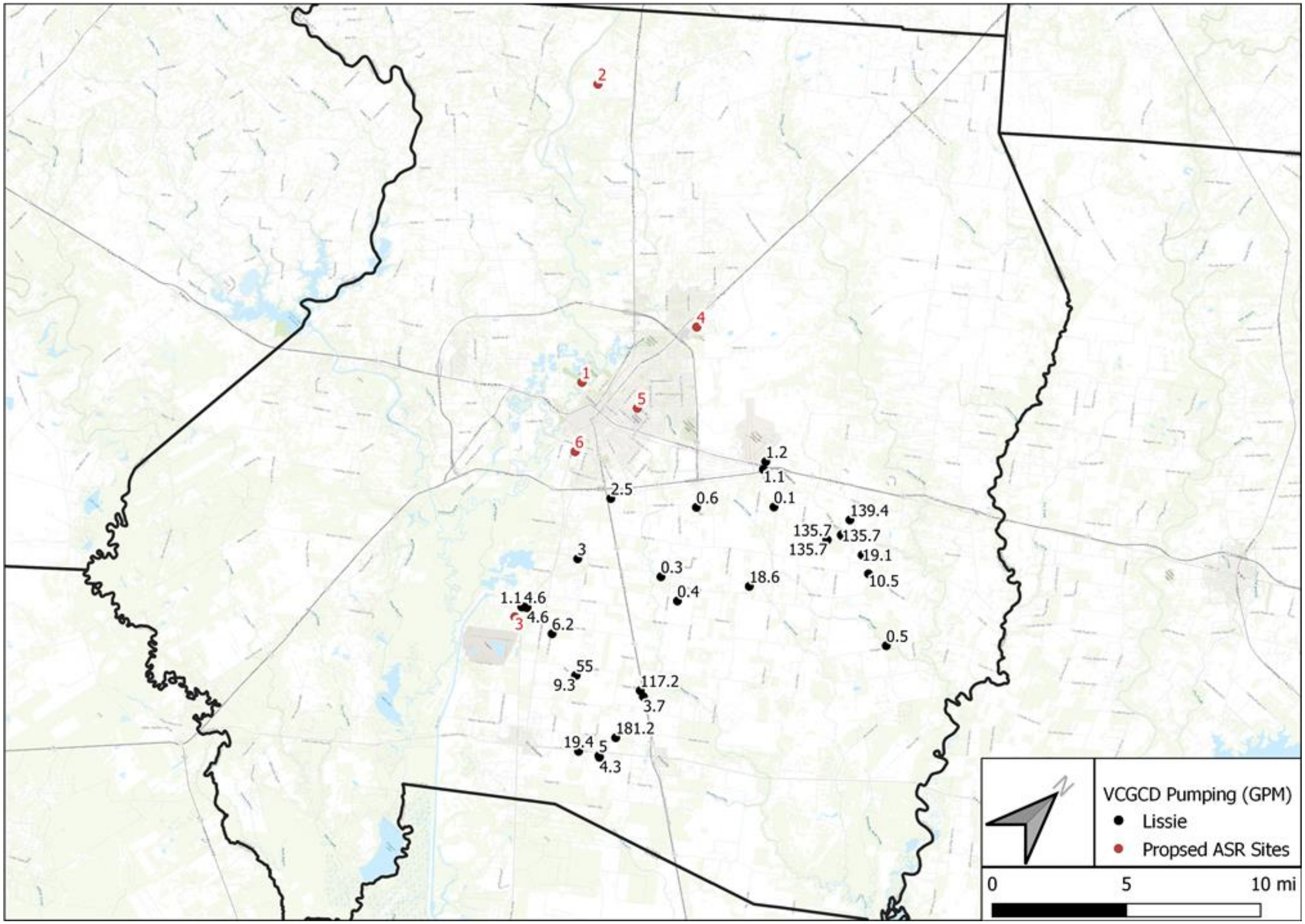

Figure 4-5 Location of permitted wells in the Lissie Formation that were assigned pumping rates for the ASR Post-development modeling scenarios and the locations of the six candidate ASR wells.

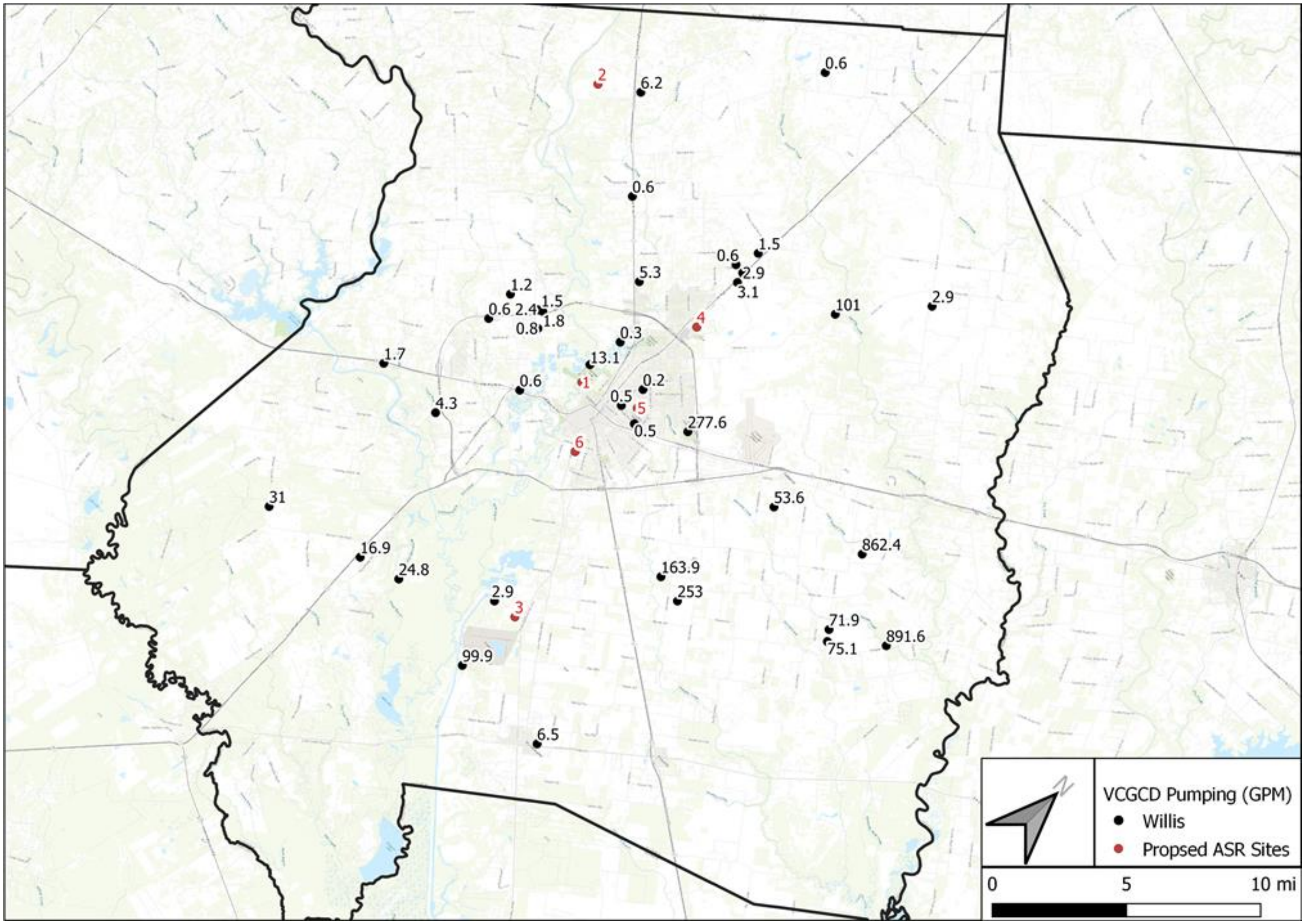

Figure 4-6 Location of permitted wells in theWillis Formation that were assigned pumping rates for the ASR Post-development modeling scenarios and the locations of the six candidate ASR wells.

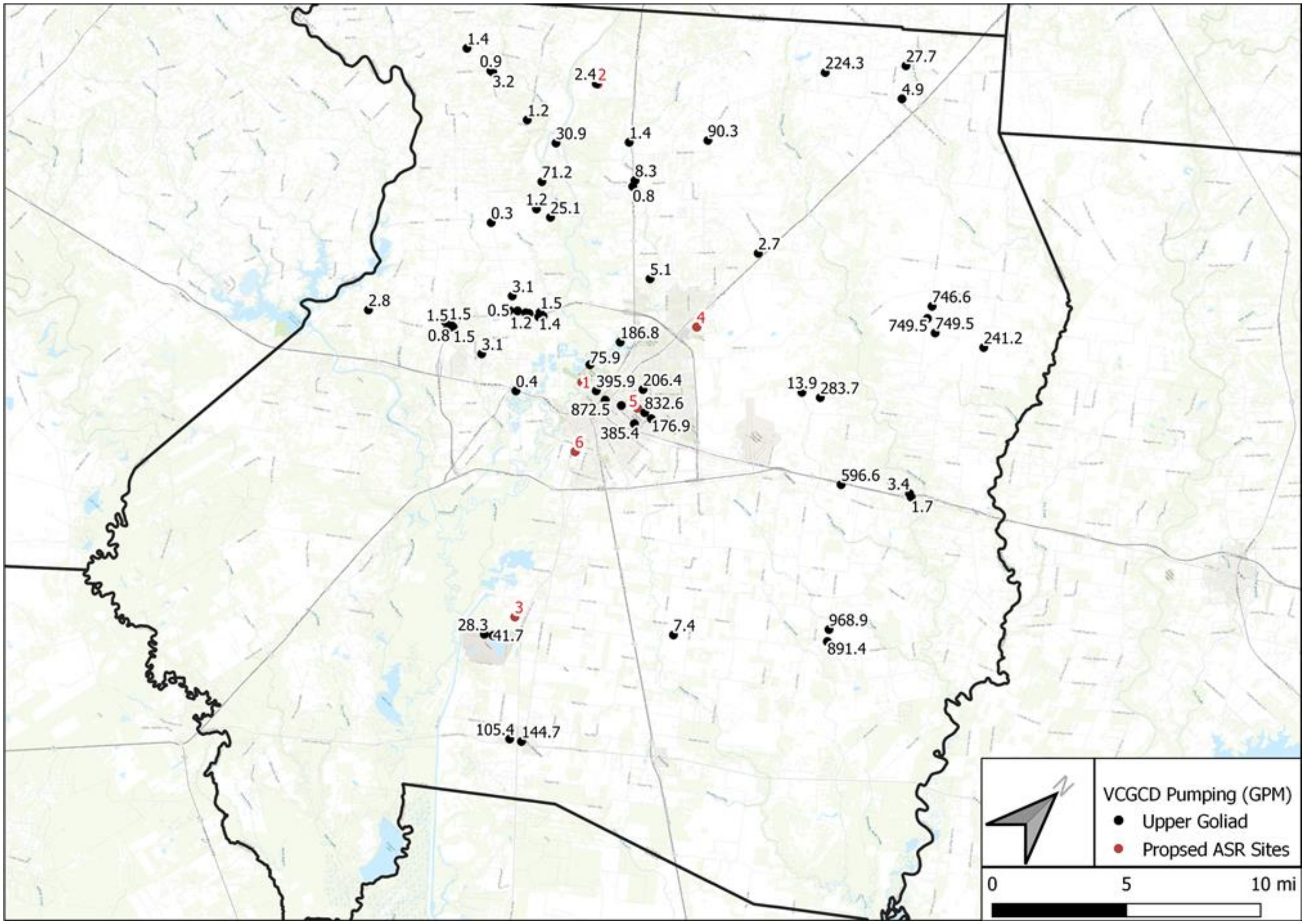

Figure 4-7 Location of permitted wells in the Upper Goliad Formation that were assigned pumping rates for the ASR Post-development modeling scenarios and the locations of the six candidate ASR wells.

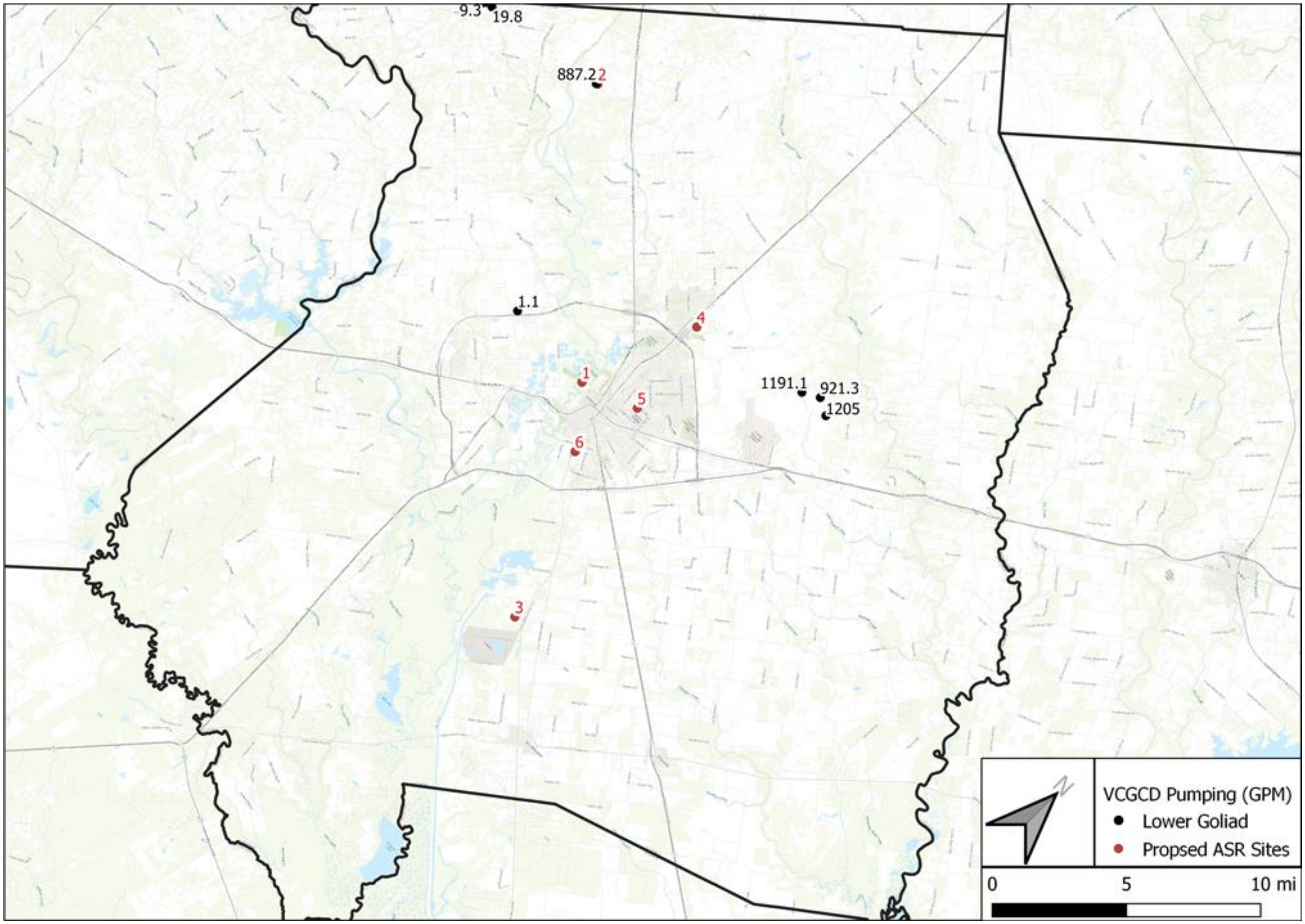

Figure 4-8 Location of permitted wells in the Lower GoliadFormation that were assigned pumping rates for the ASR Post-development modeling scenarios and the locations of the six candidate ASR wells.

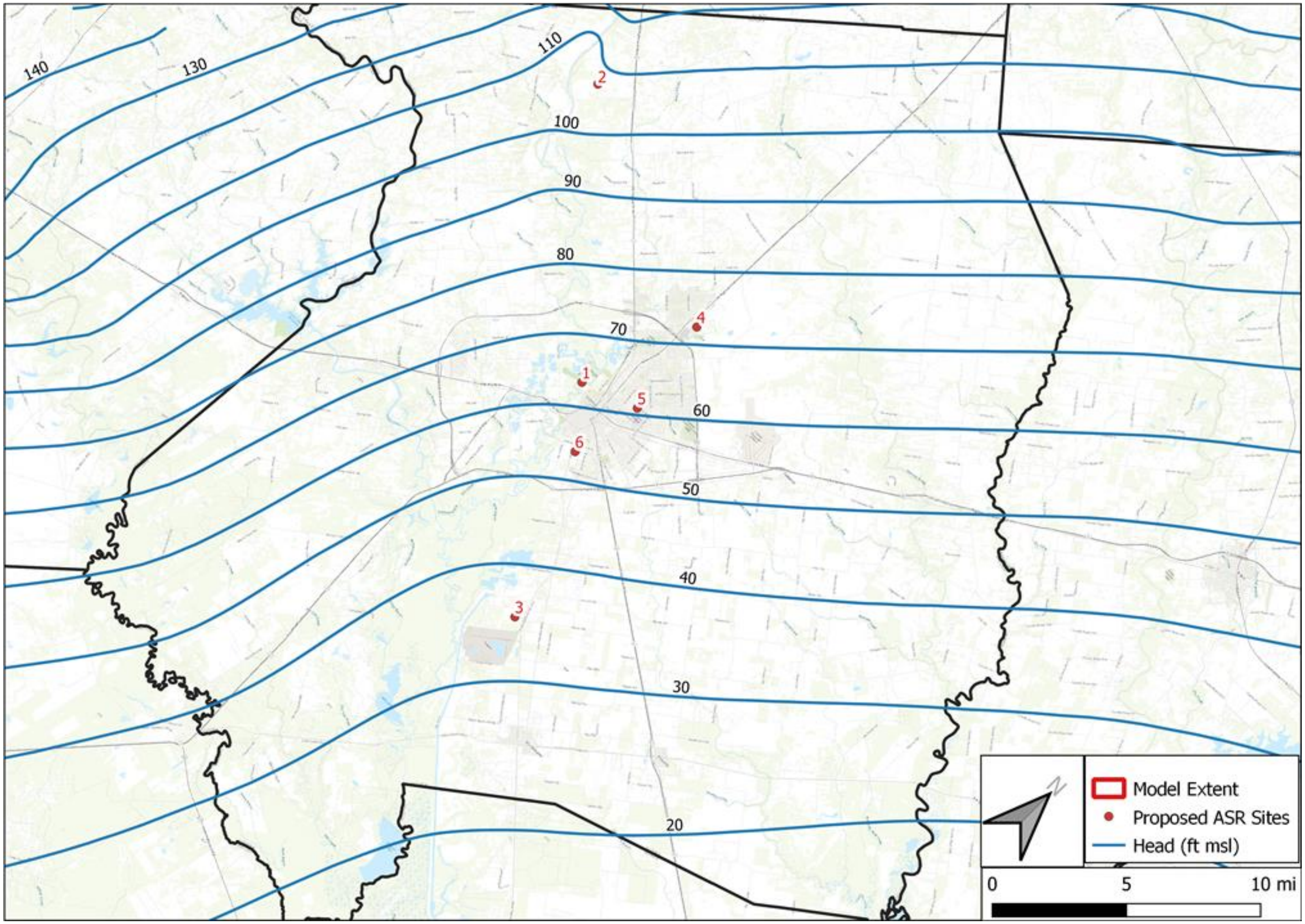

Figure 4-9 Contours for simulated hydraulic head in Model Layer 6 that represents a portion of the Upper Goliad Formation for steady-state flow condtions based on the assumption of no pumping or Pre-development scenarios.

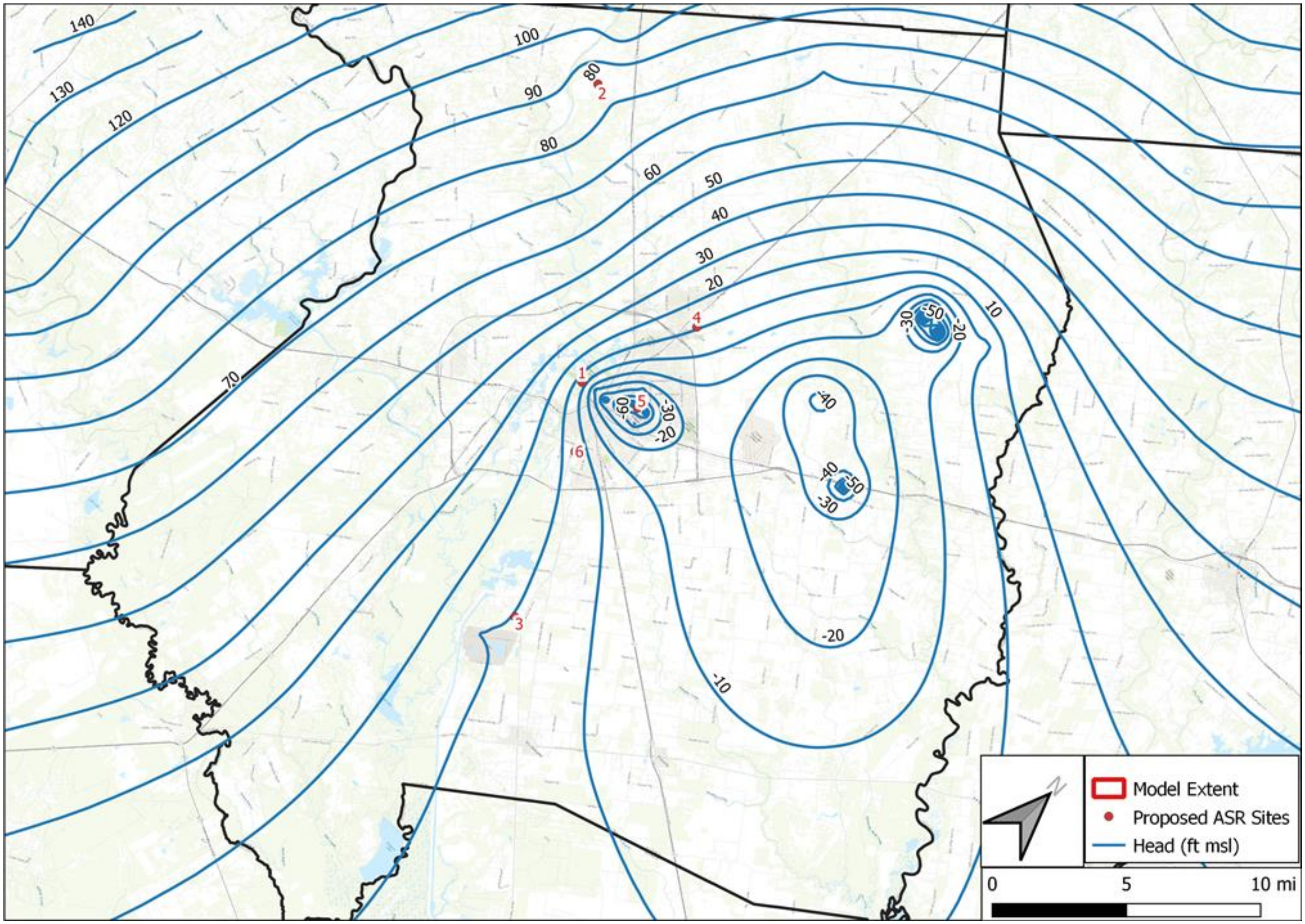

Figure 4-10 Contours for simulated hydraulic head in Model Layer 6 that represents a portion of the Upper Goliad Formation for steady-state flow condtions based on the assumption of pumping at permit well locations or Post-development scenarios.

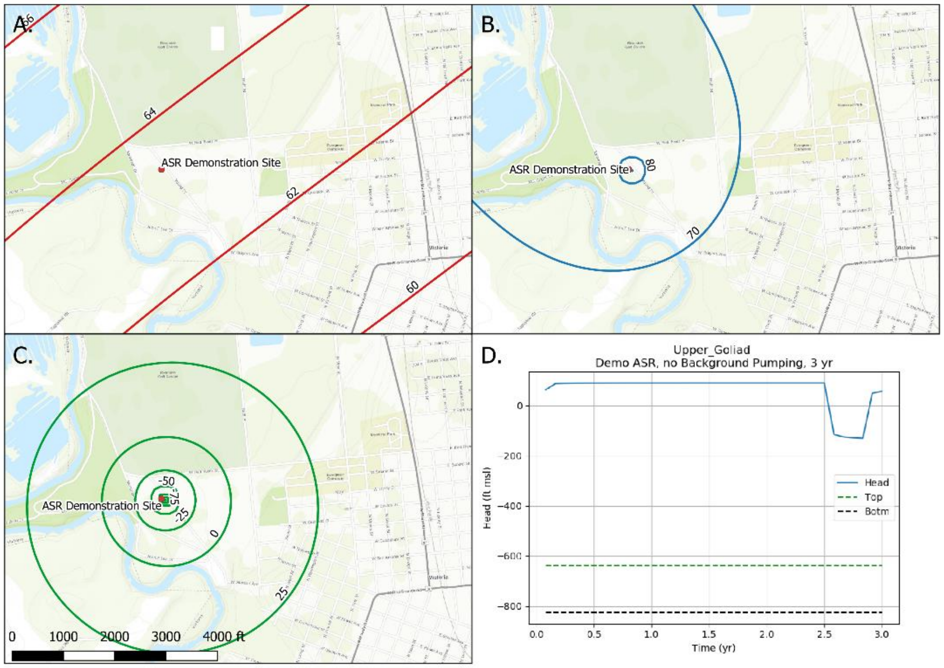

Figure 4-11a Hydraulic head contours simulated near the location of Site 1, ASR Demonstration Site, for the assumption of no pumping: (A) regional groundwater flow; (B) after 29 months of injection; and (C) after 4 months of pumping. (D) Hydraulic head in the ASR well with time.

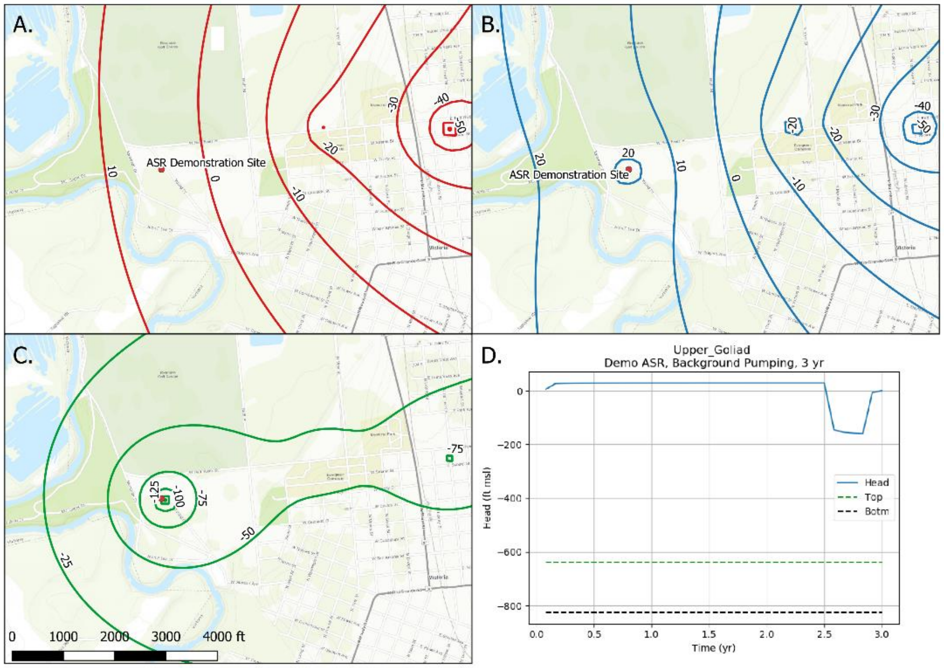

Figure 4-11b Hydraulic head contours simulated near the location of Site 1, ASR Demonstration Site, for the assumption of pumping at all permitted wells: (A) regional groundwater flow; (B) after 29 months of injection; and (C) after 4 months of pumping. (D) Hydraulic head in the ASR well with time.

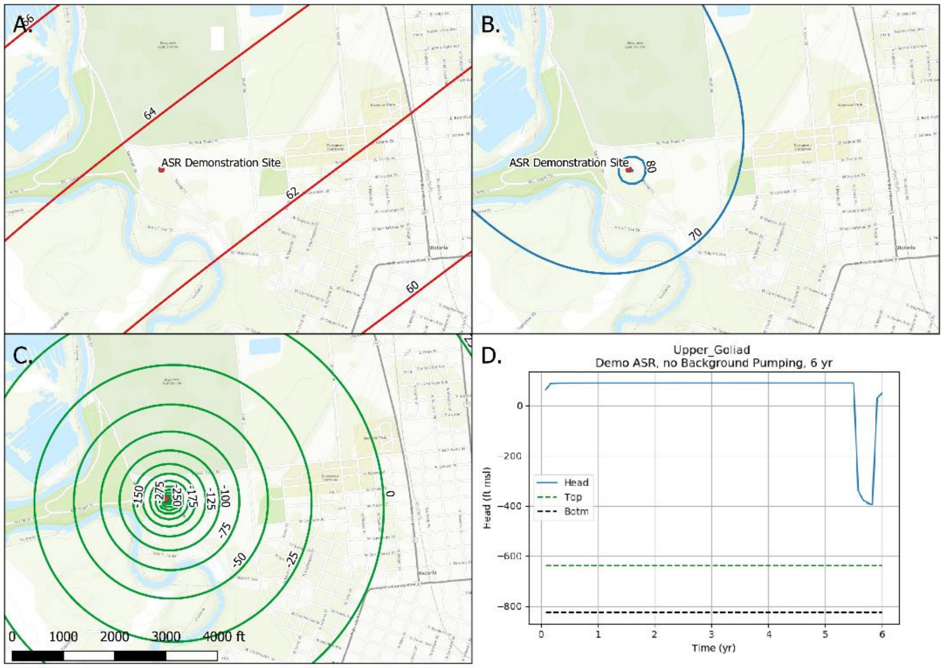

Figure 4-12a Hydraulic head contours simulated near the location of Site 1, ASR Demonstration Site, for the assumption of no pumping: (A) regional groundwater flow; (B) after 64 months of injection; and (C) after 4 months of pumping. (D) Hydraulic head in the ASR well with time.

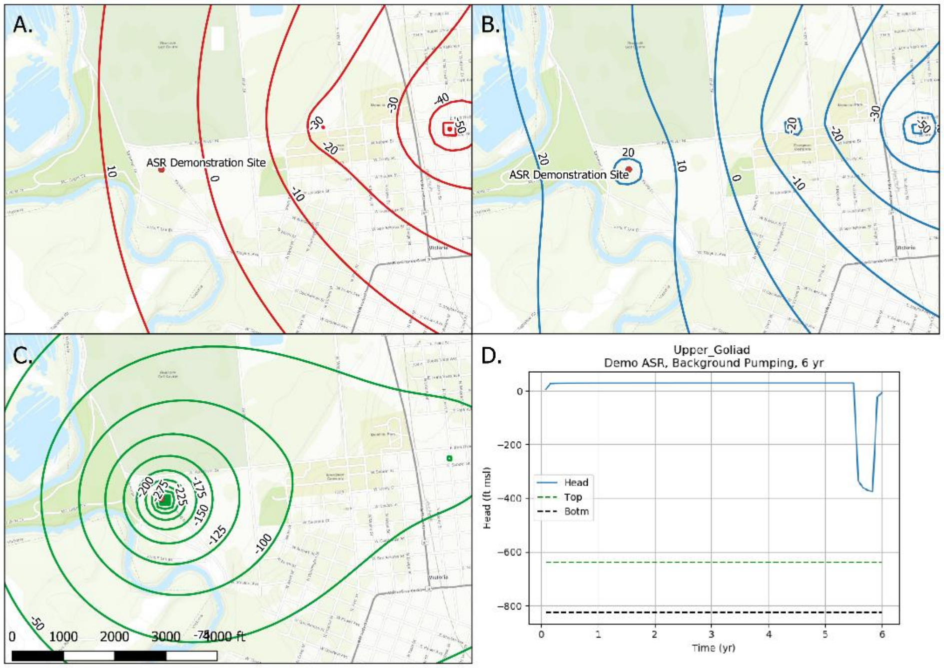

Figure 4-12b Hydraulic head contours simulated near the location of Site 1, ASR Demonstration Site, for the assumption of pumping at all permitted wells: (A) regional groundwater flow; (B) after 64 months of injection; and (C) after 4 months of pumping. (D) Hydraulic head in the ASR well with time.

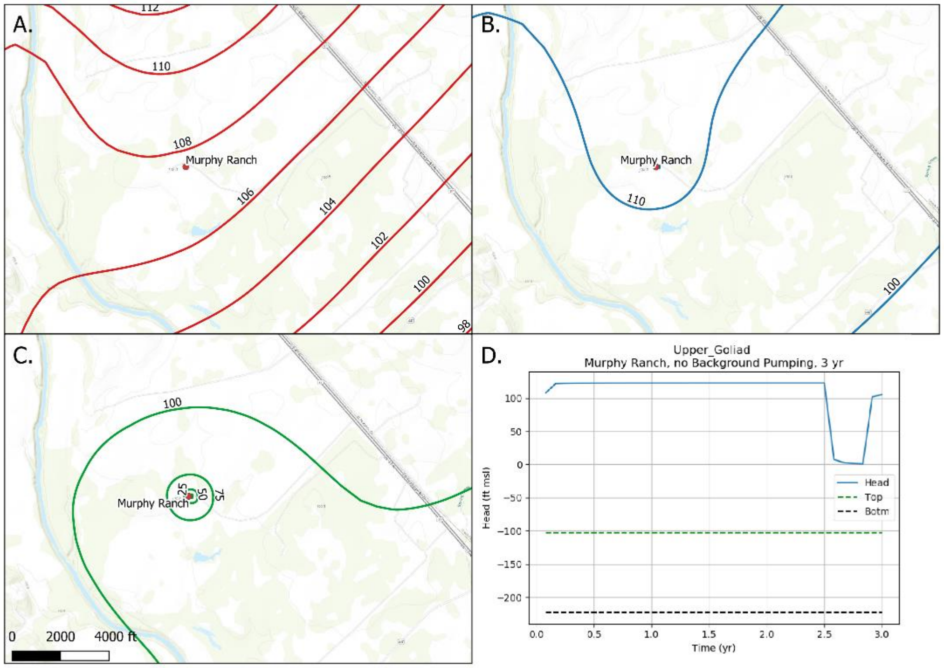

Figure 4-13a Hydraulic head contours simulated near the location of Site 2, Murphy Ranch, for the assumption of no pumping: (A) regional groundwater flow; (B) after 29 months of injection; and (C) after 4 months of pumping. (D) Hydraulic head in the ASR well with time.

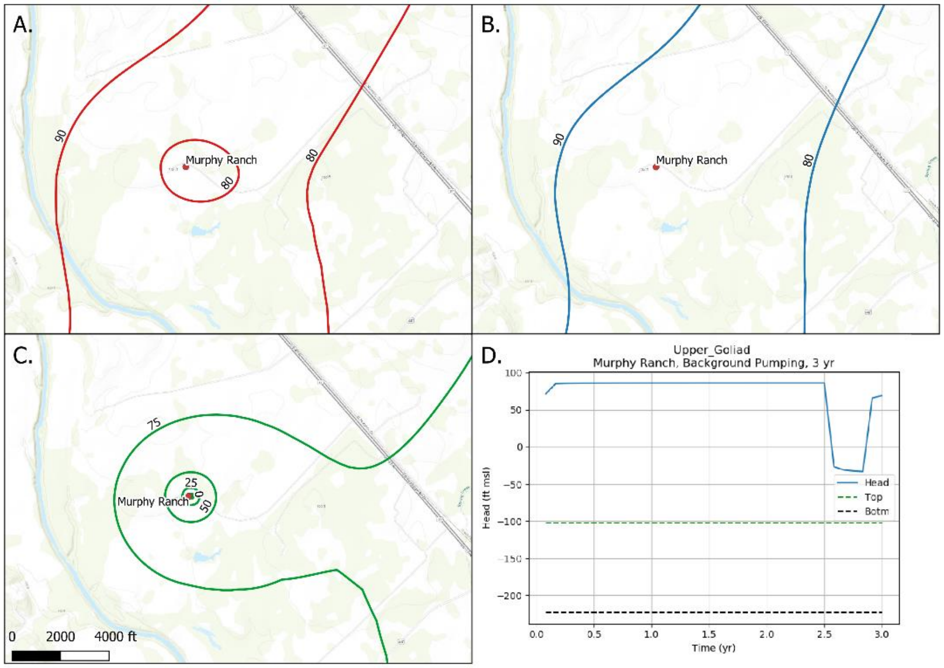

Figure 4-13b Hydraulic head contours simulated near the location of Site 2, Murphy Ranch, for the assumption of pumping at all permitted wells: (A) regional groundwater flow; (B) after 29 months of injection; and (C) after 4 months of pumping. (D) Hydraulic head in the ASR well with time.

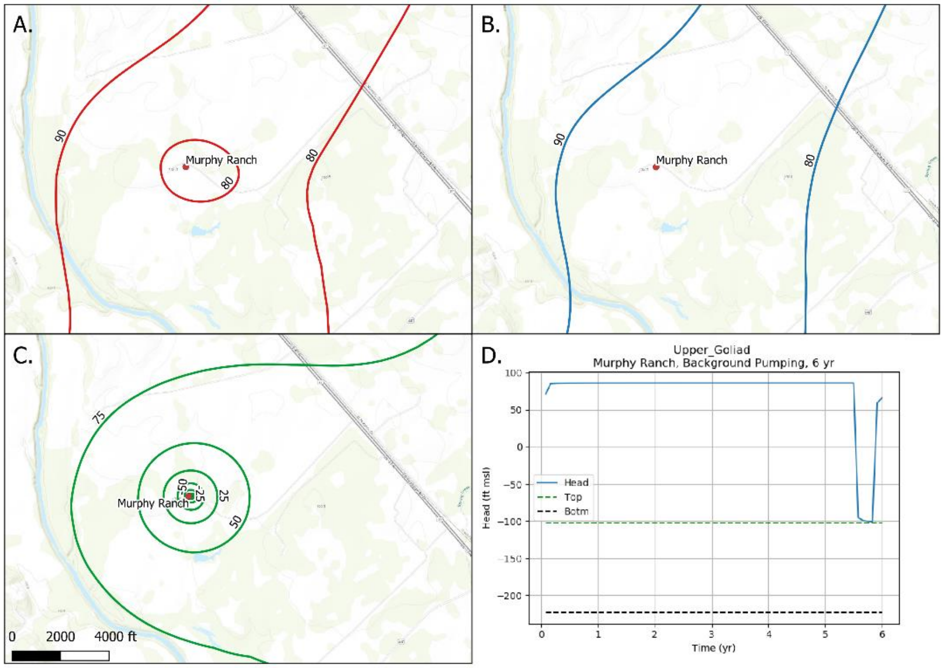

Figure 4-14a Hydraulic head contours simulated near the location of Site 2, Murphy Ranch, for the assumption of no pumping: (A) regional groundwater flow; (B) after 64 months of injection; and (C) after 4 months of pumping. (D) Hydraulic head in the ASR well with time.

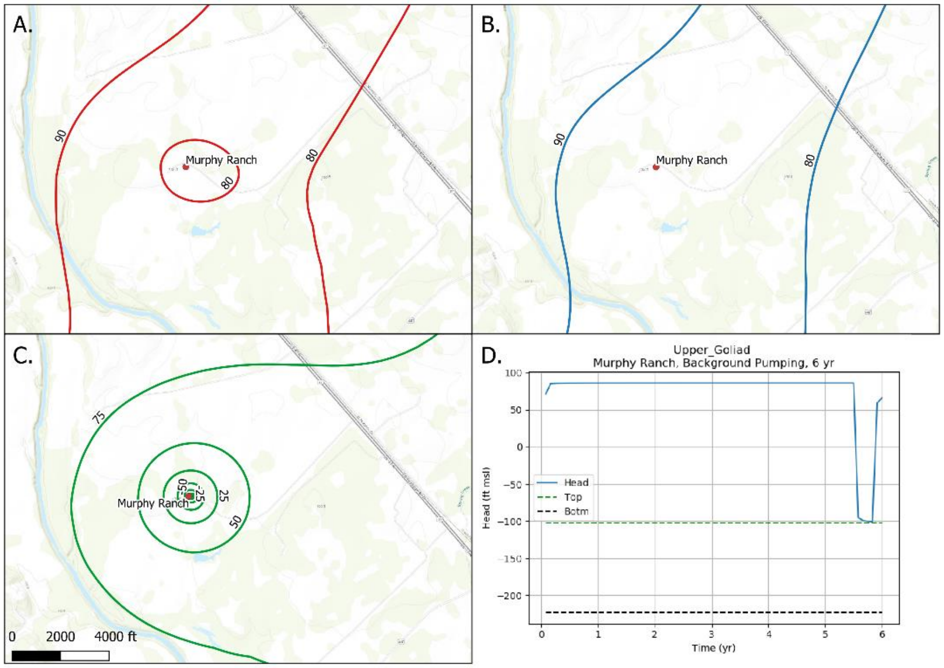

Figure 4-14b Hydraulic head contours simulated near the location of Site 2, Murphy Ranch, for the assumption of pumping at all permitted wells: (A) regional groundwater flow; (B) after 64 months of injection; and (C) after 4 months of pumping. (D) Hydraulic head in the ASR well with time.

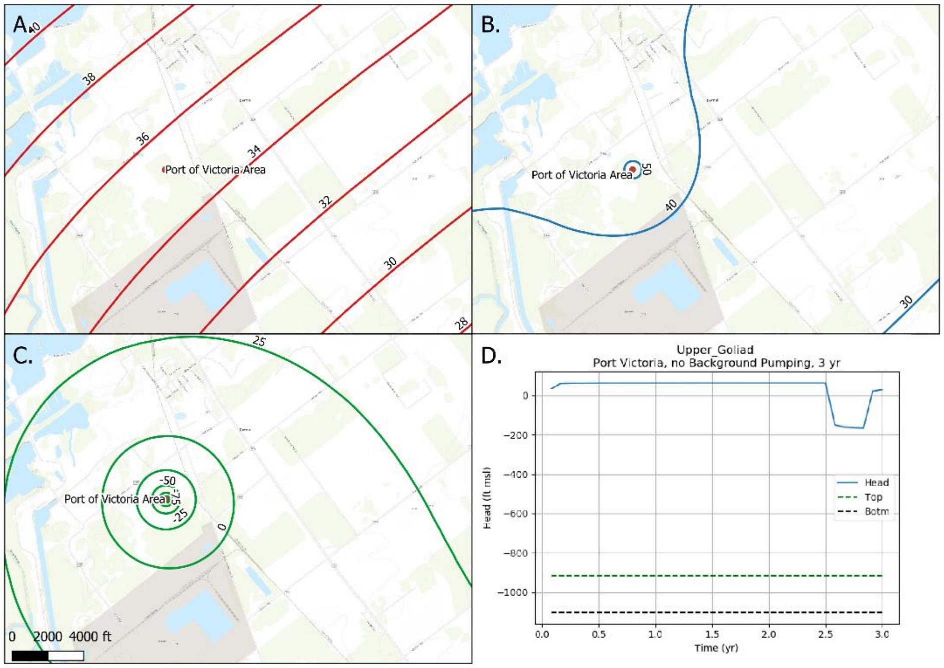

Figure 4-15a Hydraulic head contours simulated near the location of Site 3, Port Victoria, for the assumption of no pumping: (A) regional groundwater flow; (B) after 29 months of injection; and (C) after 4 months of pumping. (D) Hydraulic head in the ASR well with time.

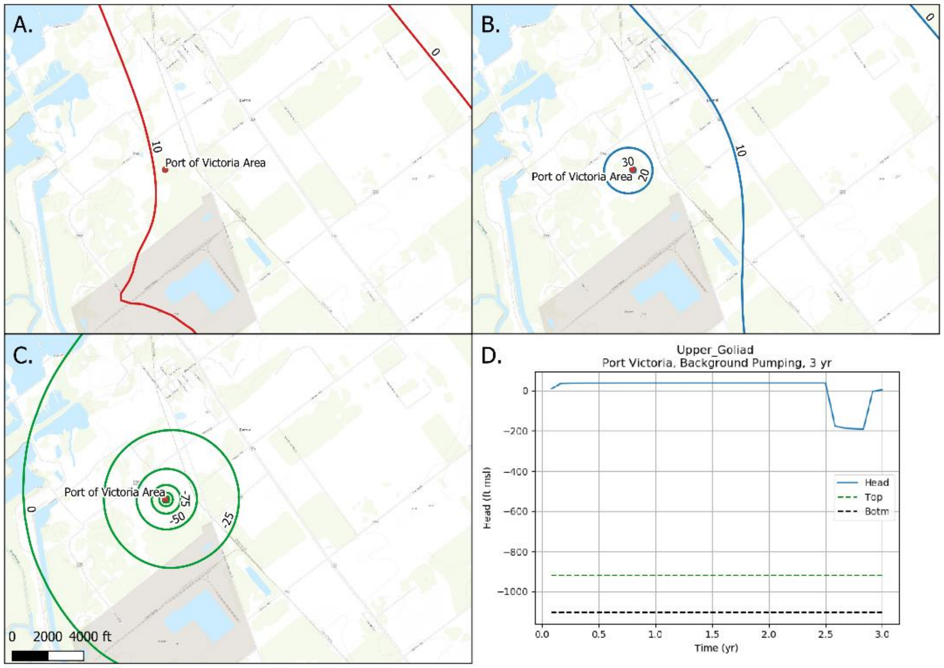

Figure 4-15b Hydraulic head contours simulated near the location of Site 3, Port Victoria, for the assumption of pumping at all permitted wells: (A) regional groundwater flow; (B) after 29 months of injection; and (C) after 4 months of pumping. (D) Hydraulic head in the ASR well with time.

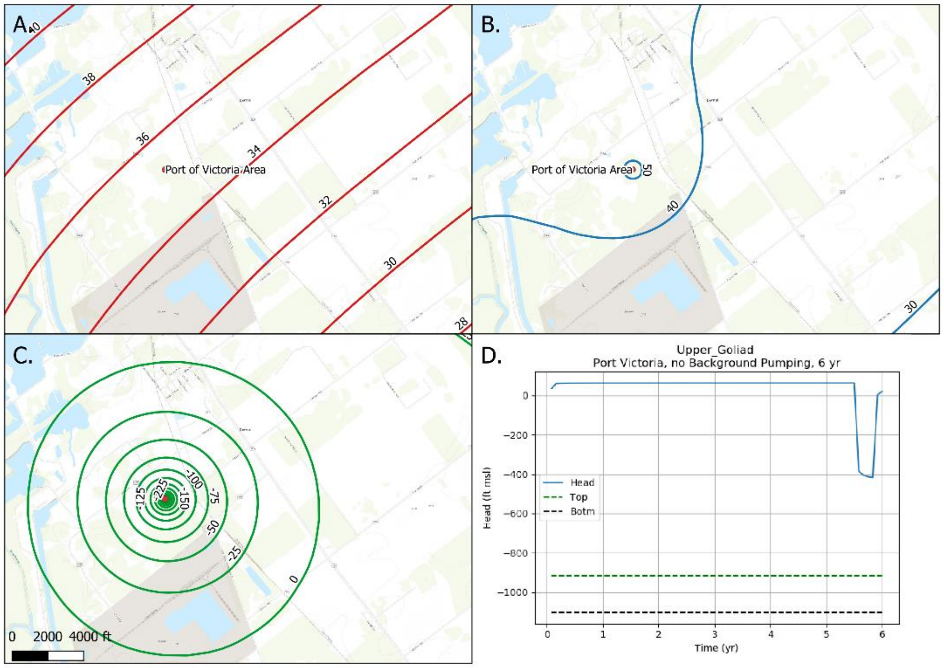

Figure 4-16a Hydraulic head contours simulated near the location of Site 3, Port Victoria Site, for the assumption of no pumping: (A) regional groundwater flow; (B) after 64 months of injection; and (C) after 4 months of pumping. (D) Hydraulic head in the ASR well with time.

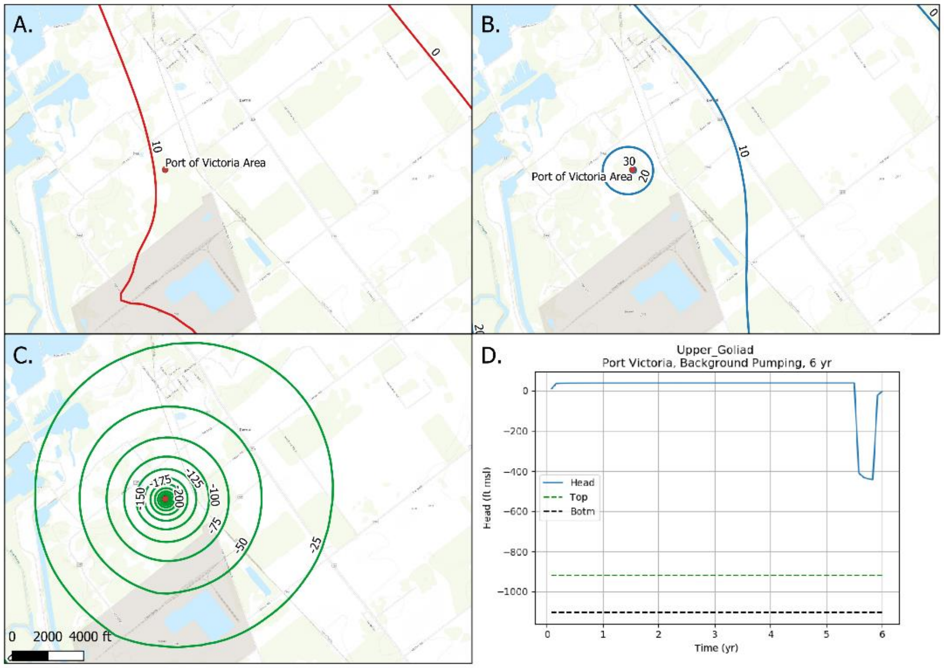

Figure 4-16b Hydraulic head contours simulated near the location of Site 3, Port Victoria, for the assumption of pumping at all permitted wells: (A) regional groundwater flow; (B) after 64 months of injection; and (C) after 4 months of pumping. (D) Hydraulic head in the ASR well with time.

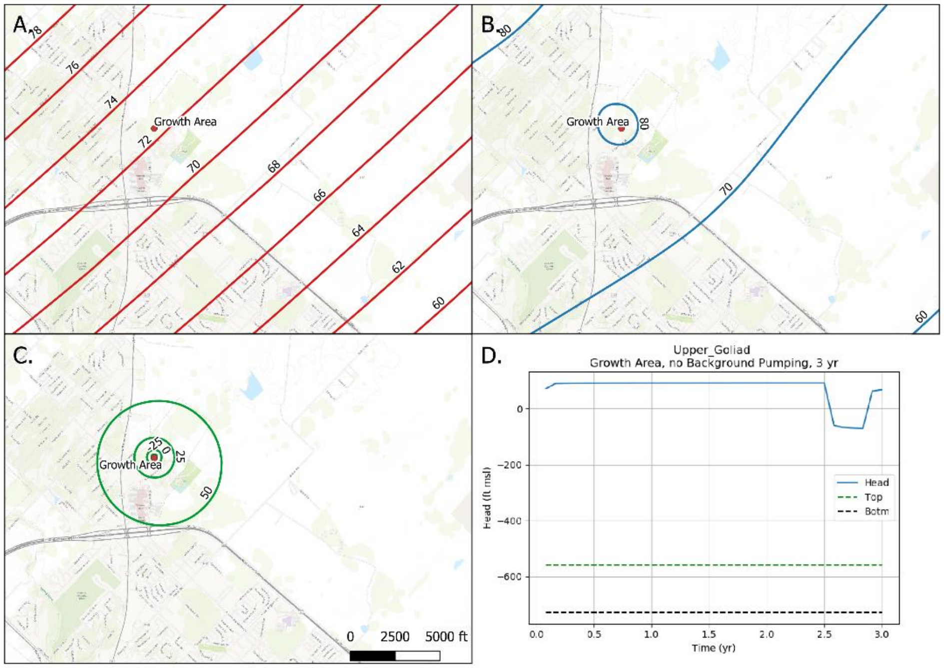

Figure 4-17a Hydraulic head contours simulated near the location of Site 4, Growth Area, for the assumption of no pumping: (A) regional groundwater flow; (B) after 29 months of injection; and (C) after 4 months of pumping. (D) Hydraulic head in the ASR well with time.

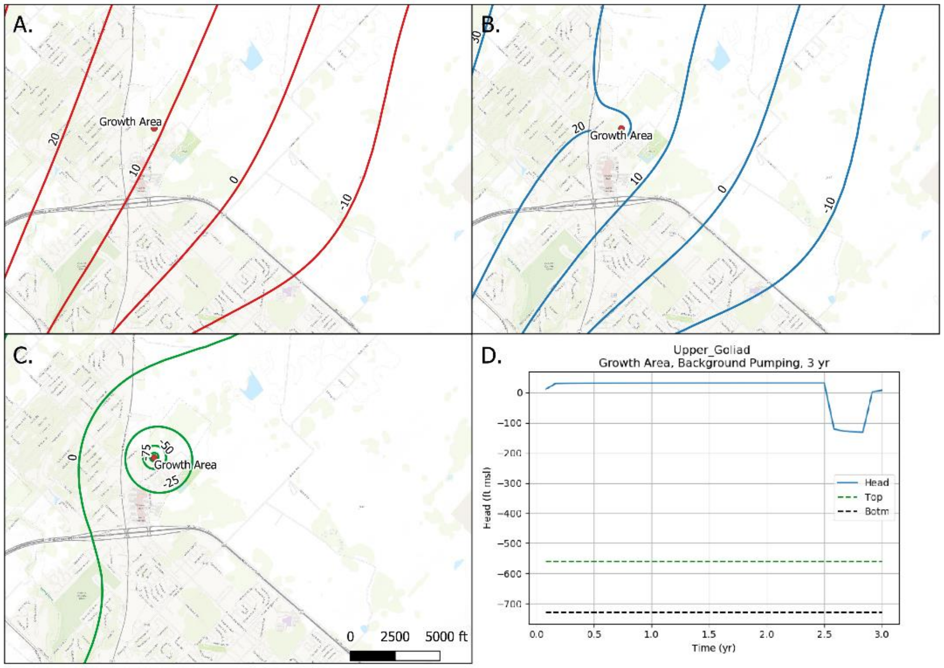

Figure 4-17b Hydraulic head contours simulated near the location of Site 4, Growth Area, for the assumption of pumping at all permitted wells: (A) regional groundwater flow; (B) after 29 months of injection; and (C) after 4 months of pumping. (D) Hydraulic head in the ASR well with time.

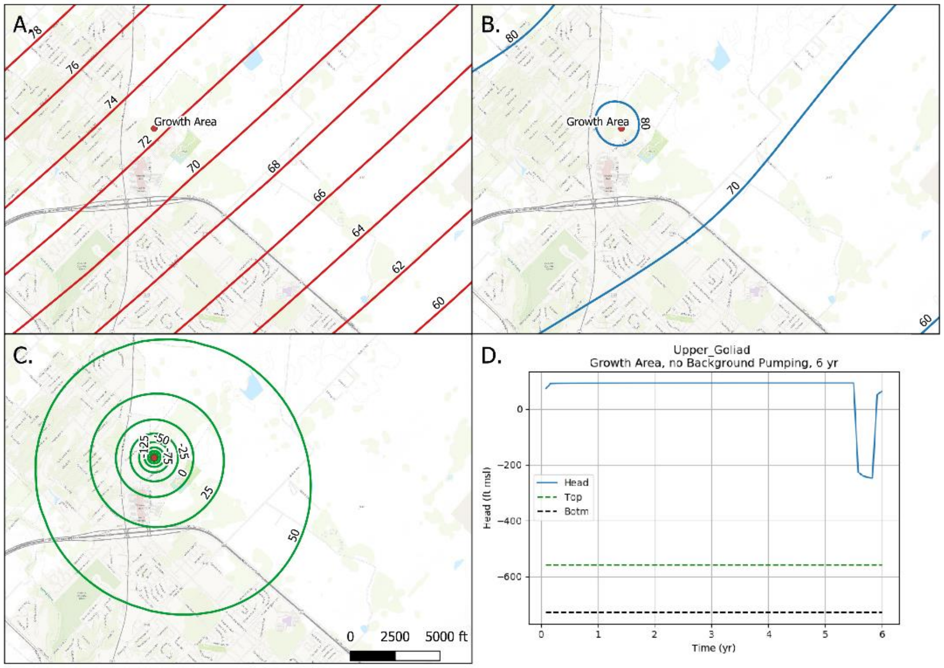

Figure 4-18a Hydraulic head contours simulated near the location of Site 4, Growth Area, for the assumption of no pumping: (A) regional groundwater flow; (B) after 64 months of injection; and (C) after 4 months of pumping. (D) Hydraulic head in the ASR well with time.

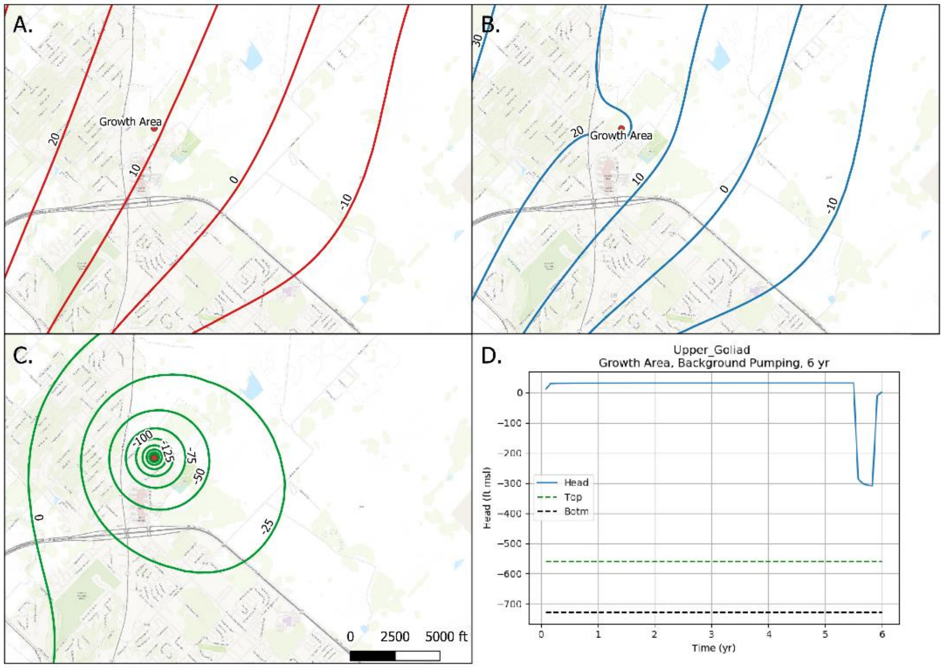

Figure 4-18b Hydraulic head contours simulated near the location of Site 4, Growth Area, for the assumption of pumping at all permitted wells: (A) regional groundwater flow; (B) after 64 months of injection; and (C) after 4 months of pumping. (D) Hydraulic head in the ASR well with time.

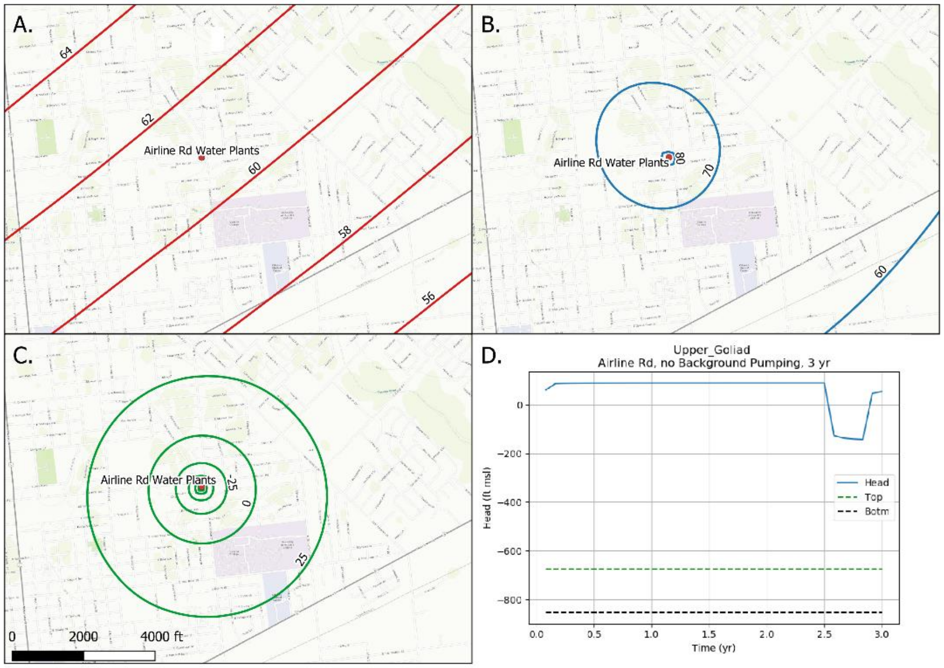

Figure 4-19a Hydraulic head contours simulated near the location of Site 5, Airline Road, for the assumption of no pumping: (A) regional groundwater flow; (B) after 29 months of injection; and (C) after 4 months of pumping. (D) Hydraulic head in the ASR well with time.

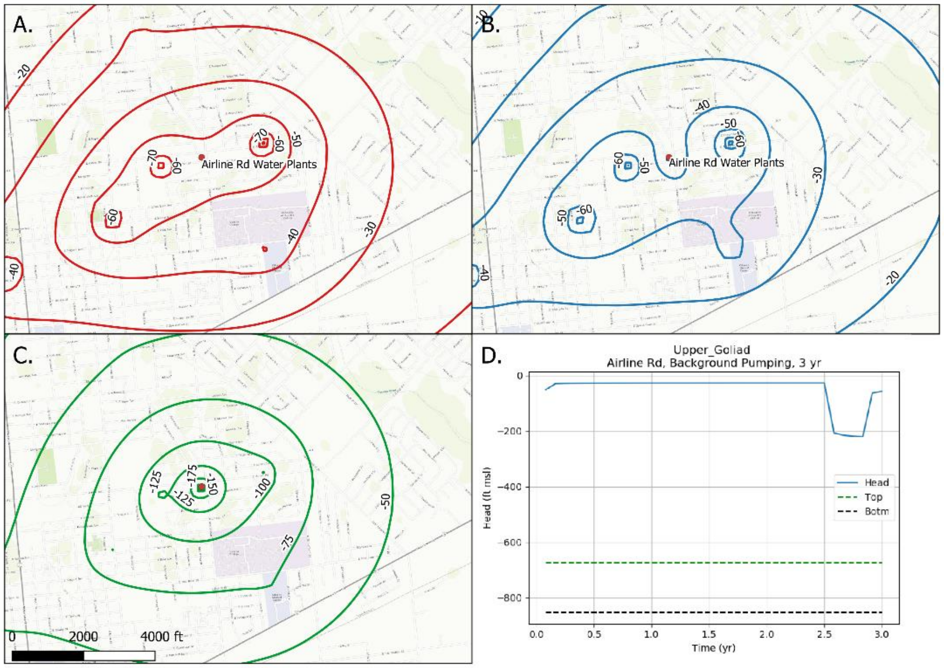

Figure 4-19b Hydraulic head contours simulated near the location of Site 5, Airline Road, for the assumption of pumping at all permitted wells: (A) regional groundwater flow; (B) after 29 months of injection; and (C) after 4 months of pumping. (D) Hydraulic head in the ASR well with time.

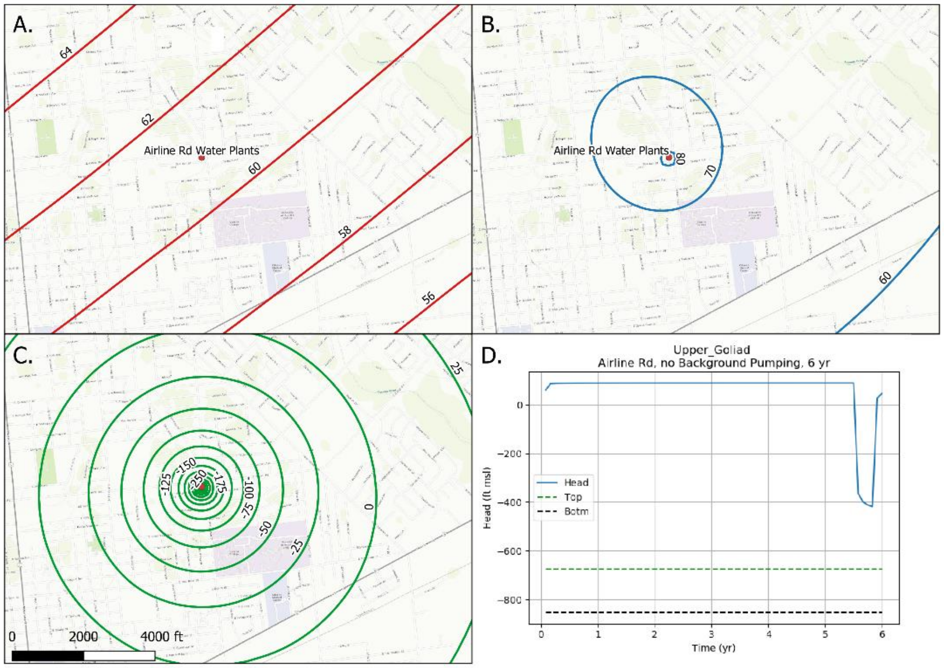

Figure 4-20a Hydraulic head contours simulated near the location of Site 5, Airline Road, for the assumption of no pumping: (A) regional groundwater flow; (B) after 64 months of injection; and (C) after 4 months of pumping. (D) Hydraulic head in the ASR well with time.

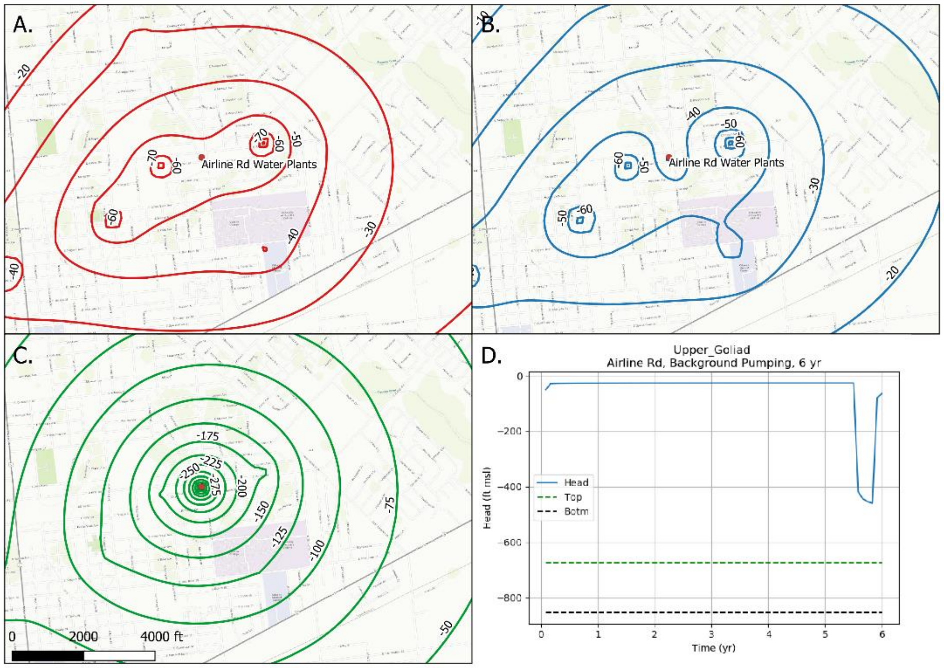

Figure 4-20b Hydraulic head contours simulated near the location of Site 5, Airline Road, for the assumption of pumping at all permitted wells: (A) regional groundwater flow; (B) after 64 months of injection; and (C) after 4 months of pumping. (D) Hydraulic head in the ASR well with time.

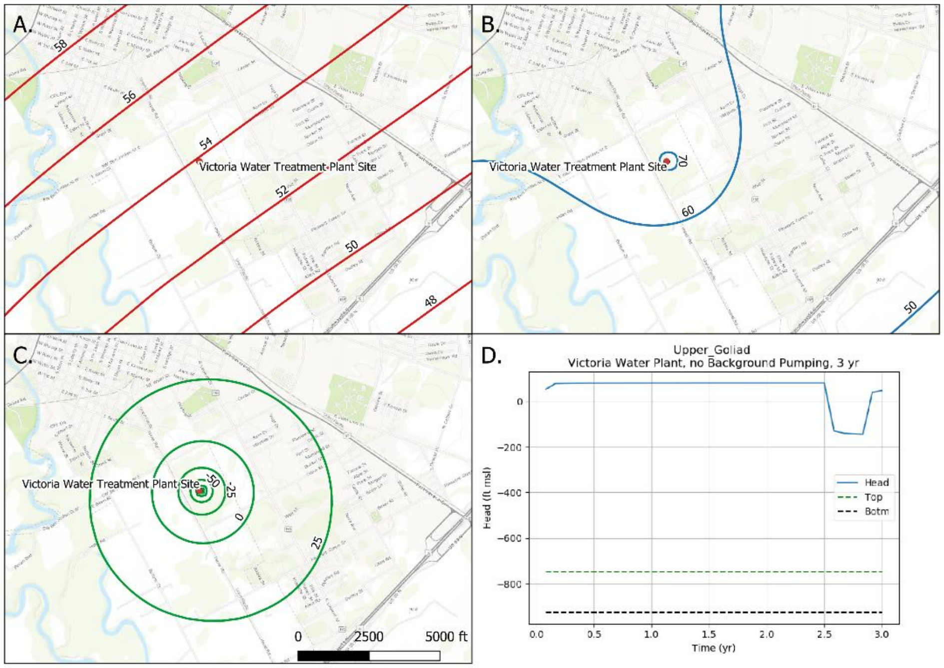

Figure 4-21a Hydraulic head contours simulated near the location of Site 6, Victoria Water, for the assumption of no pumping: (A) regional groundwater flow; (B) after 29 months of injection; and (C) after 4 months of pumping. (D) Hydraulic head in the ASR well with time.

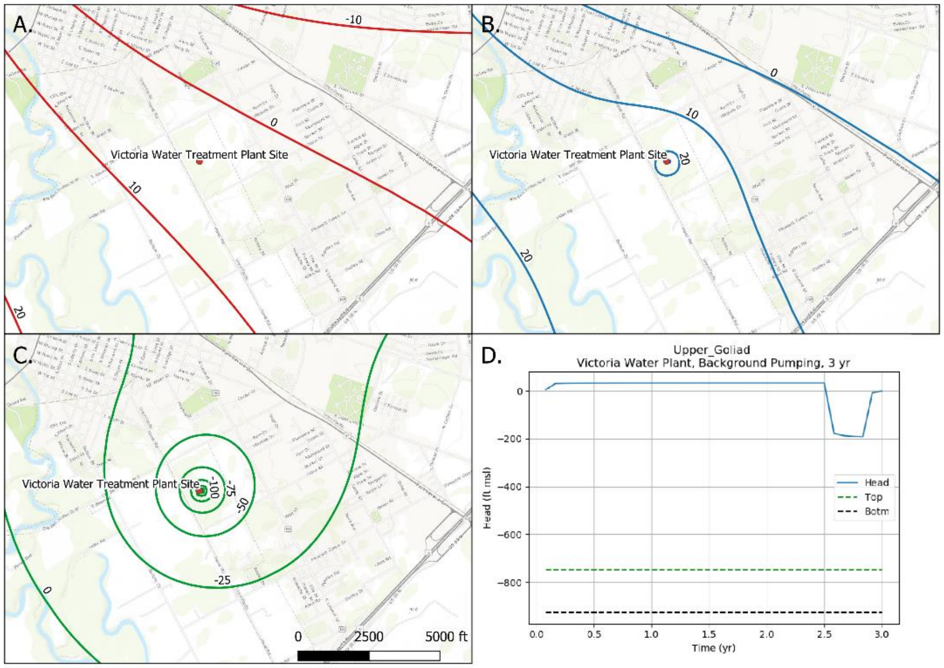

Figure 4-21b Hydraulic head contours simulated near the location of Site 6, Victoria Water, for the assumption of pumping at all permitted wells: (A) regional groundwater flow; (B) after 29 months of injection; and (C) after 4 months of pumping. (D) Hydraulic head in the ASR well with time.

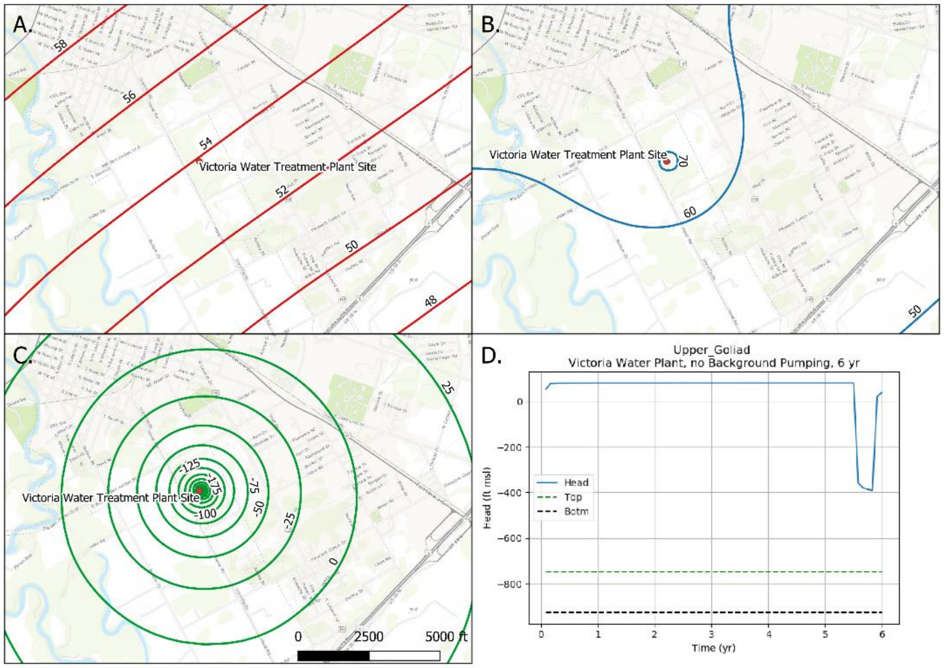

Figure 4-22a Hydraulic head contours simulated near the location of Site 6, Victoria Water, for the assumption of no pumping: (A) regional groundwater flow; (B) after 64 months of injection; and (C) after 4 months of pumping. (D) Hydraulic head in the ASR well with time.

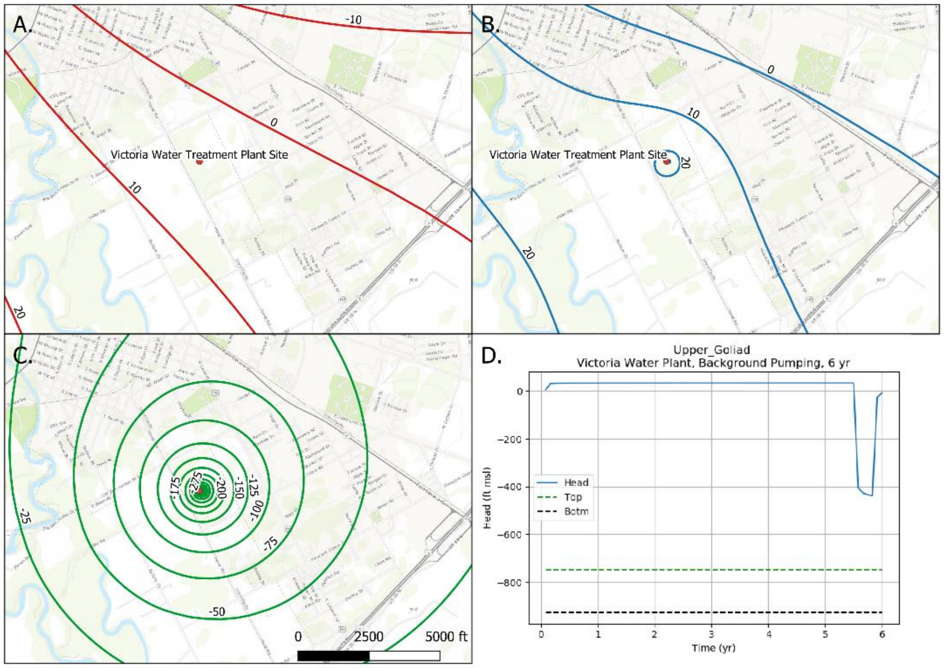

Figure 4-22b Hydraulic head contours simulated near the location of Site 6, Victoria Water, for the assumption of pumping at all permitted wells: (A) regional groundwater flow; (B) after 64 months of injection; and (C) after 4 months of pumping. (D) Hydraulic head in the ASR well with time.

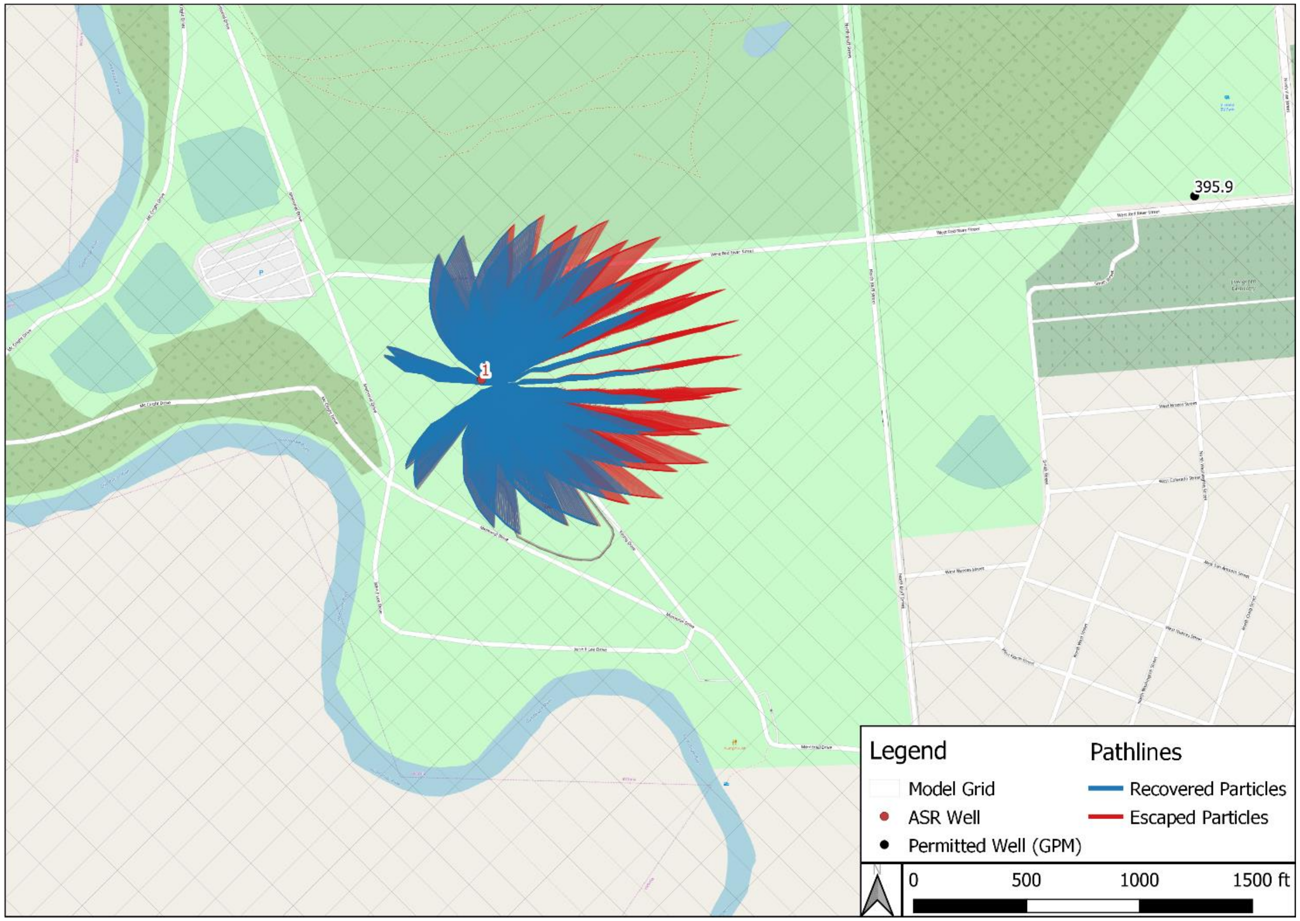

Figure 4-23 Pathlines for particles that were recovered and that escaped capture for the modeling scenario based on the Post-development scenario and a 64-month injection/4-month extraction for the ASR well operation at Site #1, ASR Demonstration Site.

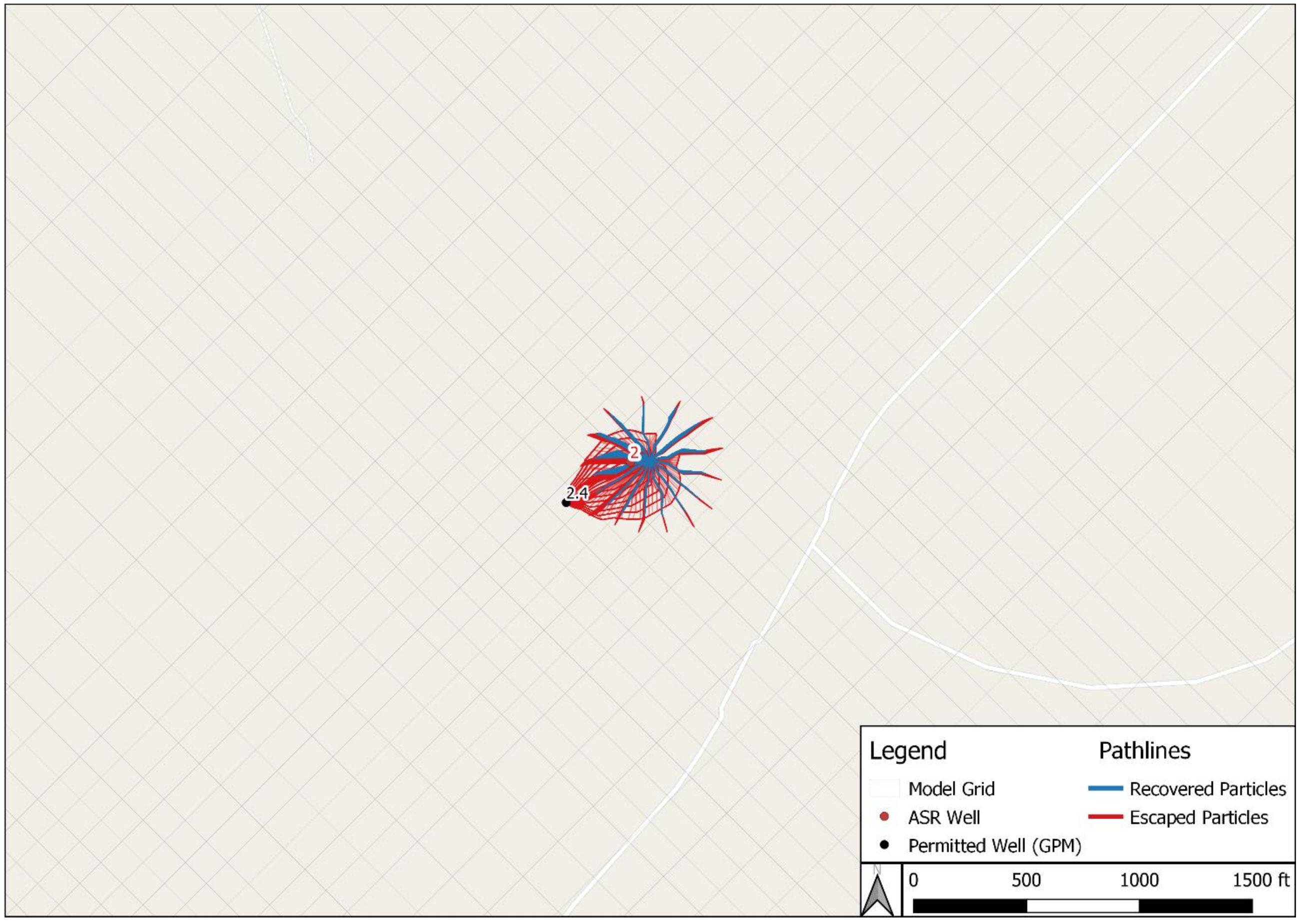

Figure 4-24 Pathlines for particles that were recovered and that escaped capture for the modeling scenario based on the Post-development scenario and a 64-month injection/4-month extraction for the ASR well operation at Site #2, Murphy Ranch Site.

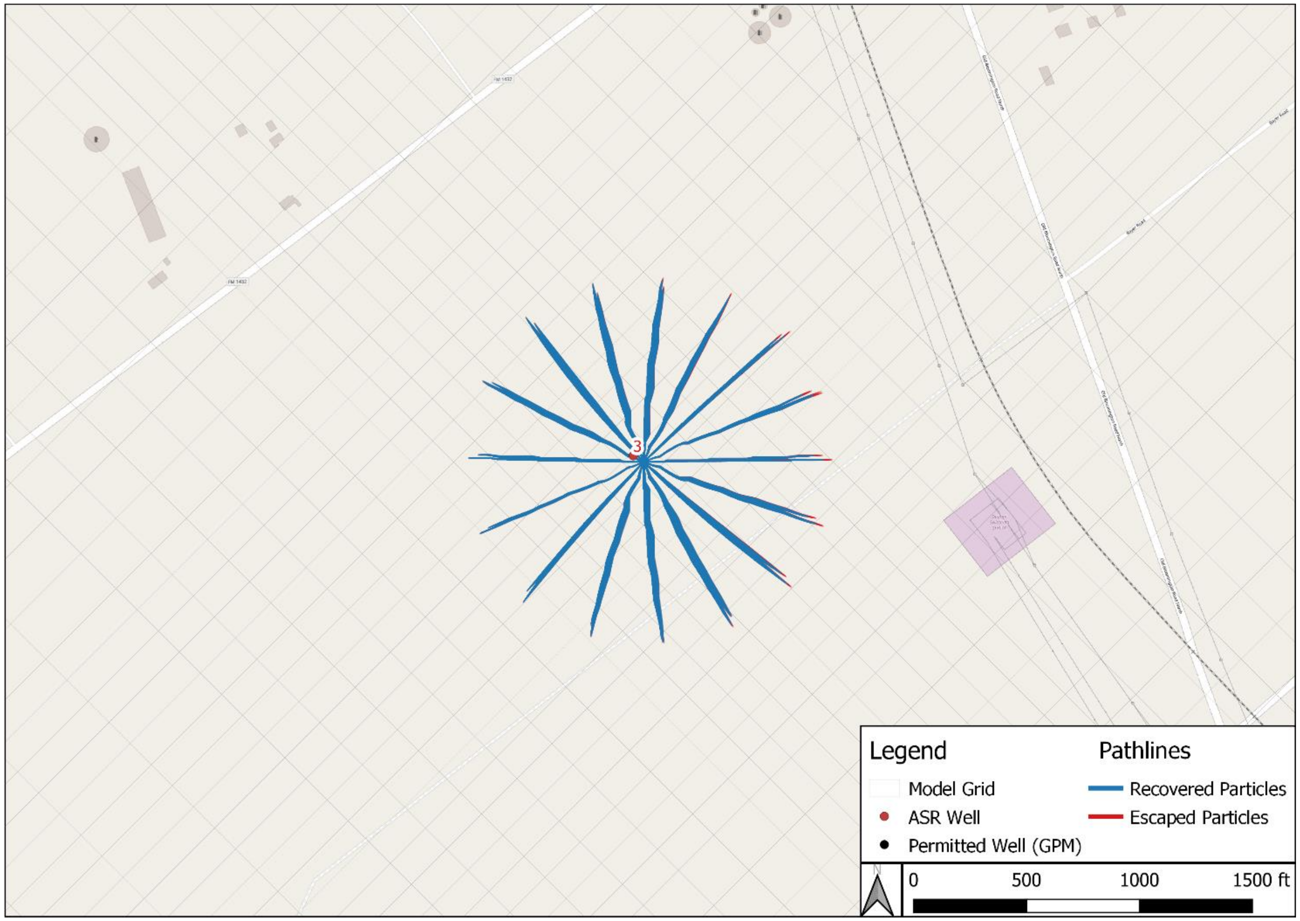

Figure 4-25 Pathlines for particles that were recovered and that escaped capture for the modeling scenario based on the Post-development scenario and a 64-month injection/4-month extraction for the ASR well operation at Site #3, Port Victoria Site.

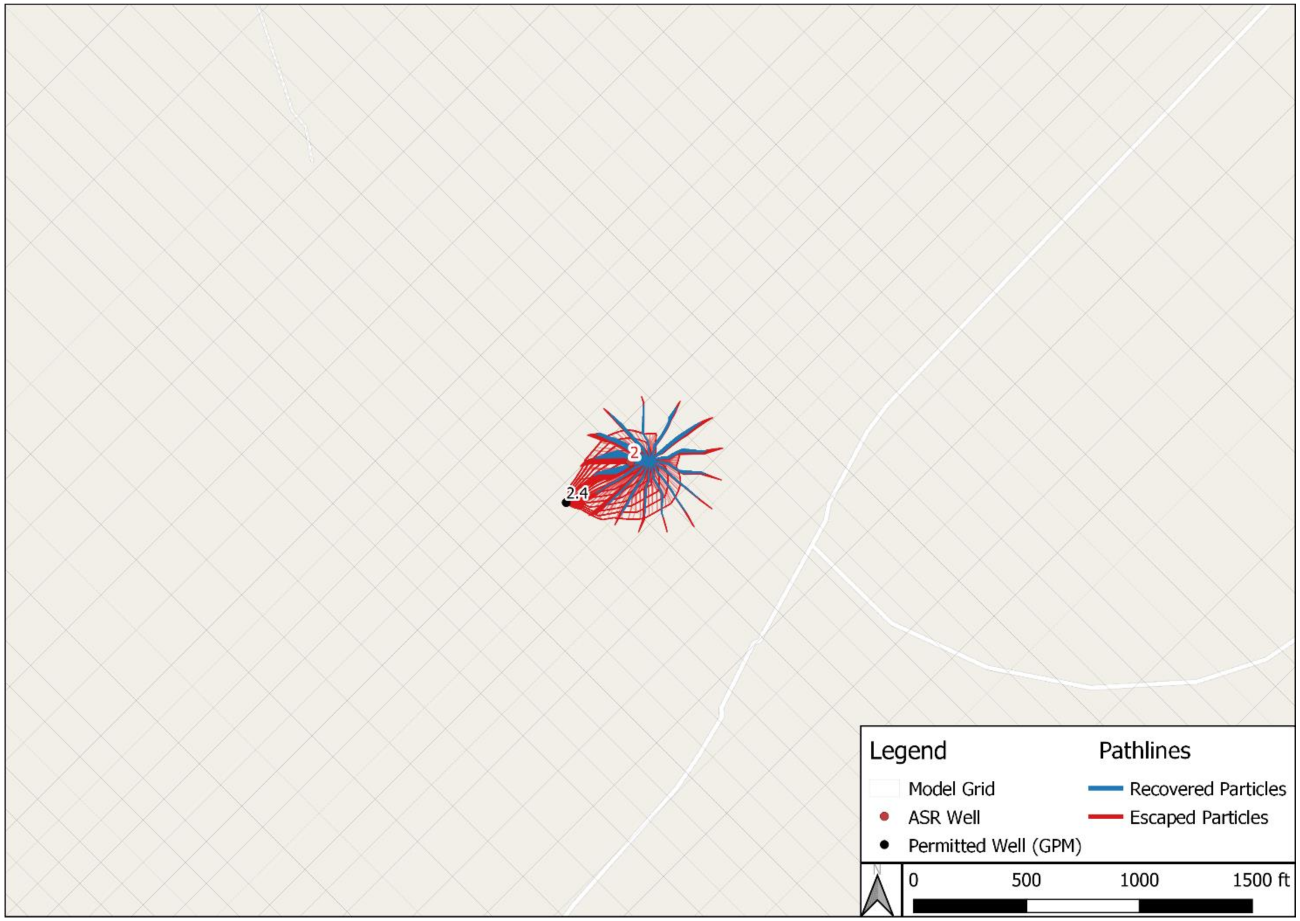

Figure 4-26 Pathlines for particles that were recovered and that escaped capture for the modeling scenario based on the Post-development scenario and a 64-month injection/4-month extraction for the ASR well operation at Site #4, Growth Area Site.

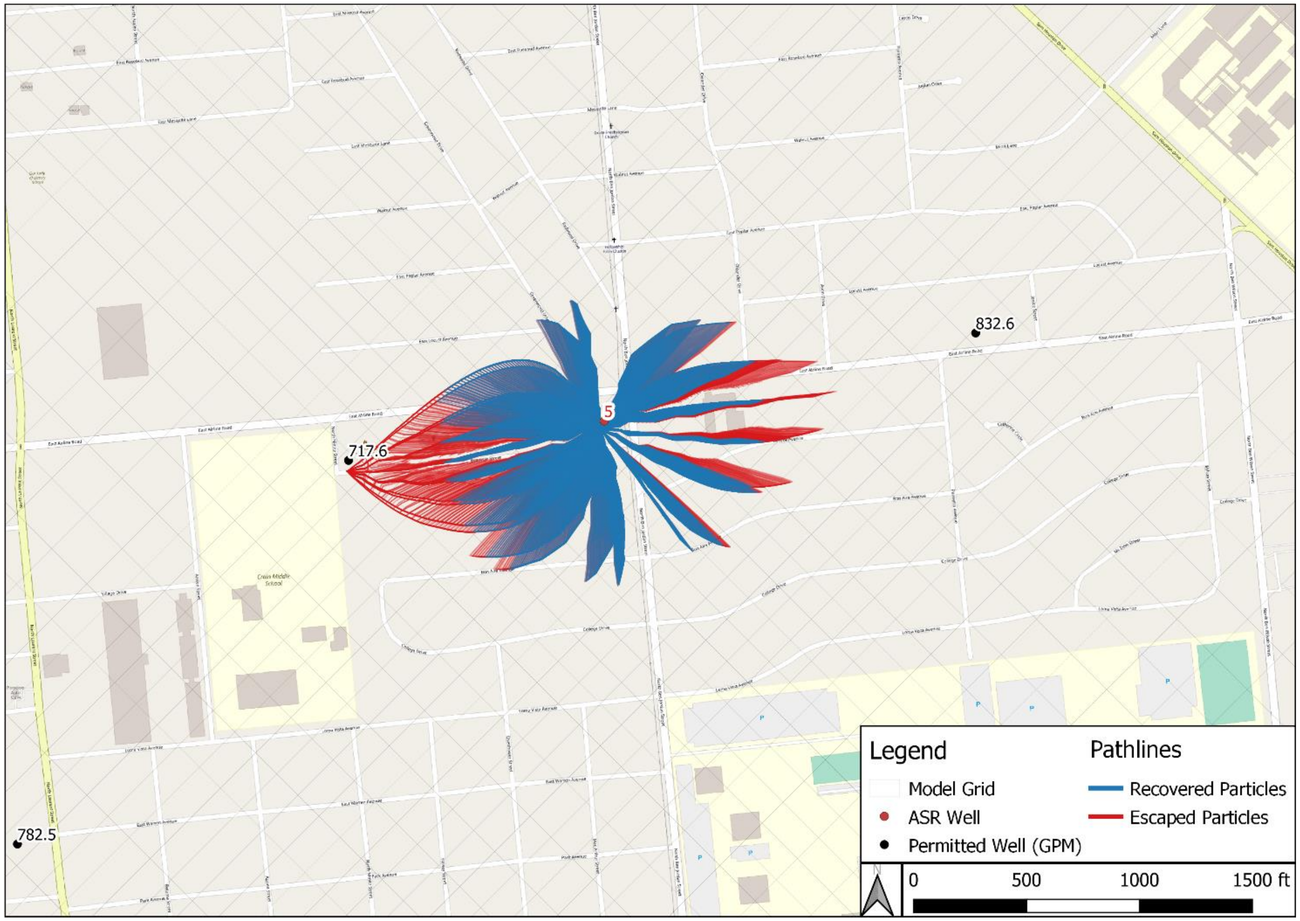

Figure 4-27 Pathlines for particles that were recovered and that escaped capture for the modeling scenario based on the Post-development scenario and a 64-month injection/4-month extraction for the ASR well operation at Site #5, Airline Road Site.

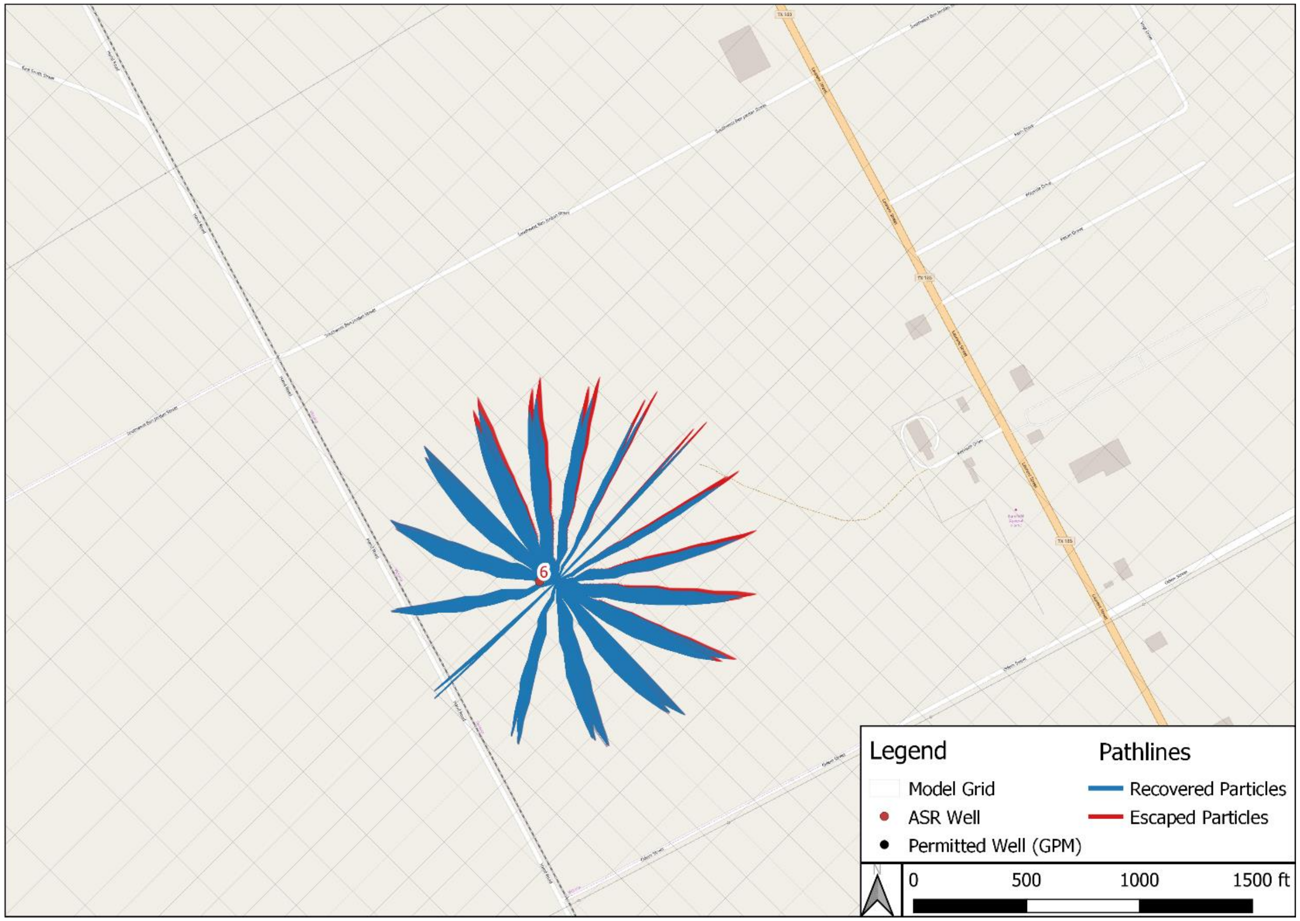

Figure 4-28 Pathlines for particles that were recovered and that escaped capture for the modeling scenario based on the Post-development scenario and a 64-month injection/4-month extraction for the ASR well operation at Site #6, Victoria Water Treatment Site.

This page intentionally left blank.

5.0 REFERENCES

American Water Works Association, 2015. Aquifer Storage and Recovery, AWWA Manual M63.

Arthur, J.D., Cowart, J.B. and Dabous, A. (2001) Florida Aquifer Storage and Recovery Geochemical Study: Year Three Progress Report. Florida Geological Survey Open File Report 83, 48 p. http://water.usgs.gov/ogw/pubs/ofr0289/jda_mobilization.htm

Austin, B.P. (2013) Email to F. Bloetscher Dated 4/10/13 Wisconsin ASR Wells.

Bear, J., and Jacobs, M. 1965. On the movement of water bodies injected into aquifers. Journal of Hydrology. 3(1) pg 37-57.

Bloetscher, F., Sham, C., Danko, J.J., and Ratick, S. 2014. Lessons Learned from Aquifer Storage and Recovery (ASR) Systems in the United States. Journal of Water Resource and Protection. Vol. 6 pg 1603-1629.

Harbaugh, A.W., 2005, MODFLOW-2005. The U.S. geological survey modular ground-water model – the ground-water flow process, Techniques and methods 6-A16: United States Geological Survey.

Harbaugh, A.W., and M.G. McDonald, 1996. User’s Documentation for MODFLOW-96, an update to the U.S. Geological Survey modular finite-difference ground-water flow model: United States Geological Survey, Open-File Report 96-485, 56 p.

Harbaugh, A.W., Banta, E.R., Hill, M.C., and McDonald, M.G., 2000, MODFLOW-2000, the U.S. Geological Survey modular groundwater model—User guide to modularization concepts and the groundwater flow process: United States Geological Survey, Open-File Report 00–92, 121 p.

Hughes, J.D., Langevin, C.D., and Banta, E.R., 2017, Documentation for the MODFLOW 6 framework: U.S. Geological Survey Techniques and Methods, book 6, chap. A57, 40 p., https://doi.org/10.3133/tm6A57.

Jones, G. W., 2015. Investigation of the Mechanisms for Mobilization of Arsenic in Two Arsenic ASR Systems in Southwest Central Florida. Graduate Theses and Dissertatoin. University of South Florida

Konikow, L.F., Goode, D.J., and Hornberger, G.Z. (1996). *A Three- Dimensional Method-of-Characteristics Solute–Transport Model (MOC3D).* U.S. Geological Survey Water Resources Investigation Report 96-4267. Reston, VA: U.S. Geological Survey.

Langevin, C.D., Hughes, J.D., Banta, E.R., Niswonger, R.G., Panday, Sorab, and Provost, A.M., 2017, Documentation for the MODFLOW 6 Groundwater Flow Model: U.S. Geological Survey Techniques and Methods, book 6, chap. A55, 197 p., https://doi.org/10.3133/tm6A55.

Malcolm Pirnie, 2011, An assessment of aquifer storage and recovery in Texas: contract report no. 0904830940 for the Texas Water Development Board, 200 p.

Maliva R. G., Guo, W. and Missimer, T, 2006. Aquifer Storage and Recovery: Recent Hydrogeological Advances and System Performance. Water Environment Research. Vol 78. Pag

Math Works, 2012. MATLAB: The Language of Technical Computing. Version 7. The MathWorks, Inc. Natick, MA

McDonald, M.G., and Harbaugh, A.W., 1988, A modular three-dimensional finite-difference ground-water flow model: United States Geological Survey: Techniques of Water-Resources Investigations, Book 6, chapter A1.

Moulder, E.A., and Frazer, D.R., 1957, Artificial recharge experiments at McDonald Field, Amarillo, Texas: U.S. Geological Survey Bulletin 5701, 34 p.

Muffles, C., Scantlebury, L., Wang, X., Tonkin, M., Neville, C., Ramadhan, M., and Craig, J., 2018. User Guide for mod-PATH3DU" A groundwater path and travel-time simulator. S. S. Papadpulos & Associates, Bethesda, MD.

Niswonger, R.G., Panday, S., and Ibaraki, M., 2011, MODFLOW-NWT, A Newton formulation for MODFLOW-2005: U.S. Geological Survey Techniques and Methods 6-A37, 44 p.

Panday, S., Langevin, C.D., Niswonger, R.G., Ibaraki, M., and Hughes, J.D., 2013, MODFLOW-USG version 1: An unstructured grid version of MODFLOW for simulating groundwater flow and tightly coupled processes using a control volume finite-difference formulation: U.S. Geological Survey Techniques and Methods, book 6, chap. A45, 66 p.

Parker, B. 2016. Addressing water needs using aquifer storage and recovery. House Research Organization- Texas House of Representatives Focus Report, prepared by House Research Organization, www.hro.house.state.tx.us. July 12, 2016. Pg 7.

Pollock, D.W., 1989, Documentation of a computer program to compute and display pathlines using results from the U.S Geological Survey modular three-dimensional finite-difference ground-water flow model: U.S. Geological Survey Open-File Report 89–381, 188 p.

Pollock, D.W. (1994). User's guide for MODPATH/MODPATH- PLOT, Version 3: A particle tracking post-processing package for MODFLOW. The U.S. Geological Survey finite-difference ground- water flow model. U.S. Geological Survey Open-File Report 94– 464, Reston, VA: U.S. Geological Survey.

Pollock, D.W., 2012, User guide for MODPATH version 6—A particle-tracking model for MODFLOW: U.S. Geological Survey Techniques and Methods, book 6, chap. A41, 58 p.

Reese, R. (2002) Inventory and Review of Aquifer Storage and Recovery in Southern Florida. U.S. Geological Survey Water-Resources Investigations Report 02-4036, USGS, Tallahassee.

Rhamadhan, M., 2015, A Semi-Analytical Particle Tracking Algorithm for Arbitrary Unstructured Grids. Unpublished MASc. Thesis. University of Waterloo, Waterloo Ontario.

Sundstrom, R.W., and Hood, J.W., 1952, Results of artificial recharge of the ground-water reservoir at El Paso, Texas: U.S. Geological Survey Bulletin 5206, 18 p.

TCEQ, 2018, TCEQ-20772, Application for Class V Underground Injection Control (UIC) Wells for an Aquifer Storage and Recovery (ASR) Project, TCEQ website https://view.officeapps.live.com/op/view.aspx?src=https%3A%2F%2Fwww.tceq.texas.gov%2Fassets%2Fpublic%2Fpermitting%2Fwaste%2Fuic%2FASR%2520applicaton%2520form.docx.

Texas Water Development Board, 1997, H.B. 1989 — Aquifer storage and recovery, a report to the 75th Legislature: Texas Water Development Board, 119 p.

TWDB, 2018. Aquifer Storage and Recovery Web Page. http://www.twdb.texas.gov/innovativewater/asr/index.asp. Texas Water Development Board, Austin Texas.

Ward, J., and Dillion, P. 2009. Robust Design of Managed Recharge Policy in Australia: Facilitating Recycycling of Stormwater and Reclaimed Water via Aquifer in Australia – Milestone Report 3.1. National Commission – Rising National Standards Project. National Water Commission. Australian Government.

Werth, C. University of Texas. Personal communication, March, 2019.

Young, S.C., Knox, P.R., Baker, E., Budge, T., Hamlin, S., Galloway, B., Kalbouss, R., and Deeds, N., 2010, Hydrostratigraphic of the Gulf Coast Aquifer from the Brazos River to the Rio Grande: Texas Water Development Board Report, 203 p.

Young, S. C., and R. Kushnereit. 2018. Characterization of Brackish Groundwater Resources in Victoria County. Prepared for the Victoria Groundwater Conservation District, Prepared by INTERA. Austin. Texas

Zheng, C. (1990). MT3D User's Manual: A Modular Three-Dimensional Transport Model for Simulation of Advection, Dispersion, and Chemical Reactions of Contaminants in Groundwater Systems. Bethesda, MD: S.S. Papadopulos and Associates.

Zheng, C., 1992, PATH3D, A ground-water path and travel-time simulator, version 3.2 user's manual, S.S. Papadopulos & Associates, Inc., Bethesda, MD.

This page intentionally left blank.

Appendix A

Table A-1: List of permitted wells and their pumping rates used to generate the Post-development modeling scenario

Well ID	Latitude	Longitude	Pumping Rate (GPM)	Top of Screen	Bottom of Screen	Model Layer(s)
GW-000005	28.82097	-96.9843	98394.91	-363	-899	4,5,6,7
GW-000006	28.82074	-96.9876	138146.9	-359	-909	4,5,6,7
GW-000007	28.82208	-96.9789	160275.8	-352	-902	4,5,6,7
GW-000008	28.82215	-96.9734	34045.37	-355	-703	4,5,6
GW-000009	28.81067	-97.0197	79190.35	-451	-989	4,5,6,7
GW-000010	28.81388	-96.9789	74282.77	-300	-870	3,4,5,6
GW-000011	28.81266	-97.0098	76207.64	-334	-894	4,5,6,7
GW-000012	28.83051	-96.9894	39761.54	-280	-877	3,4,5,6,7
GW-000013	28.8162	-96.9924	150727.7	-308	-922	3,4,5,6,7
GW-000014	28.81234	-97.0018	167957.3	-343	-953	4,5,6,7
GW-000091	28.6753	-97.0494	6082.3	-18	-28	2
GW-000107	28.92172	-97.225	1793.682	-109	-129	8,9
GW-000108	28.92362	-97.2233	1793.682	-90	-130	9
GW-000139	28.69334	-96.8989	1788.912	-186	-226	2
GW-000239	28.86673	-96.8608	114848.1	-864	-914	6
GW-000240	28.84061	-97.0196	36016.76	-201	-251	3,4
GW-000246	28.8765	-97.0331	983.9014	-138	-188	4
GW-000309	28.6329	-97.0033	1646.991	-154	-174	2
GW-000311	28.6474	-96.8951	27864.09	-906	-956	5
GW-000312	28.64401	-96.9015	20289.84	-892	-942	5
GW-000314	28.67845	-96.9525	16054.89	-943	-993	6
GW-000314	28.67845	-96.9525	10898.05	-943	-993	6
GW-000315	28.67567	-96.9569	10898.05	-941	-991	6
GW-000315	28.67567	-96.9569	16054.89	-941	-991	6
GW-000317	28.66558	-96.9605	11806.82	-15	-71	2
GW-000318	28.66542	-96.9634	5605.257	9	-21	2
GW-000319	28.66492	-96.9629	6082.3	-5	-35	2
GW-000340	28.9329	-97.1396	171258.5	-222	-620	6,7,8,9,10
GW-000366	28.97341	-96.8549	46440.15	-646	-696	6,7
GW-000376	28.83307	-96.8814	10336.33	-131	-301	2,3
GW-000377	28.90129	-96.7978	21.46694	22	-28	1
GW-000451	28.66477	-96.9628	4484.205	65	3	2
GW-000464	28.96394	-96.8924	144273.3	-517	-567	6
GW-000466	28.96111	-96.8828	144273.3	-582	-632	6
GW-000474	28.84709	-96.8395	26131.23	-186	-236	2
GW-000475	28.84696	-96.839	26131.23	-186	-236	2

Well ID	Latitude	Longitude	Pumping Rate (GPM)	Top of Screen	Bottom of Screen	Model Layer(s)
GW-000476	28.83979	-96.8439	26131.23	-191	-241	2
GW-000477	28.83993	-96.8437	26131.23	-186	-236	2
GW-000478	28.84729	-96.822	166011	-490	-540	3
GW-000510	28.82055	-97.0236	17137.77	-54	-260	2,3,4
GW-000532	28.8306	-96.9516	53428.83	-307	-357	3
GW-000542	28.89472	-97.1325	5945.15	-59	-115	4
GW-000559	28.89314	-96.9068	231962.2	-911	-961	7,8
GW-000560	28.88839	-96.9173	231962.2	-906	-956	7,8
GW-000561	28.88806	-96.8966	231962.2	-983	-1033	8
GW-000568	28.69248	-96.9664	560.5257	-175	-255	2,3
GW-000569	28.70027	-96.9517	202.7433	-102	-144	2
GW-000571	28.82246	-97.0706	471.0801	-72	-87	3
GW-000678	28.89875	-97.1921	170.5429	-99	-149	7
GW-000683	28.85101	-96.891	29.8152	19	-1	1
GW-000687	28.92223	-97.1002	298.152	16	-4	3,4
GW-000693	28.89894	-97.1908	614.193	-29	-79	6
GW-000696	28.8886	-96.8264	653.5491	-603	-633	4
GW-000697	28.8878	-96.8242	322.0041	-510	-535	4
GW-000713	28.75967	-97.1455	548.1225	-159	-179	4
GW-000719	28.90239	-96.9946	200.3581	75	25	2
GW-000732	28.7456	-96.8723	2862.259	-196	-805	2,3,4,5
GW-000732	28.7456	-96.8723	57567.66	-196	-805	2,3,4,5
GW-000733	28.76038	-96.8848	48776.11	-95	-480	2,3
GW-000754	28.80008	-96.8007	186046.8	-243	-643	2,3,4
GW-000755	28.82029	-96.7726	171735.5	-249	-649	2,3
GW-000756	28.80541	-96.8051	200358.1	-253	-653	2,3,4
GW-000768	28.67051	-96.8546	954.0862	-146	-166	2
GW-000773	28.67014	-96.8537	834.8255	-146	-166	2
GW-000972	28.76378	-96.9024	31622	-81	-456	2,3
NW-000101	28.82362	-97.0683	280.2628	-30	-110	3
NW-000111	28.86357	-97.1035	4840.795	-69	-109	4
NW-000116	28.69361	-96.8986	10578.43	-180	-220	2
NW-000118	28.81541	-97.0621	156.2316	-100	-140	3
NW-000119	28.87111	-96.8569	357.7823	-4	-34	1,2
NW-000149	28.90056	-96.9936	369.7084	70	60	2
NW-000161	28.90945	-97.0814	1592.131	-135	-175	4,5
NW-000206	28.78333	-97.105	298.152	44	24	2
NW-000207	29.06699	-96.9865	53.66735	97	77	2
NW-000208	28.90223	-97.0758	119.2608	10	0	3

Well ID	Latitude	Longitude	Pumping Rate (GPM)	Top of Screen	Bottom of Screen	Model Layer(s)
NW-000209	28.78472	-97.1061	298.152	-161	-181	4
NW-000210	28.74444	-97.1161	322.0041	-96	-116	3
NW-000211	28.81858	-97.0873	596.3039	-99	-119	4
NW-000212	28.78444	-97.1047	298.152	-136	-156	4
NW-000217	28.77	-97.0983	816.9363	37	17	2
NW-000314	28.82214	-97.065	214.6694	-160	-180	4
NW-000320	28.78431	-97.1071	298.152	36	16	2
NW-000332	28.65232	-96.8872	1252.238	-318	-338	3
NW-000346	28.78444	-97.1039	298.152	-141	-161	4
NW-000361	28.78194	-97.0664	954.0862	4	-14	2
NW-000371	28.87139	-97.0367	1013.717	-72	-92	3
NW-000384	28.78361	-97.1025	149.076	-156	-196	4
NW-000388	28.78455	-97.0765	593.9187	-156	-256	3,4
NW-000397	28.81472	-97.0786	1107.933	13	-1007	2,3,4,5,6,7,8,9
NW-000406	29.06722	-96.9872	119.2608	100	80	2
NW-000409	28.82389	-97.0672	351.8193	-90	-110	3
NW-000410	28.86166	-97.1133	238.5216	-111	-131	4
NW-000416	28.81704	-97.0742	178.8912	-117	-137	4
NW-000426	28.92413	-97.2186	3807.997	-90	-150	9
NW-000428	28.88305	-97.0594	218.2472	70	50	2
NW-000429	28.81861	-97.0889	226.5955	19	-1	2,3
NW-000430	28.78416	-97.1053	298.152	-156	-196	4
NW-000431	28.84278	-96.9067	0.119261	-13	-23	2
NW-000432	28.84306	-96.9061	0.119261	-9	-25	2
NW-000433	28.84306	-96.9061	0.119261	56	46	1
NW-000434	28.84278	-96.9061	0.119261	-5	-25	2
NW-000435	28.84306	-96.9055	0.119261	53	43	1
NW-000436	28.84333	-96.9058	0.119261	53	43	1
NW-000437	28.78444	-97.1028	238.5216	-136	-156	4
NW-000443	28.85612	-96.8419	26833.68	-49	-109	2
NW-000451	28.7836	-97.1062	232.5585	-132	-152	4
NW-000453	28.87433	-97.1224	13714.99	-78	-138	4,5
NW-000454	28.92667	-96.9955	801.4324	-71	-151	3,4
NW-000460	28.82245	-97.0679	295.7667	-113	-133	3,4
NW-000474	28.84389	-96.9019	214.6694	-24	-44	2
NW-000481	28.90624	-97.0799	155.039	25	-15	3,4
NW-000483	28.68386	-96.8547	34871.85	-64	-144	2
NW-000499	28.81801	-97.0725	238.5216	-132	-152	4
NW-000510	28.83946	-97.1277	64.40082	-18	-38	4

Well ID	Latitude	Longitude	Pumping Rate (GPM)	Top of Screen	Bottom of Screen	Model Layer(s)
NW-000513	28.89305	-97.1551	238.5216	-96	-136	5,6
NW-000533	28.85447	-96.8372	238.5216	-35	-55	1,2
NW-000559	28.84692	-96.8217	3667.269	-189	-214	2
NW-000563	28.77585	-96.9578	477.0431	-28	-48	2
NW-000573	28.65974	-97.0447	3249.856	-117	-177	2,3
NW-000590	28.93138	-96.9353	19439.51	-89	-209	2,3
NW-000591	28.82027	-97.0667	262.3737	-195	-235	4
NW-000595	28.78778	-97.0947	333.9302	34	-6	2
NW-000600	28.6458	-97.1067	5963.039	-60	-100	2,3
NW-000601	28.69054	-97.0339	5963.039	-68	-98	2
NW-000609	28.86302	-96.8718	178.8912	2	-18	1,2
NW-000618	28.65531	-96.9536	19236.76	-239	-279	2,3
NW-000622	28.78083	-97.1022	298.152	-156	-196	4
NW-000625	28.80417	-96.9158	119.2608	-120	-140	2
NW-000626	28.75862	-97.0464	6618.973	17	-33	2
NW-000629	28.72317	-97.0381	131.1869	-46	-66	2
NW-000632	28.84778	-96.9042	228.9807	-27	-67	2
NW-000638	28.89448	-96.9939	119.2608	86	66	2
NW-000651	28.86312	-96.871	136.9114	2	-18	1,2
NW-000672	28.66555	-97.0183	4770.431	-249	-289	3
NW-000682	29.05501	-97.0089	5333.342	27	-13	4
NW-000707	28.78445	-97.1006	298.152	-136	-176	4
NW-000708	28.86381	-96.8724	178.8912	2	-18	1,2
NW-000709	28.78445	-97.1014	298.152	-154	-194	4
NW-000715	28.84192	-96.8109	2027.433	-82	-102	2
NW-000718	28.89869	-97.2123	262.3737	20	-20	6
NW-000722	29.02238	-97.0421	43291.66	58	-62	2,3,4,5
NW-000747	28.66471	-96.8655	3732.862	-164	-204	2
NW-000750	28.79279	-96.8589	3577.823	-170	-230	2
NW-000759	28.73991	-96.9471	572.4517	-140	-180	2
NW-000780	28.86472	-96.8725	135.9573	12	-8	1
NW-000795	28.80102	-97.0883	119.2608	-45	-65	3
NW-000803	28.71023	-96.8597	707.2164	-144	-184	2
NW-000809	28.86901	-96.8655	357.7823	-3	-23	1,2
NW-000824	28.81194	-97.0825	88.25298	-199	-284	4,5
NW-000827	28.71138	-96.8636	22562.95	-187	-267	2
NW-000846	28.95221	-97.0658	17390.61	-173	-223	5
NW-000869	28.91322	-96.9942	560.5257	-71	-91	3
NW-000872	28.90322	-96.9933	71.55647	70	50	2

Well ID	Latitude	Longitude	Pumping Rate (GPM)	Top of Screen	Bottom of Screen	Model Layer(s)
NW-000887	28.9075	-96.9925	596.3039	-75	-95	3
NW-000973	28.78139	-97.1039	286.2259	24	4	2
NW-001059	28.91394	-97.0006	120.4534	-105	-125	3
NW-001142	28.90167	-96.7883	87.65667	15	-5	1
NW-001160	28.70113	-96.9506	894.4559	-102	-122	2
NW-001161	28.70194	-96.9492	894.4559	-112	-122	2
NW-001188	28.80778	-96.9981	238.5216	34	14	1,2
NW-001194	28.94611	-97.1161	1192.608	17	7	3
NW-001230	28.70105	-96.9269	1192.608	-60	-80	2
NW-001252	28.78103	-97.1012	298.152	24	4	2
R1GW-000001	28.78434	-97.0496	53.66735	-42	-44	2
R1GW-000238	28.78448	-97.0441	119.2608	-177	-197	3
R1GW-000257	28.78278	-97.0456	73.94168	-220	-280	3,4
R1GW-000465	28.97041	-96.8954	144273.3	-49	-627	2,3,4,5,6,7
R1GW-000469	28.74438	-97.0722	834.8255	-157	-197	3
R1GW-000521	28.90152	-96.9933	40.54867	80	65	2
R1GW-000530	29.04055	-96.9967	951.701	-71	-111	4
R1GW-000556	28.89972	-96.7831	1192.608	-19	-39	1